

Politecnico Di Milano

School of Industrial and Information Engineering
Master's Degree in Electrical Engineering



Simulation, Implementation and Testing of Three-phase
Controlled Power Inverter Behavior

Supervisor: Prof. Francesco Castelli Dezza.

Masters of Science Thesis:

Syed Zaigham Abbas

Matricola: 10340561

April 2016

Abstract

With the increase in the use of renewable sources, the study of control schemes for better control of distributed generation systems and grid connection has become very vital to achieve better stability of the system. This thesis provides a study of the control scheme for interconnection between a DC source and an AC grid.

A possible control scheme is studied and simulated in Simulink. The system behavior is analyzed by subjecting it to different changes in parameters and grid conditions. . Possible modifications are applied to the scheme enable it to perform in the desired way in case of unsymmetrical grid conditions.

The implementation of the scheme is done by using dSpace and Simulink model. Only Low Voltage implementation is performed and tested in this thesis.

Acknowledgements

I express my sincere gratitude to my supervisor Professor Francesco Castelli Dezza for guiding me in making this thesis according to the standards of Politecnico Di Milano.

This thesis has been possible with the help provided by Professor Felipe Córcoles Lopez and Santiago Bogarra Rodríguez of UPC Barcelona, Special thanks to Jaume Saura Perisé for all the guidance provided during the implementation phase.

I would also like to thank Politecnico Di Milano and Universitat Politècnica de Catalunya for providing me with the opportunity and enough resources to undertake my thesis work in Barcelona through the Erasmus Exchange program.

Table of Contents

Abstract	i
Acknowledgements.....	ii
Table of Contents.....	iii
List of Figures	v
List of Tables	vii
1. Introduction.....	1
1.1 Motivation	1
1.2 Objectives and Scope of the Project	2
1.3 Structure of the Thesis.....	2
2. DC/AC Links and Voltage Source Converters	3
2.1 Introduction.....	3
2.2 The Distributed Source-Grid Interconnection	3
2.3 Voltage Source Converter (VSC)	4
2.4 VSC Average Model	5
2.5 VSC Control.....	6
2.6 Mathematical Model of the Three-Phase Inverter in <i>abc</i> coordinates:.....	6
2.7 dq0 Transformation.....	7
2.8 Inner Loop for AC Current Control	9
2.9 The Outer Loop for DC Voltage Control	14
2.10 Outer Loop Modifications for Large Sources	19
2.11 The Phase Locked Loop	19
2.11.1 Tuning of the Phase Locked Loop PI	20
3. Simulations of the Control Scheme using Continuous Model	24
3.1 Introduction.....	24
3.2 Simulations	24
3.2.1 Current Controller (Inner Loop) Simulation.....	24
3.2.2 Simulation of the Overall Control Scheme.....	26
3.2.3 Changes in DC Source Current	26
3.2.4 Response to Changes in Grid Voltage Amplitude	28
3.2.5 Response to Changes in Phase of Grid voltage.....	29
3.2.6 Response to Unsymmetrical Sags	30
Conclusions.....	30
4. Unsymmetrical Conditions	32

4.1	Introduction.....	32
4.2	Symmetrical Components.....	32
4.2.1	Transformation of Symmetrical Components into dq Reference Frame	33
4.3	Control Strategies.....	34
4.3.1	Current Control.....	34
4.3.2	Cross Coupling and Introduction of Notch Filters.....	36
4.3.3	Outer Loop Strategies for PQ Control.....	38
4.3.4	Control Scheme Block Diagram.....	39
4.4	Current Reference Calculation.....	41
4.4.1	Instantaneous Power Expressions.....	41
4.5	PLL Modifications.....	43
4.6	Simulation Results.....	44
	Conclusions.....	50
5.	Discrete Inverter Influence.....	52
5.1	Introduction.....	52
5.2	Space Vector PWM.....	52
5.3	Simulations.....	58
5.3.1	Results.....	58
5.3.2	Introduction of Low-Pass Filters.....	61
5.4	Unsymmetrical Conditions.....	64
	Conclusions.....	67
6.	Implementation.....	68
6.1	Introduction.....	68
6.2	Block Diagram.....	68
6.3	The Hardware.....	68
6.3.1	dSPACE 1104.....	68
6.3.2	The Inverter.....	69
6.4	Control Desk.....	70
6.5	The Simulink Model.....	70
6.6	Tests and Results.....	72
	Conclusions.....	76
7.	Conclusions and Recommendations.....	77
	References.....	78
	Appendices.....	79
A.	Continuous Model Simulink Blocks.....	79

B. Discrete Models in Simulink	85
C. Simulink Models for Real Time Implementation on dSpace.....	87

List of Figures

Figure 1-1 REN21 Report findings	1
Figure 2-1 General structure for distributed power system having different input power sources.....	3
Figure 2-2 VSC Average Model	5
Figure 2-3 DC Source and AC Grid Connection Block Diagram.....	5
Figure 2-4 DC Source and AC Grid Connection.....	5
Figure 2-5 Cascaded Control Scheme	6
Figure 2-6 Equivalent Circuits for the dq Equations.....	9
Figure 2-7 A Feedback System with Control	11
Figure 2-8 PI Controller.....	11
Figure 2-9 Current Control	11
Figure 2-10 Feedback System with Plant and Current Controller	12
Figure 2-11 Current Control Closed Loop	12
Figure 2-12 Open loop and Closed Loop Gain	13
Figure 2-13 Rise Time, Overshoot and Settling Time	14
Figure 2-14 Currents at the Inverter	15
Figure 2-15 Voltage and Current Loop Block Diagram	15
Figure 2-16 Voltage Control Open Loop.....	16
Figure 2-17 Voltage Control Closed Loop	16
Figure 2-18 Current Reference Generation	17
Figure 2-19 Control Scheme with Inverter Average Model	18
Figure 2-20 Outer Loop Modifications for Large DC Source.....	19
Figure 2-21 Reference Current Calculation for Large DC Source [6].....	19
Figure 2-22 Synchronous Reference Frame Phase Locked Loop	20
Figure 2-23 PLL Model according to [7]	20
Figure 2-24 PLL Response at initiation	22
Figure 2-25 PLL Response (frequency)	22
Figure 2-26 PLL Response to Change in Reference Voltage Phase	22
Figure 2-27 PLL Response to Change in Reference Voltage Amplitude	23
Figure 2-28 PLL response to changes in grid voltage frequency	23
Figure 3-1 Current Control Model.....	25
Figure 3-2 Current Control Test Results.....	26
Figure 3-3 DC Source Current and DC Bus Voltage	27
Figure 3-4 AC Currents and Voltages	27
Figure 3-5 Response under Grid Voltage Changes (+ .1 p.u.).....	28
Figure 3-6 Response to Changes in Grid Voltage Phase	29
Figure 3-7 PLL Response	29
Figure 3-8 DC Voltage, P and Q Under Unsymmetrical Sags	30
Figure 3-9 AC Currents Under Unsymmetrical Conditions	30
Figure 4-1 Symmetrical Components of Three Phase Voltage.....	33

Figure 4-2 dq Transformation of Positive and Negative Sequence	34
Figure 4-3 Double SRF Current Control	35
Figure 4-4 Positive and Negative Sequence Controllers	35
Figure 4-5 Oscillations in dq components of unbalanced quantities	37
Figure 4-6 Removing the oscillations using notch filters	37
Figure 4-7 DSRF Current control with notch filters	38
Figure 4-8 Reference power for the current reference calculation	39
Figure 4-9 Control Scheme For PQ control in Double Synchronous Reference Frame ...	40
Figure 4-10 PLL behavior before and during sag	43
Figure 4-11 SOGI Quadrature Signals Generator	43
Figure 4-12 DSOGI PLL Block Diagram	44
Figure 4-13 System behavior during type E Voltage Sags (DC Voltage and Current)	44
Figure 4-14 System behavior during type E Voltage Sags (AC Voltage and Current).....	45
Figure 4-15 System behavior during type E Voltage Sags (qd components)	45
Figure 4-16 System behavior during type E Voltage Sags (P and Q)	46
Figure 4-17 PLL Response	46
Figure 4-18 System behavior during type B Voltage Sags (AC voltages and currents) ...	47
Figure 4-19 System behavior during type B Voltage Sags (qd Components)	47
Figure 4-20 System behavior during type B Voltage Sags (P and Q)	48
Figure 4-21 System behavior during type A Voltage Sags (DC Side Voltage and Currents)	48
Figure 4-22 System behavior during type A Voltage Sags (AC voltages and Currents)...	49
Figure 4-23 System behavior during type A Voltage Sags (qd components)	49
Figure 4-24 System behavior during type A Voltage Sags (P and Q)	50
Figure 4-25 PLL behavior during symmetrical sag (type A)	50
Figure 5-1 The eight Space Vectors forming a hexagon.....	54
Figure 5-2 Application of Zero and Non-Zero Vectors	55
Figure 5-3 Switching Pattern with asymmetric pulsation.....	56
Figure 5-4 Symmetric pulsation using $V_7(111)$ as zero vector	57
Figure 5-5 Symmetric pulsation using $V_0(000)$ as zero vector	57
Figure 5-6 Symmetric pulsation using $V_7(111)$ and $V_0(000)$ as zero vector.....	58
Figure 5-7 Control Scheme with Inverter and SVPWM.....	59
Figure 5-8 DC Voltage when DC Current Reference is Changed	59
Figure 5-9 AC Voltages and Currents	60
Figure 5-10 dq Currents and Voltages	60
Figure 5-11 Inverter Voltages.....	61
Figure 5-12 Introduction of Filters	62
Figure 5-13 AC Voltages before and after the Filters	62
Figure 5-14 AC Currents before and after the Filters.....	63
Figure 5-15 dq Components of the filtered quantities	63
Figure 5-16 Reference voltages without and with the use of filters	64
Figure 5-17 System behavior during type E Voltage Sags (DC Voltage and Current)	65
Figure 5-18 System behavior during type E Voltage Sags (AC Voltage and Current).....	65
Figure 5-19 System behavior during type E Voltage Sags (dq Voltage and Current).....	66
Figure 5-20 System behavior during type E Voltage Sags (p and q)	66
Figure 6-1 dSpace Setup	68
Figure 6-2 dSpace pin-out and display.....	69
Figure 6-3 Simulink model to read and scale inputs	71

Figure 6-4 Mechanism to reset the integrator	72
Figure 6-5 AC Currents and Voltages	72
Figure 6-6 DC Current Changes	73
Figure 6-7 DC Voltage	73
Figure 6-8 dq Currents	74
Figure 6-9 AC Currents and Voltages	75
Figure 6-10 Transformed Voltages in dq frame	75
Figure 6-11 Transformed Currents in dq frame	76
Figure 7-1 Performance of IARC, PNSC,AARC and BPS [6]	77
Figure A 1 PLL Simulink Block	79
Figure A 2 System model in Simulink	80
Figure A 3 Control Block in Simulink	81
Figure A 4 abc to dq transformation block	82
Figure A 5 dq0 to abc transformation block	83
Figure A 6 Converter DC side Current Calculation	84
Figure B 1 Main System Model in Simulink	85
Figure B 2 SVPWM Generation Block	86
Figure C 1 Simulink top level model for real time implementation	87
Figure C 2 Simulink block for enabling/disabling the IGBTs	88

List of Tables

Table 3-1 Parameters used for current control simulations	25
Table 3-2 Parameters used for cascaded control simulation	26
Table 5-1 Switching Vectors and Corresponding voltages in abc and alpha-beta frames	54
Table 5-2 Calculation of Times in Different Sectors [8]	56
Table 6-1 Inverter Information	69
Table 6-2 Parameters used in dSpace tests	74

1. Introduction

1.1 Motivation

Fossil fuels are the major source of energy these days. Due to the adverse effects of CO₂ emissions on the environment, the focus has now been shifting towards clean and renewable energy sources. The energy demand is very high and renewable energy sources represent a reliable alternative to the traditional sources. Wind, Solar and hydro-electric power systems are now being used as cleaner and more environment friendly energy sources. Based on renewables contributed 19 percent to our global energy consumption and 22 percent to our electricity generation in 2012 and 2013, respectively [1].

Estimated Renewable Energy Share of Global Final Energy Consumption, 2013

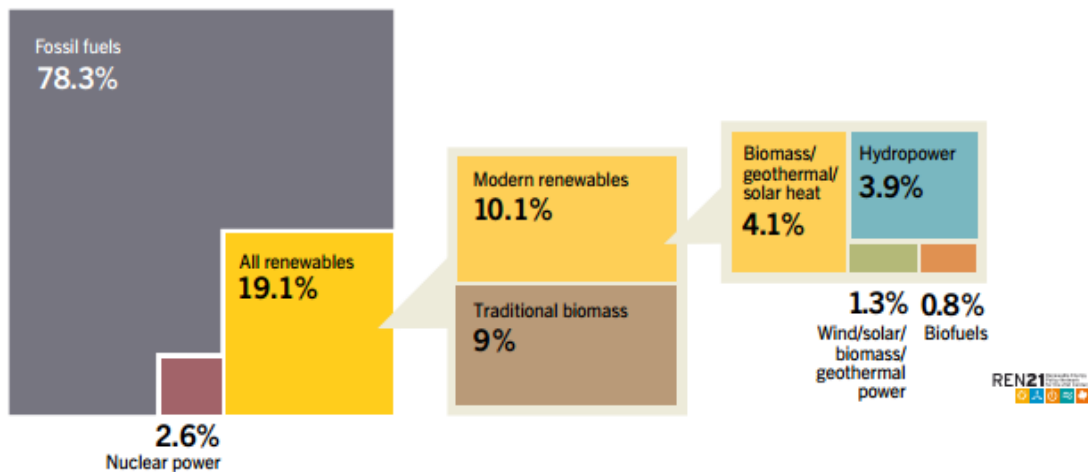


Figure 1-1 REN21 Report findings

With the increase in use of renewable sources in modern power systems, the power system design is changing from the traditional design, where energy from large generation plants is transmitted to large consumption centers which is further distributed to the consumers, to distributed systems where distributed generation stations are spread throughout the system.

One of the main drawbacks of distributed generation systems based on renewable sources is their controllability. If the systems are not properly controlled to the main grid, it can lead to the instability, or even failure of the system. Moreover, the standards for interconnecting these systems to the utility network are stressing more and more the capability of the DPGS to run over short grid disturbances. Therefore, the control strategies applied to distributed systems become of high interest.

1.2 Objectives and Scope of the Project

The main goals of this thesis are:

- understanding of the VSC-based transmission system concept
- mathematical modelling of the system and investigating a possible control scheme
- simulation and analysis of the developed control scheme using Simulink
- testing and possibly modifying the control scheme for unsymmetrical sags
- implementation of the tested scheme using dSpace and inverter

1.3 Structure of the Thesis

This thesis focuses on the development and testing of a control scheme for the VSC based transmission system using Simulink and developing a test setup for the system to be implemented on dSpace. The thesis is structured in the following way:

- Chapter 1 introduces the thesis, including the motivation for research and the main objectives.
- Chapter 2 provides a short overview of the VSC, mathematical modeling using the average VSC model and developing a possible control scheme
- Chapter 3 presents the simulation results for the control scheme using a linear continuous model of the VSC
- Chapter 4 deals with the study of the control during unsymmetrical sags and possible modifications to tackle such situations.
- Chapter 5 presents an overview of the SVPWM modulation scheme for implementation of the control using the discrete VSC model.
- Chapter 6 contains the study of the test setup to implement the system using dSpace and inverter and the results of said experiments.

2. DC/AC Links and Voltage Source Converters

2.1 Introduction

In this chapter first the interconnection between a grid and the distributed power source is introduced. The main components of such an interconnection are the Voltage Source Converter (VSC), the control mechanism and the filter. The average model of the VSC is introduced, to develop the control scheme using a linear model before testing it with the actual inverter. The mathematical model for the whole system is developed from the circuit equations and then a suitable control scheme is discussed.

2.2 The Distributed Source-Grid Interconnection

The interconnection between the distributed generation source and grid is of great importance to achieve a smoother integration of the distributed source into the grid. The input energy source determines the power conversion system at the point of common coupling (PCC). The following figure shows a general power system for the said interconnection [2].

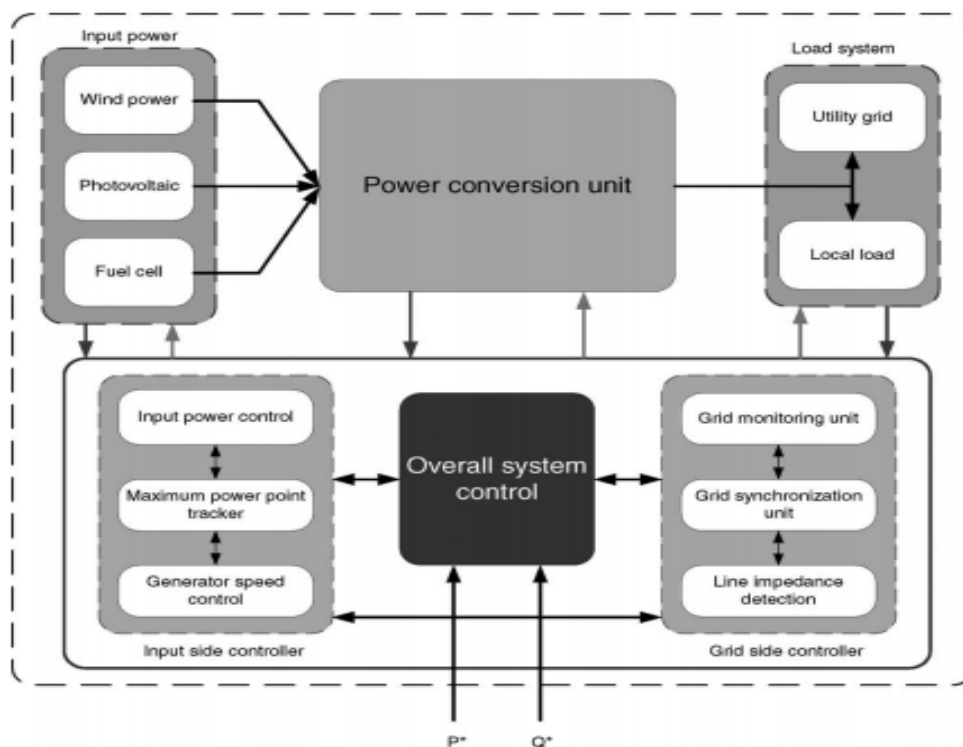


Figure 2-1 General structure for distributed power system having different input power sources

2.3 Voltage Source Converter (VSC)

The main requirement in a power transmission system is the precise control of active and reactive power flow to maintain the system voltage stability. This is achieved through an electronic converter and its ability of converting electrical energy from AC to DC or vice versa.

Depending upon the input and output there are two types of converters (a) Voltage Source Inverter (VSI) & (b) Current Source converter (CSC).

(a) Voltage Source Converter (VSC): In VSC, input voltage is maintained constant and the amplitude of output voltage does not depend on the load. However, the waveform of load current as well as its magnitude depends upon the nature of the load impedance.

(b) Current Source Inverter (CSI): In these type of converter input current is constant but adjustable. The amplitude of output current from CSI is independent of load. However the magnitude of output voltage and its waveform output from CSC is dependent upon the nature of load impedance. A CSC does not require any feedback diodes whereas these are required in VSC.

Conventional line commutated current source converters make use of filters, series capacitors or shunt banks to fulfil the reactive power demands of the conversion process. These converters generally make use of thyristors that can only be turned ON (not OFF) by the control action.

Insulated-gate bipolar transistor (IGBT) devices provide both the options of Tuning ON and OFF by the control action. They have good controllability and thus help in maintaining a good power quality.

The high frequency switching capabilities of the IGBTs make it possible to use high frequency pulse-width modulation (PWM) techniques which allow high performance control of the current while minimizing the low frequency current harmonics without the need of large passive filters. The high frequency modulation also makes it possible to use a low frequency model of the converter and to approximate the behavior of the inverters as ideal controllable voltage sources. This is possible thanks to the low pass nature of the physical systems connected to the inverters, which have the ability to filter the high frequency content of the voltage applied by the inverters. This allows to apply the well-known linear system analysis tools to study the system and design its controllers.

2.4 VSC Average Model

VSC is based on discrete switching states of the IGBT, but for design purposes only, it can be modeled by a continuous counterpart that has decoupled DC and AC sides. In this thesis, first the control scheme is designed using this average model [3].

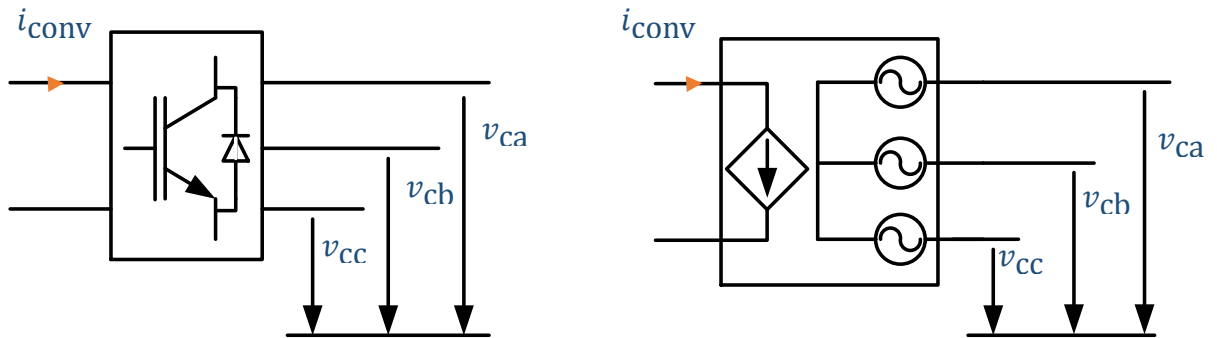


Figure 2-2 VSC Average Model

A filter is connected between the VSC and the grid to avoid any short circuit.

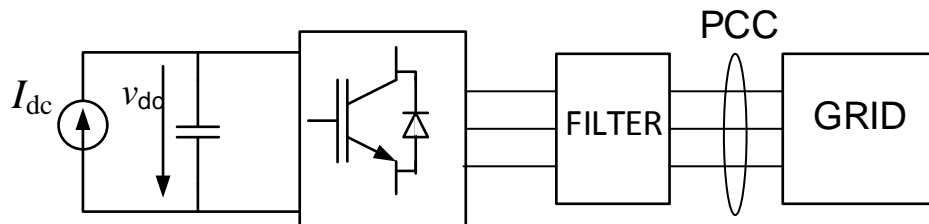


Figure 2-3 DC Source and AC Grid Connection Block Diagram

The basic model for such a connection between an AC grid and a VSC is shown in figure below:

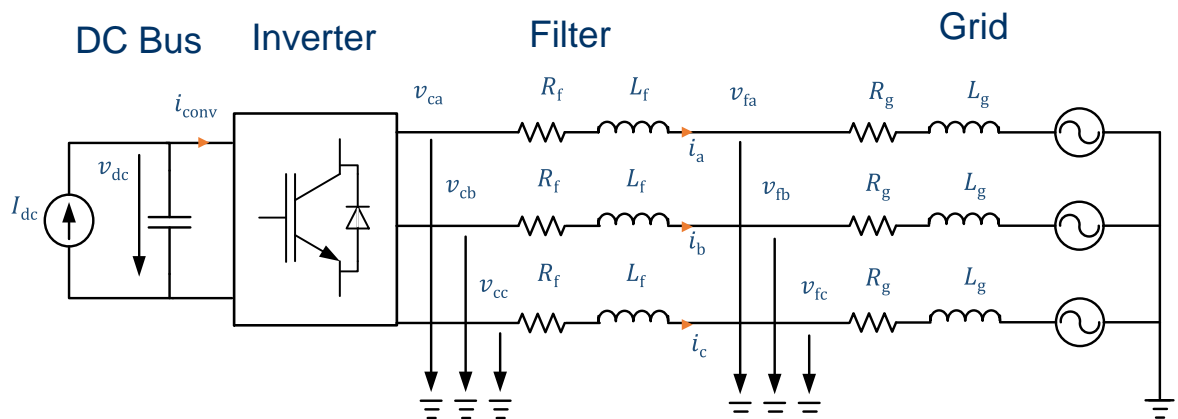


Figure 2-4 DC Source and AC Grid Connection

2.5 VSC Control

The control scheme used in this thesis is a cascaded control with two control loops. The mathematical model of the system and description of the loops is given in the following sections.

The two control loops are:

- The Inner Loop
The lower level control (current loop) regulates the AC current in d and q components. VSC has it as the basic control loop.
- The Outer loop
This loop controls the DC side bus voltage and gives a current reference for the inner loop.

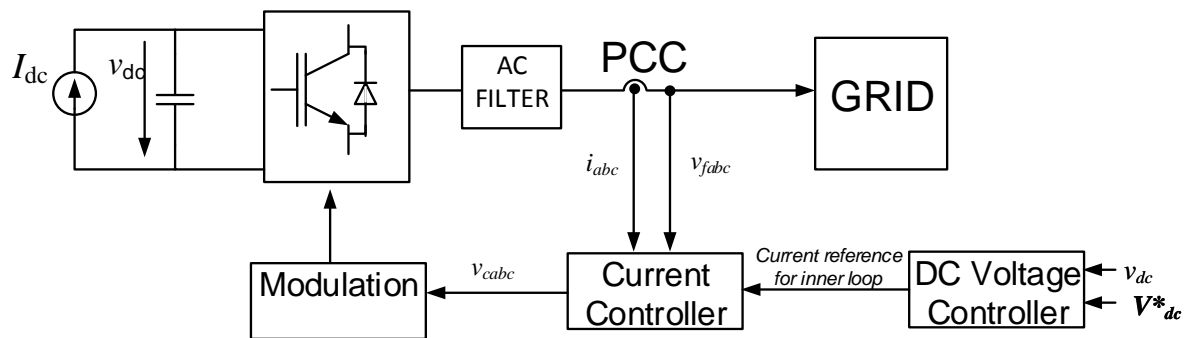


Figure 2-5 Cascaded Control Scheme

2.6 Mathematical Model of the Three-Phase Inverter in abc coordinates:

From Figure 2-4, following equations can be written for the various voltages and currents

$$v_{ca} = i_a(R_f + L_f \frac{d}{dt}) + v_{fa}$$

$$v_{cb} = i_b(R_f + L_f \frac{d}{dt}) + v_{fb}$$

(2.1)

$$v_{cc} = i_c(R_f + L_f \frac{d}{dt}) + v_{fc}$$

Similar equations can be written for the voltages at the filter in terms of the grid voltages. In matrix form the equations are given below:

$$\begin{bmatrix} v_{ca} \\ v_{cb} \\ v_{cc} \end{bmatrix} = \begin{bmatrix} R_f & 0 & 0 \\ 0 & R_f & 0 \\ 0 & 0 & R_f \end{bmatrix} \begin{bmatrix} i_a \\ i_b \\ i_c \end{bmatrix} + \begin{bmatrix} L_f & 0 & 0 \\ 0 & L_f & 0 \\ 0 & 0 & L_f \end{bmatrix} \frac{d}{dt} \begin{bmatrix} i_a \\ i_b \\ i_c \end{bmatrix} + \begin{bmatrix} v_{fa} \\ v_{fb} \\ v_{fc} \end{bmatrix}$$

$$\begin{bmatrix} v_{fa} \\ v_{fb} \\ v_{fc} \end{bmatrix} = \begin{bmatrix} R_g & 0 & 0 \\ 0 & R_g & 0 \\ 0 & 0 & R_g \end{bmatrix} \begin{bmatrix} i_a \\ i_b \\ i_c \end{bmatrix} + \begin{bmatrix} L_g & 0 & 0 \\ 0 & L_g & 0 \\ 0 & 0 & L_g \end{bmatrix} \frac{d}{dt} \begin{bmatrix} i_a \\ i_b \\ i_c \end{bmatrix} + \begin{bmatrix} v_{ga} \\ v_{gb} \\ v_{gc} \end{bmatrix}$$

2.7 dq0 Transformation

To design a control scheme, it is useful to have constant quantities in steady state. The electrical quantities in the abc reference frame are oscillating in nature. To convert them into constant quantities, $dq0$ is applied.

abc model coordinates written in matrix form:

$$[v_c] = [R_f][i] + [L_f] \frac{d}{dt} [i] + [v_f] \quad (2.4.1)$$

The $dq0$ transformation is given by

$$[x_{qdo}] = [P][x_{abc}]$$

Where the transformation matrix $[P]$ is given by

$$[P] = \sqrt{\frac{2}{3}} \begin{bmatrix} \cos(\theta) & \cos(\theta - \frac{2\pi}{3}) & \cos(\theta + \frac{2\pi}{3}) \\ -\sin(\theta) & -\sin(\theta - \frac{2\pi}{3}) & -\sin(\theta + \frac{2\pi}{3}) \\ \frac{1}{\sqrt{2}} & \frac{1}{\sqrt{2}} & \frac{1}{\sqrt{2}} \end{bmatrix}$$

Multiplying the system equation with the transformation matrix on both sides we get,

$$[P][v_c] = [P][R_f][i] + [P] \frac{d}{dt} \{ [L_f][i] \} + [P][v_f]$$

$$[P][v_c] = [P][R_f][P]^{-1}[P][i] + [P] \frac{d}{dt} \{ [L_f][P]^{-1}[P][i] \} + [P][v_f]$$

$$[v_{cqdo}] = [R_f][i_{dqo}] + [P] \frac{d}{dt} \{ [L_f][P]^{-1}[i_{dqo}] \} + [v_{fdqo}]$$

$$[v_{cqdo}] = [R_f][i_{dqo}] + [P][L_f] \frac{d}{dt} \{ [P]^{-1}[i_{dqo}] \} + [v_{fdqo}]$$

Applying the product rule on the derivative of two terms, we get

$$[v_{cqdo}] = [R_f][i_{dqo}] + [P] \frac{d}{dt} \{ [P]^{-1} [L_f][i_{dqo}] \} + [P][L_f][P]^{-1} \frac{d}{dt} \{ [i_{dqo}] \} + [v_{fdqo}]$$

$$[v_{cqdo}] = [R_f][i_{dqo}] + [\omega][L_f][i_{dqo}] + [L_f] \frac{d}{dt} \{ [i_{dqo}] \} + [v_{fdqo}]$$

Where,

$$[P][L_f][P]^{-1} = [L_f]$$

$$[\omega] = [P] \frac{d}{dt} [P]^{-1} = \begin{bmatrix} 0 & 0 & 0 \\ 0 & 0 & -\frac{d\psi}{dt} \\ 0 & \frac{d\psi}{dt} & 0 \end{bmatrix} = \begin{bmatrix} 0 & 0 & 0 \\ 0 & 0 & -\omega_\psi \\ 0 & \omega_\psi & 0 \end{bmatrix}$$

$$\begin{bmatrix} v_{c0} \\ v_{cd} \\ v_{cq} \end{bmatrix} = \begin{bmatrix} R_f & 0 & 0 \\ 0 & R_f & 0 \\ 0 & 0 & R_f \end{bmatrix} \begin{bmatrix} i_0 \\ i_d \\ i_q \end{bmatrix} + \begin{bmatrix} 0 & 0 & 0 \\ 0 & 0 & -\omega_\psi \\ 0 & \omega_\psi & 0 \end{bmatrix} \begin{bmatrix} L_f & 0 & 0 \\ 0 & L_f & 0 \\ 0 & 0 & L_f \end{bmatrix} \begin{bmatrix} i_0 \\ i_d \\ i_q \end{bmatrix} + \begin{bmatrix} L_f & 0 & 0 \\ 0 & L_f & 0 \\ 0 & 0 & L_f \end{bmatrix} \frac{d}{dt} \begin{bmatrix} i_0 \\ i_d \\ i_q \end{bmatrix} + \begin{bmatrix} v_{f0} \\ v_{fd} \\ v_{fq} \end{bmatrix}$$

$$\begin{bmatrix} v_{c0} \\ v_{cd} \\ v_{cq} \end{bmatrix} = \begin{bmatrix} R_f & 0 & 0 \\ 0 & R_f & -\omega_\psi L_f \\ 0 & \omega_\psi L_f & R_f \end{bmatrix} \begin{bmatrix} i_0 \\ i_d \\ i_q \end{bmatrix} + \begin{bmatrix} L_f & 0 & 0 \\ 0 & L_f & 0 \\ 0 & 0 & L_f \end{bmatrix} \frac{d}{dt} \begin{bmatrix} i_0 \\ i_d \\ i_q \end{bmatrix} + \begin{bmatrix} v_{f0} \\ v_{fd} \\ v_{fq} \end{bmatrix} \quad (2.4.2)$$

And

$$\begin{bmatrix} v_{f0} \\ v_{fd} \\ v_{fq} \end{bmatrix} = \begin{bmatrix} R_g & 0 & 0 \\ 0 & R_g & -\omega_\psi L_g \\ 0 & \omega_\psi L_g & R_g \end{bmatrix} \begin{bmatrix} i_0 \\ i_d \\ i_q \end{bmatrix} + \begin{bmatrix} L_g & 0 & 0 \\ 0 & L_g & 0 \\ 0 & 0 & L_g \end{bmatrix} \frac{d}{dt} \begin{bmatrix} i_0 \\ i_d \\ i_q \end{bmatrix} + \begin{bmatrix} v_{g0} \\ v_{gd} \\ v_{gq} \end{bmatrix}$$

The zero component voltage equations are:

$$v_{c0} = R_f i_0 + L_f \frac{di_0}{dt} + v_{f0}$$

$$v_{f0} = R_g i_0 + L_g \frac{di_0}{dt} + v_{g0}$$

But

$$i_0 = 0 \Rightarrow v_{c0} = v_{f0} = v_{g0}$$

From the transformation equation, $v_{c0} = \frac{v_{ca} + v_{cb} + v_{cc}}{\sqrt{3}} = 0$

So equation 2.4.2 can be simplified as

$$\begin{bmatrix} v_{cd} \\ v_{cq} \end{bmatrix} = \begin{bmatrix} R_f & -\omega_\psi L_f \\ \omega_\psi L_f & R_f \end{bmatrix} \begin{bmatrix} i_d \\ i_q \end{bmatrix} + \begin{bmatrix} L_f & 0 \\ 0 & L_f \end{bmatrix} \frac{d}{dt} \begin{bmatrix} i_d \\ i_q \end{bmatrix} + \begin{bmatrix} v_{fd} \\ v_{fq} \end{bmatrix}$$

Similar equations can be derived for the d and q components of \mathbf{v}_f .

$$\Psi = \theta_e = \arctan\left(\frac{v_{g\beta}}{v_{g\alpha}}\right) \Rightarrow \omega_\Psi = \frac{d\Psi}{dt} = \frac{d\theta_e}{dt} = \omega_g$$

$$\Psi = \omega_g t + \Psi_0 \Rightarrow \omega_\Psi = \frac{d\Psi}{dt} = \frac{d\{\omega_g t + \Psi_0\}}{dt} = \omega_g$$

Where $\omega_g = \omega_{\text{voltage}} = 2\pi f$

So we have the following final set of equations,

$$v_{cd} = R_f i_d + L_f \frac{di_d}{dt} - \omega_g L_f i_q + v_{fd} \quad (2.4.3)$$

$$v_{cq} = R_f i_q + L_f \frac{di_q}{dt} + \omega_g L_f i_d + v_{fq} \quad (2.4.4)$$

The above system of equations can be represented by the following circuits

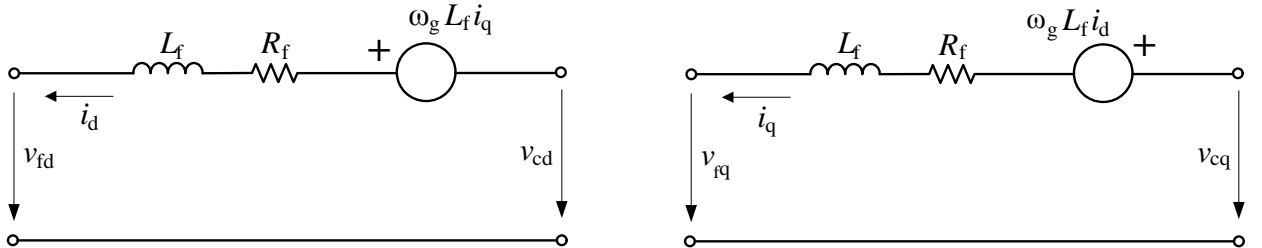


Figure 2-6 Equivalent Circuits for the dq Equations

2.8 Inner Loop for AC Current Control

The objective here is to control the current i_{abc} by applying a voltage v_{abc} with the power converter. Laplace transform of the equations 2.4.3 and 2.4.4 is

$$v_{cd} = (R_f + sL_f)i_d - \omega_g L_f i_q + v_{fd}$$

$$v_{cq} = (R_f + sL_f)i_q + \omega_g L_f i_d + v_{fq}$$

From which we get

$$(R_f + sL_f)i_d = v_{cd} + \omega_g L_f i_q - v_{fd}$$

$$(R_f + sL_f)i_q = v_{cq} - L_f i_d - v_{fq}$$

To control the current i_d , v_{cd} should vary because in the equation R_f , L_f and ω_g are constants. The reference voltages to be imposed by the inverter (v_{cd}^* and v_{cq}^*) are obtained from the above equations as

$$v_{cd}^* = (R_f + sL_f)i_d - \omega_g L_f i_q + v_{fd} \quad v_{cd}^* = \hat{v}_{cd} - \omega_g L_f i_q + v_{fd}$$

$$v_{cq}^* = (R_f + L_f)i_q + \omega_g L_f i_d + v_{fq} \quad v_{cq}^* = \hat{v}_{cq} + \omega_g L_f i_d + v_{fq}$$

Where \hat{v}_{cd} and \hat{v}_{cq} are the terms and the outputs of the controller. Note that the equations are now decoupled in terms of i_q and i_d . The system gain is:

$$G(s) = \frac{i_d(s)}{\hat{v}_{cd}(s)} = \frac{i_q(s)}{\hat{v}_{cq}(s)} = \frac{1}{R_f + L_f s}$$

PI Controllers

Proportional-Integral (PI) controllers are one of the most commonly used types of controllers. A PI controller provides a control signal that has a component proportional to the tracking error of a system and a component proportional to the accumulation of this error over time, and is represented by the following equation:

$$u(t) = K_p \cdot e(t) + K_i \int_0^t e(\tau) d\tau$$

Where $u(t)$ the control is signal and $e(t)$ is the tracking error. In Laplace domain the above equation can be written as:

$$U(s) = \left(K_p + \frac{K_i}{s} \right) \cdot E(s)$$

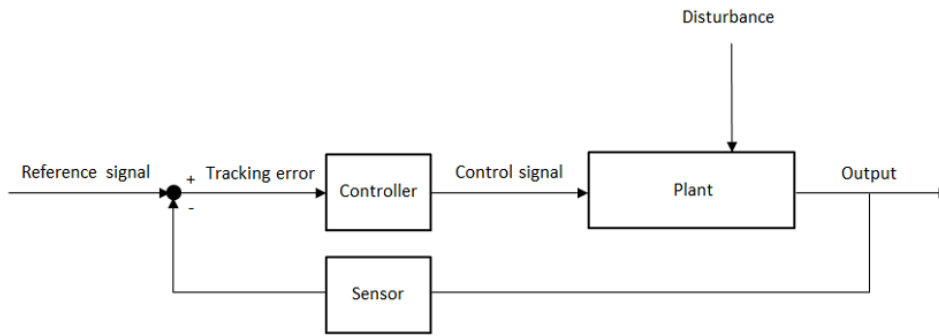


Figure 2-7 A Feedback System with Control

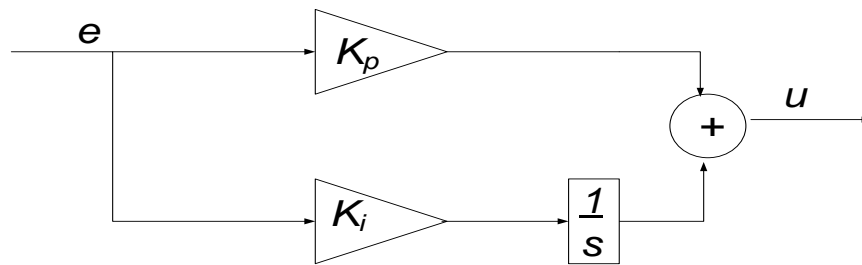


Figure 2-8 PI Controller

The control scheme of the currents, using PI controllers, is as follows

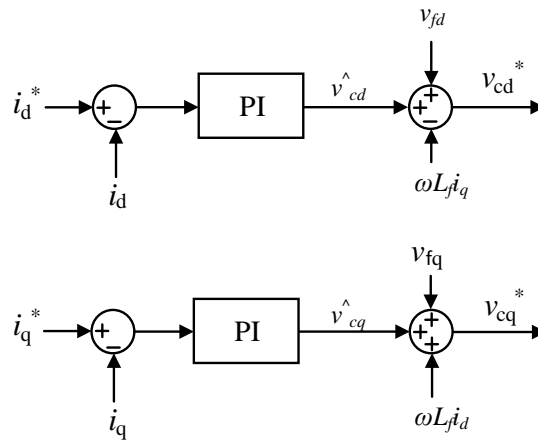


Figure 2-9 Current Control

PI Controller Setting for the Inner Loop:

The line diagram of the system and the inner control loop can be drawn as follows

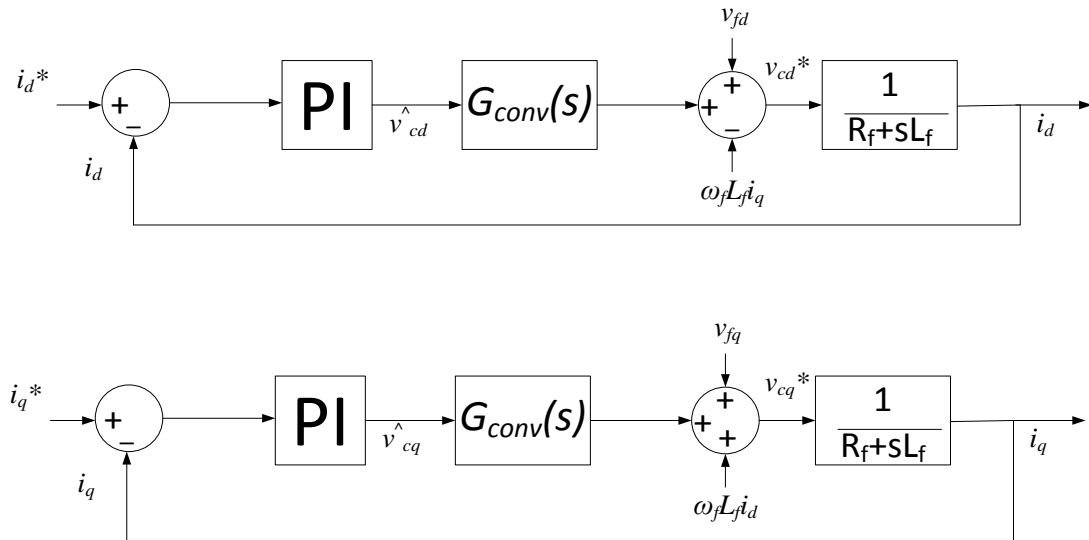


Figure 2-10 Feedback System with Plant and Current Controller

In the current control loop (inner loop), the drive is considered ideal, so the gain is $G_{conv}(s) = 1$. Neglecting the disturbances, the transfer function of the above system can be represented as

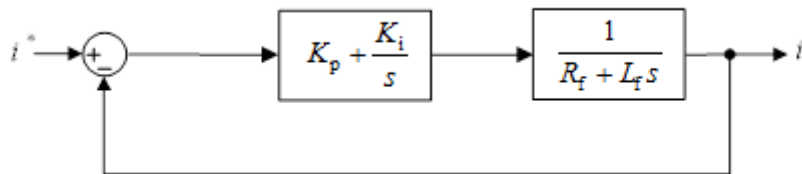


Figure 2-11 Current Control Closed Loop

The closed loop transfer function and the open loop transfer function of a feedback system are related as:

$$G_{closedloop}(s) = \frac{G_{openloop}(s)}{1 + G_{openloop}(s)H(s)}$$

Here

$$H(s) = 0$$

$$G_{openloop}(s) = \frac{K_p s + K_i}{s(R_f + L_f s)}$$

So the closed loop transfer function is given as:

$$G_{closedloop}(s) = \frac{K_p s + K_i}{L_f s^2 + (R_f + K_p)s + K_i}$$

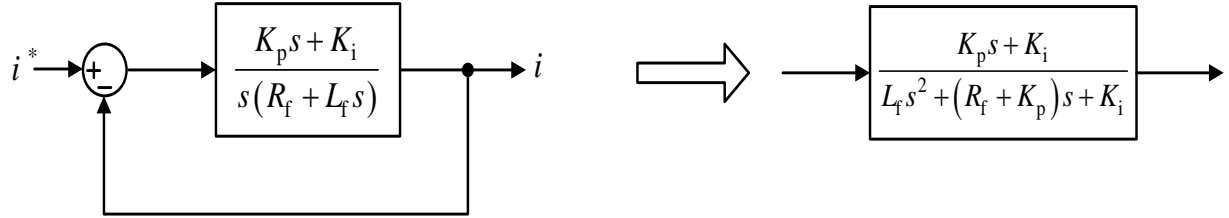


Figure 2-12 Open loop and Closed Loop Gain

The denominator of the closed loop transfer function is,

$$L_f s^2 + (R_f + K_p)s + K_i = 0 \xrightarrow{\cdot \frac{1}{L_f}} s^2 + \left(\frac{R_f + K_p}{L_f} \right) s + \frac{K_i}{L_f} = 0$$

Comparing the above equation with the characteristic second order equation

$$s^2 + 2\xi\omega_n s + \omega_n^2 = 0$$

We get

$$\boxed{\begin{aligned} K_p &= 2\xi\omega_n L_f - R_f \\ K_i &= L_f \omega_n^2 \end{aligned}}$$

ξ is the damping factor and is generally taken as 0.707. It can be also calculated based on the overshoot (M_p) desired [4]. Typical values of the overshoot: $\leq 20\%$ M_p (0.2 pu):

$$M_p = e^{-\frac{\pi\xi}{\sqrt{1-\xi^2}}} \Rightarrow \xi = \sqrt{\frac{\ln^2(M_p)}{\ln^2(M_p) + \pi^2}} ; 0 \leq M_p \leq 1$$

ω_n is the natural frequency of the system

$$\omega_n = -\frac{\ln(\varepsilon)}{\xi t_s} \xrightarrow{\varepsilon=2\%} \omega_n = \frac{4}{\xi t_s}$$

Where

- t_s = settling time (time when the response is considered to have reached the set point within an allowable error, ϵ).
- ϵ = error: error allowed the response to set point (generally considered $\epsilon = 2\%$ or 3% ,

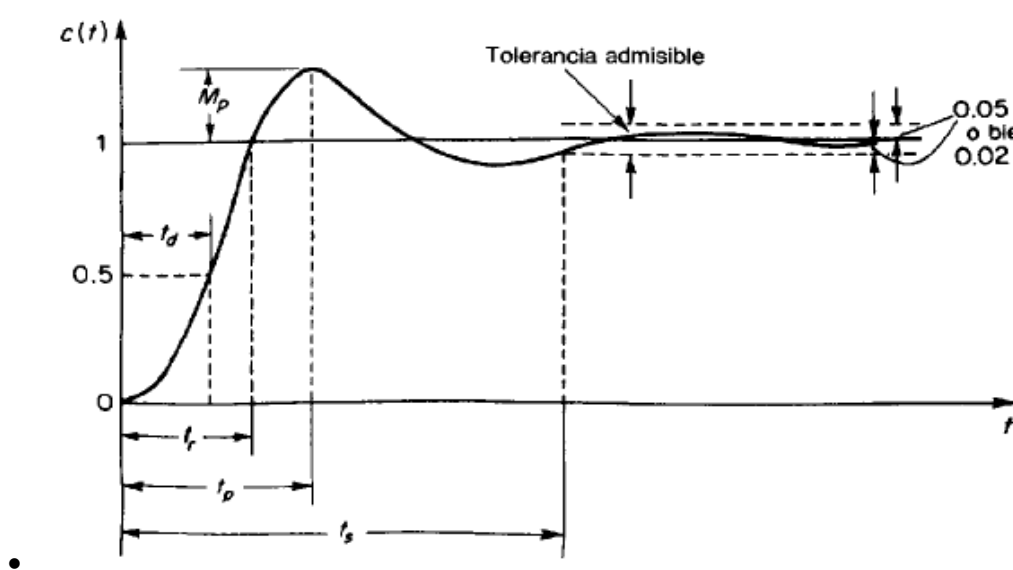


Figure 2-13 Rise Time, Overshoot and Settling Time

According to [3] or [5] the constants can also be calculated as:

$$K_p = \alpha_i L_f$$

$$K_p = \alpha_i R_f$$

Where $\alpha_i = \frac{\ln(9)}{t_s}$.

2.9 The Outer Loop for DC Voltage Control

The outer loop controls the voltage of the DC bus. The DC voltage control is achieved through the control of power exchanged by the converter with the grid. Increasing or decreasing the injected power with respect to the power produced by the DC system decreases or increases the voltage level to keep it under control. The output of the DC voltage controller provides the reference current for the inner loop. The constant current source I_{dc} can be modeled as a constant power source, value:

$$I_{dc} = \frac{P^*}{v_{dc}}$$

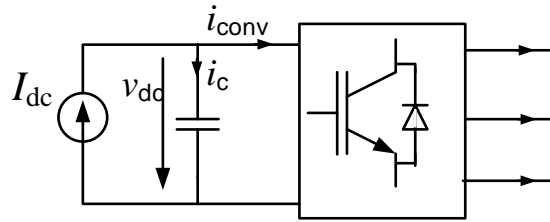


Figure 2-14 Currents at the Inverter

The current in the DC bus capacitor is

$$i_c = C \frac{dv_{dc}}{dt} = I_{dc} - i_{conv}$$

We want to keep a constant DC side voltage, so that $\frac{dv_{dc}}{dt} = 0 \Rightarrow I_{dc} = i_{conv}$

And $P_{dc} = v_{dc}I_{dc}$

Using the power balance on the DC and AC side

$$P_{dc} = P_{AC}$$

Where $P_{AC} = v_{cd}i_d + v_{cq}i_q$, but we have $v_{cq} = 0$ which implies that $P_{AC} = v_{cd}i_d$

Or

$$P_{dc} = P_{AC} \Rightarrow v_{cd}i_d = v_{dc}I_{dc}$$

We can observe that if the current i_d is regulated, we can control the bus voltage v_{dc} .

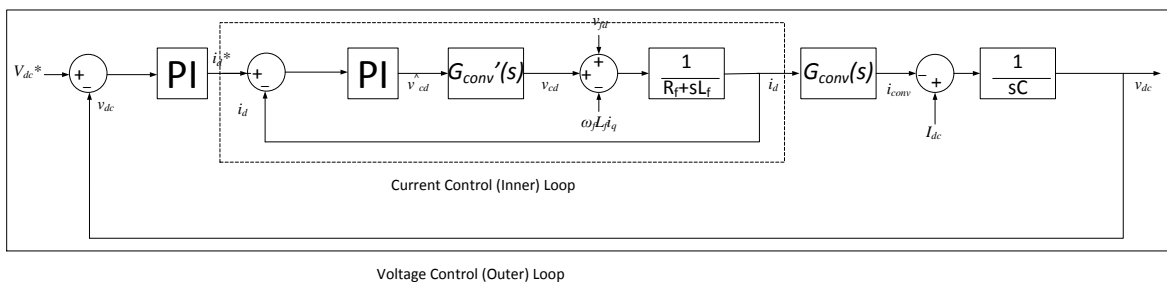


Figure 2-15 Voltage and Current Loop Block Diagram

PI Controller Setting for the Outer Loop

$$i_c = C \frac{dv_{dc}}{dt} = C \frac{dv_c}{dt}$$

Which in Laplace domain gives:

$$V_c(s) = \frac{1}{Cs} I_c(s)$$

A PI controller is used with the following transfer function:

$$G_{PI} = K_p + \frac{K_i}{s}$$

. The open loop transfer function of the voltage control loop, neglecting the disturbances and the inner loop is

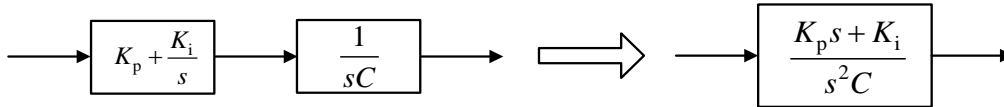


Figure 2-16 Voltage Control Open Loop

As the relation between open loop transfer function and closed loop transfer function of a feedback system is given as;

$$G_{closedloop}(s) = \frac{G_{openloop}(s)}{1 + G_{openloop}(s)H(s)}$$

Where H(s) is the loop gain, which in our case is 1. We can write the equations for the close loop as shown below.

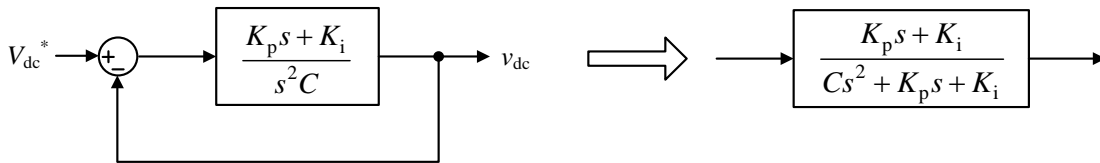


Figure 2-17 Voltage Control Closed Loop

To obtain the poles of the system, we put the denominator of the system equation =0.

$$Cs^2 + K_p s + K_i = 0 \xrightarrow{\cdot \frac{1}{C}} s^2 + \frac{K_p}{C} s + \frac{K_i}{C} = 0$$

Equating the coefficients of the above equation with the coefficients of the characteristic equation of a second order system $s^2 + 2\xi\omega_n s + \omega_n^2 = 0$, we have:

$$\boxed{\begin{matrix} K_p = 2\xi\omega_n C \\ K_i = C\omega_n^2 \end{matrix}}$$

Where ξ and ω_n are obtained the same way as in the case of the current PI.

The dynamics of the outer control loop is greater than the inner loop. The internal loop is designed to achieve short settling times, and the external loop is designed keeping in mind the stability and regulation, and it can be designed to be slower than the internal current loop. This also means we can consider both loops to be decoupled. According to [3], [6], ω_n for the outer loop should be tuned to be at least three to five times slower than the inner loop time constant.

The voltage controller PI generates the reference current i_d^* . This can be shown in the figure below, based on the reference [7]:

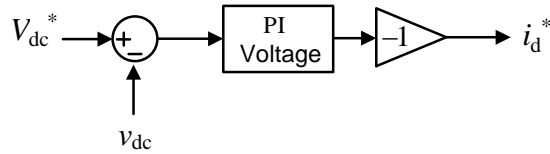


Figure 2-18 Current Reference Generation

Based on the discussion above, the overall control scheme is shown in the figure below:

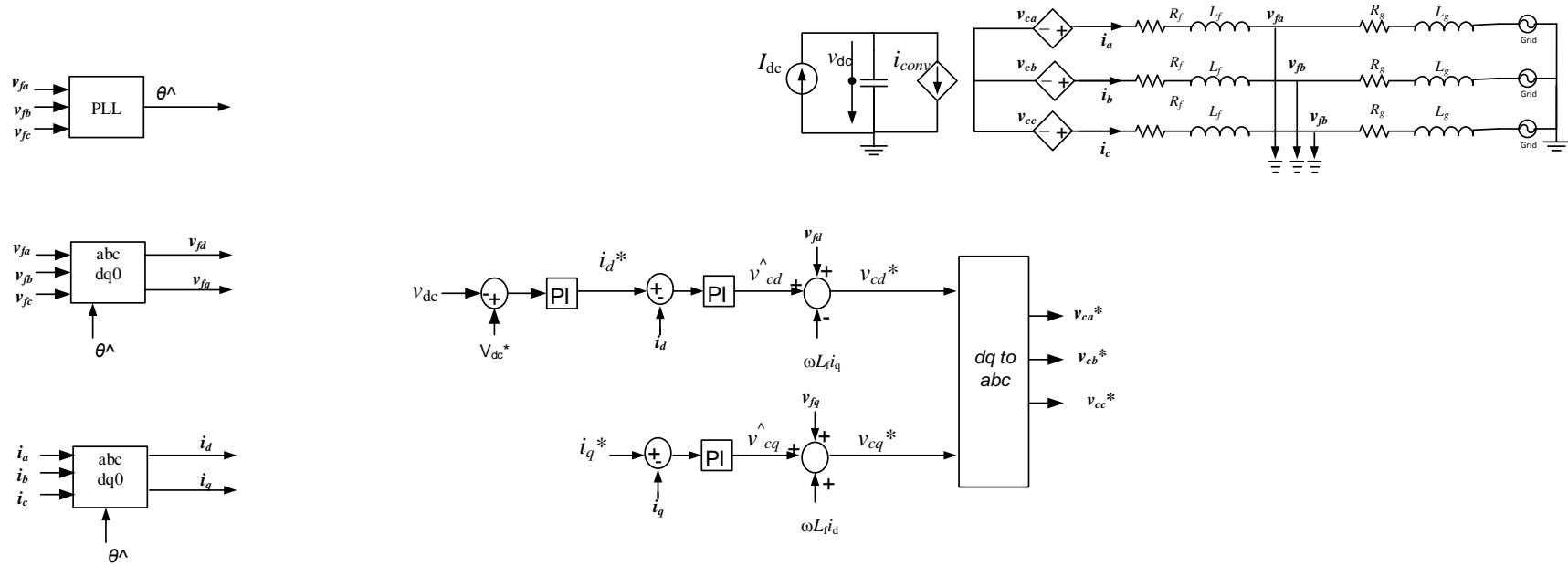


Figure 2-19 Control Scheme with Inverter Average Model

2.10 Outer Loop Modifications for Large Sources

If the DC generation source is large and produces more power than that required by the grid, the power delivered to the system has to be controlled. For this purpose the outer loop needs some modifications so that the current references generated for the inner loop are calculated from the desired power that needs to be delivered to the AC side. A possible modification is suggested in [6] as the PQ open-loop voltage oriented control based on synchronous dq frame is given below:

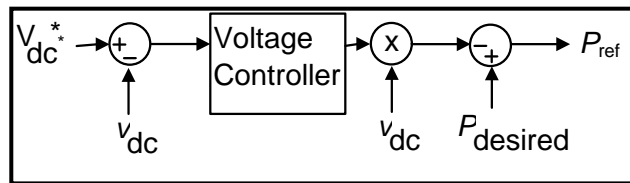


Figure 2-20 Outer Loop Modifications for Large DC Source

From P_{ref} calculated in the above figure, the reference currents for the inner loop can be calculated from the following equations:

$$\begin{bmatrix} i_d^* \\ i_q^* \end{bmatrix} = \frac{1}{v_{fd}^2 + v_{fq}^2} \begin{bmatrix} v_{fd} & -v_{fq} \\ v_{fq} & v_{fd} \end{bmatrix} \begin{bmatrix} P_{ref} \\ Q_{ref} \end{bmatrix}$$

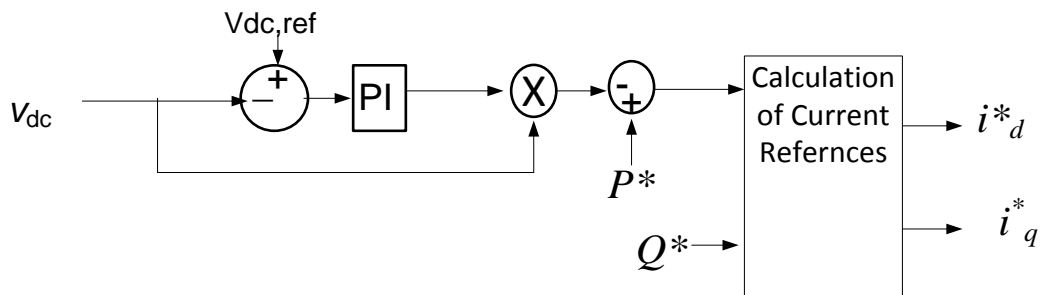


Figure 2-21 Reference Current Calculation for Large DC Source [6]

2.11 The Phase Locked Loop

The abc to dq0 conversion needs the value of the angle θ that is determined by a phase locked loop. The scheme of the phase locked loop implemented here is shown in the

figure below [6]

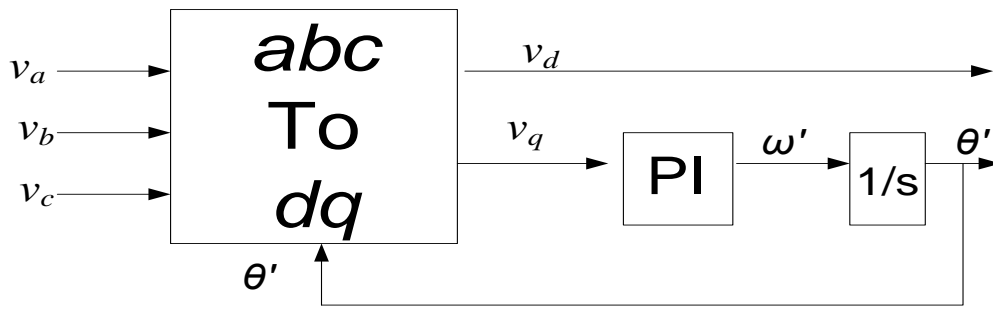


Figure 2-22 Synchronous Reference Frame Phase Locked Loop

In applications related to the three phase systems, the PLL based on the synchronous reference frame is normally used. It is used in the conversion of the three phase voltage vector from the *abc* reference frame to the *dq* reference frame using Park's Transformation. The angular position of the *dq* reference frame is controlled by a feedback loop that regulates the *q* component to zero.

2.11.1 Tuning of the Phase Locked Loop PI

The PLL can be adjusted keeping in view the fact that we align the d axis with v_{fd} which results in the voltage along the q-axis being null ($v_{fq}=0$). A feedback loop controls the angular position of the dq frame, and regulates the q component to zero. According to [7] the model for a three phase PLL system is given below:

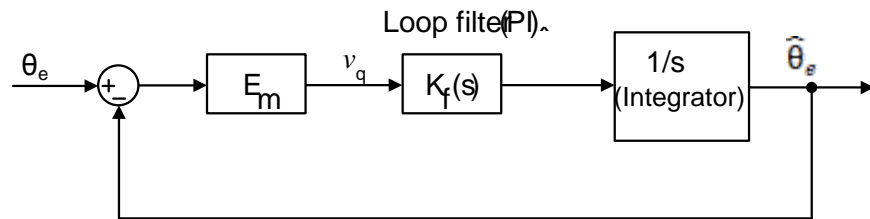


Figure 2-23 PLL Model according to [7]

Where the voltage v_d is given by,

$$v_q = E_m \sin \delta$$

The quantity $\delta = \theta_e - \hat{\theta}_e$ is very small, which implies that,

$$v_q = E_m \delta$$

And the angular frequency of the PLL is given by

$$\hat{\omega} = \frac{d\hat{\theta}}{dt} = K_f v_q = K_f E_m \delta$$

The closed loop transfer function of the previous figure is given by

$$H(s) = \frac{K_f(s)E_m}{s + K_f(s)E_m}$$

Where $K_f(s)$ is the gain of the PI, given by:

$$K_f(s) = K_p + \frac{K_i}{s}$$

Putting this value into the expression for the transfer function gives a second order equation, whose poles are obtained by putting the denominator =0.

$$s + K_f(s)E_m = s + \left(K_p + \frac{K_i}{s}\right)E_m = 0 \longrightarrow s^2 + K_p E_m s + K_i E_m = 0$$

Comparing the above equation with the characteristic second order equation

$$s^2 + 2\xi\omega_n s + \omega_n^2 = 0$$

We get,

$$\boxed{K_p = \frac{2\xi\omega_n}{E_m} \quad K_i = \frac{\omega_n^2}{E_m}}$$

The values of the parameters are

- $\xi = 1/\sqrt{2} =$ Damping factor
- $E_m = \frac{V_L}{\sqrt{3}}\sqrt{2} =$ Peak value of the phase voltage (= 326,6 V if $V_L = 400$ V)
- $\omega_n = 100\pi$ rad/s = natural frequency of the voltage

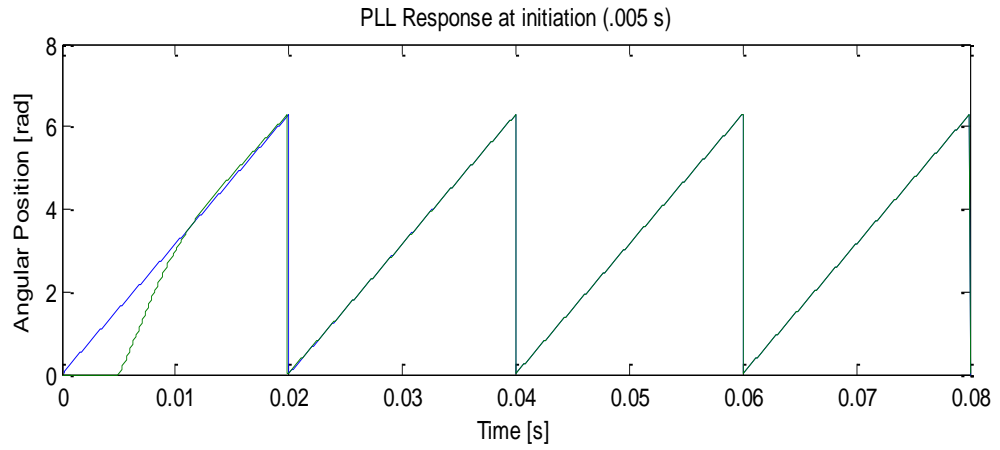


Figure 2-24 PLL Response at initiation

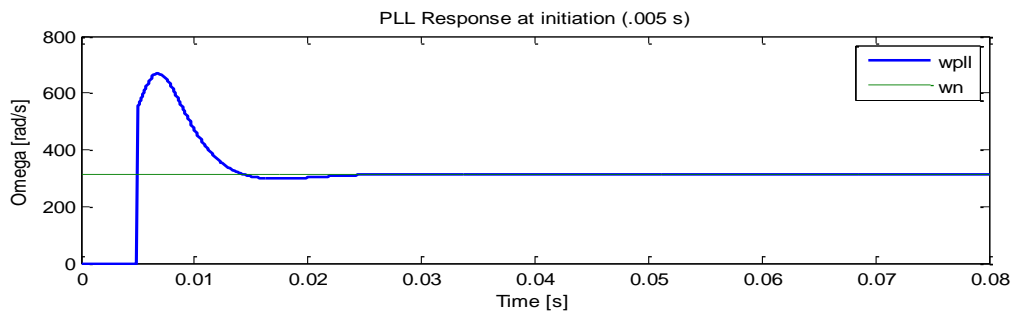


Figure 2-25 PLL Response (frequency)

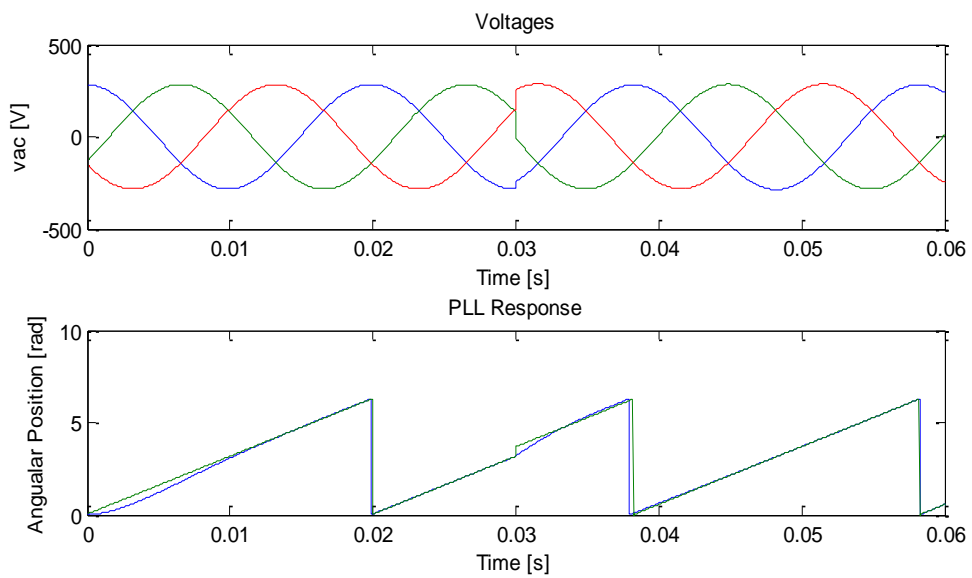


Figure 2-26 PLL Response to Change in Reference Voltage Phase

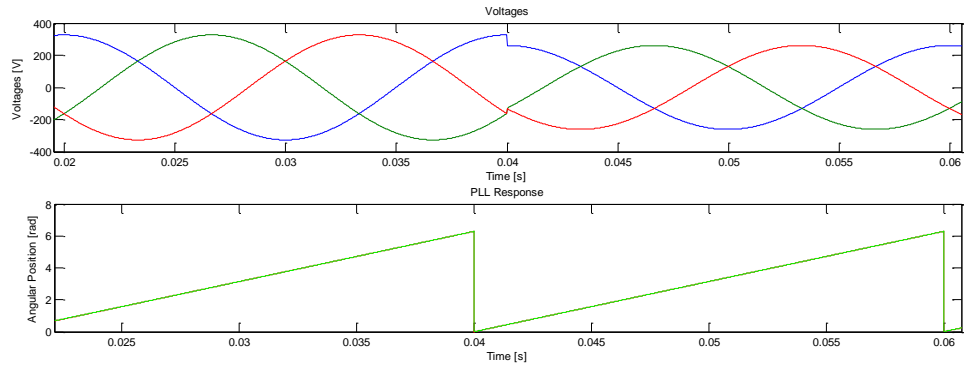


Figure 2-27 PLL Response to Change in Reference Voltage Amplitude

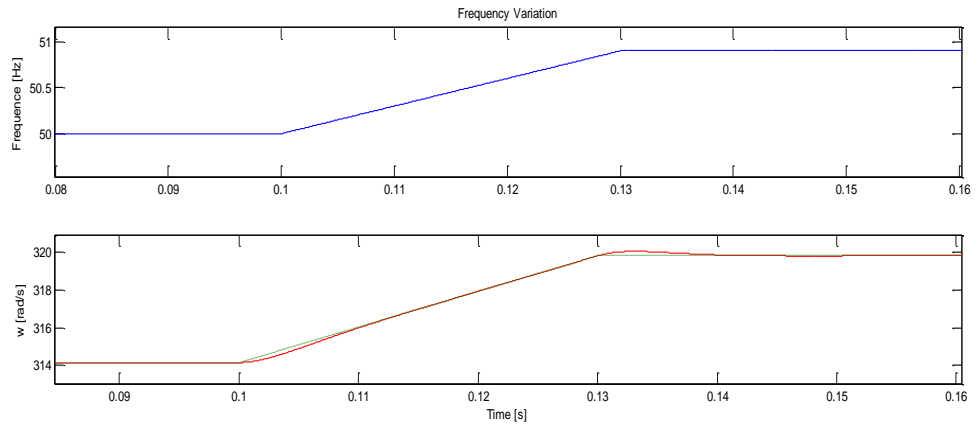


Figure 2-28 PLL response to changes in grid voltage frequency

3. Simulations of the Control Scheme using Continuous Model

3.1 Introduction

This chapter discusses the simulation of the control scheme discussed in Chapter 2 in Simulink using the average VSC model. The simulation results are presented for different scenarios, including symmetrical and unsymmetrical voltage sags.

The control scheme is tested first using the continuous model shown in Figure 2-2. The current i_d in the figure, which in our case is i_{conv} , is calculated by using the power balance and neglecting the power losses in the converter as,

$$i_{conv} = \frac{p_{AC}}{v_{dc}} = \frac{v_{ca}i_a + v_{cb}i_b + v_{cc}i_c}{v_{dc}}$$

The overall control scheme using the continuous model has been described in Figure 2-19.

3.2 Simulations

For the purpose of simulation, different scenarios are implemented, for example normal operation, change in DC source current and changes in ac grid parameters like phase, frequency and amplitude, and the response of the control scheme is simulated. The circuit diagram implemented in Simulink is given in the appendix.

3.2.1 Current Controller (Inner Loop) Simulation

To test the current controller, a reference value of i_d is selected, and the controller is tested. The following block diagram is implemented,

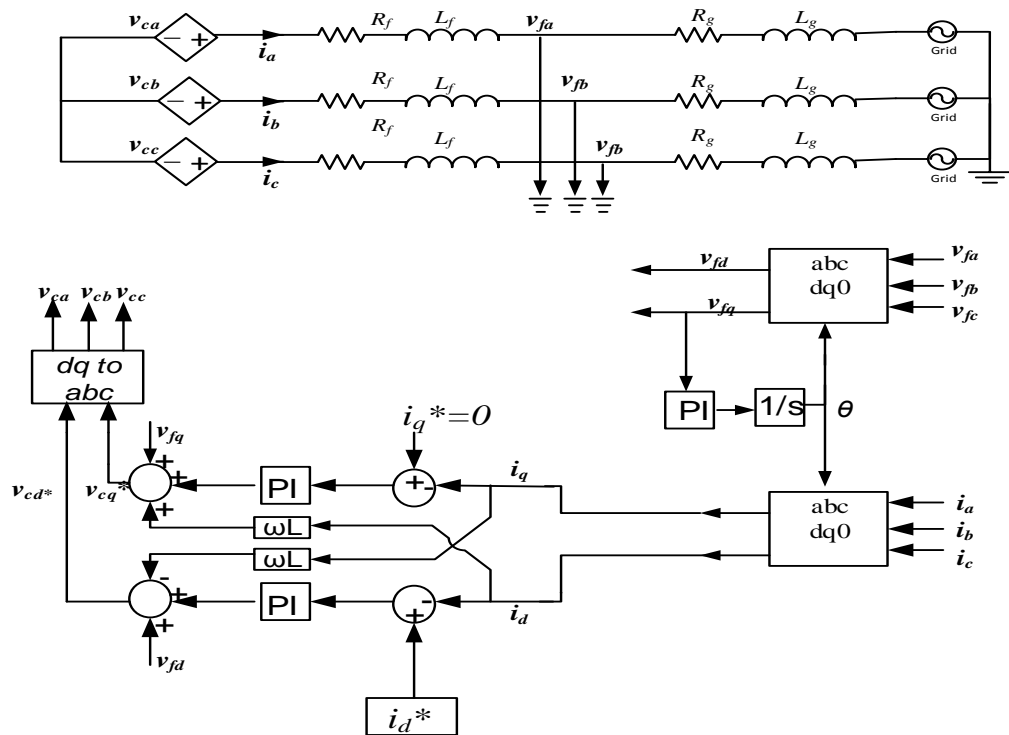


Figure 3-1 Current Control Model

The parameters used in the simulation are summarized in the following table.

Parameter	Value
R_f	.05 Ω
L_f	5.1 mH
R_g	.0073 Ω
L_g	.76mH
ω	100 π (rad/sec)
Vrms(Phase-to-Phase)	400 V
i^*	25A (0-0.025s) and 15A(0.025s onwards)

Table 3-1 Parameters used for current control simulations

The results of the inner loop simulation are given below:

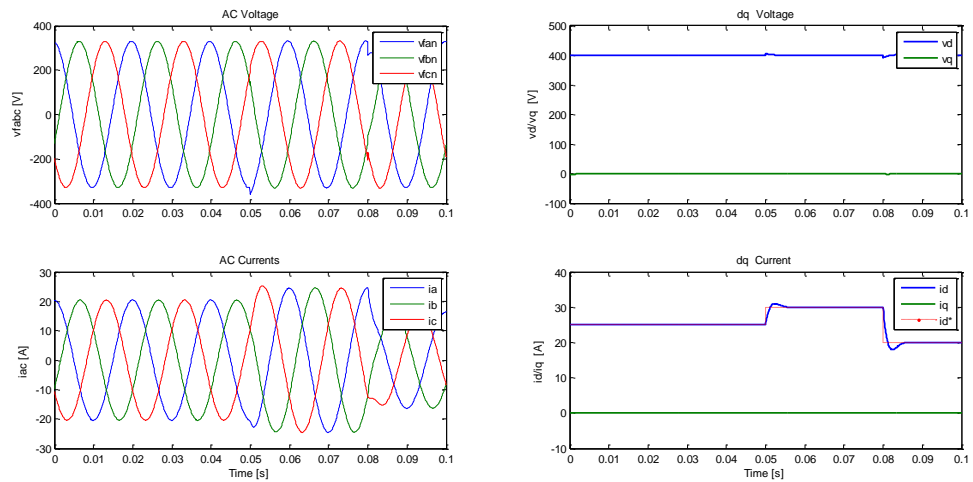


Figure 3-2 Current Control Test Results

3.2.2 Simulation of the Overall Control Scheme

In the following few sections, the overall control scheme shown in Figure 2-19 will be tested using the continuous model. The following parameters are used during the simulation.

Parameter	Value
R_f, L_f, R_g, L_g	Same as before
V_{dc}	1000V
ω	100π (rad/sec)
V_{rms} (Phase-to-Phase)	400 V

Table 3-2 Parameters used for cascaded control simulation

3.2.3 Changes in DC Source Current

First the DC source current is changed and the response of the system is recorded. Change in the current provided by the source, changes the current injected into the AC side, so that power balance is maintained.

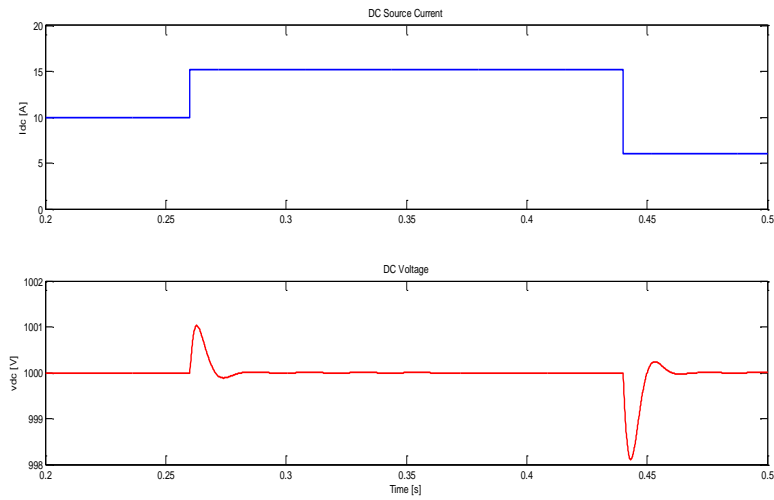


Figure 3-3 DC Source Current and DC Bus Voltage

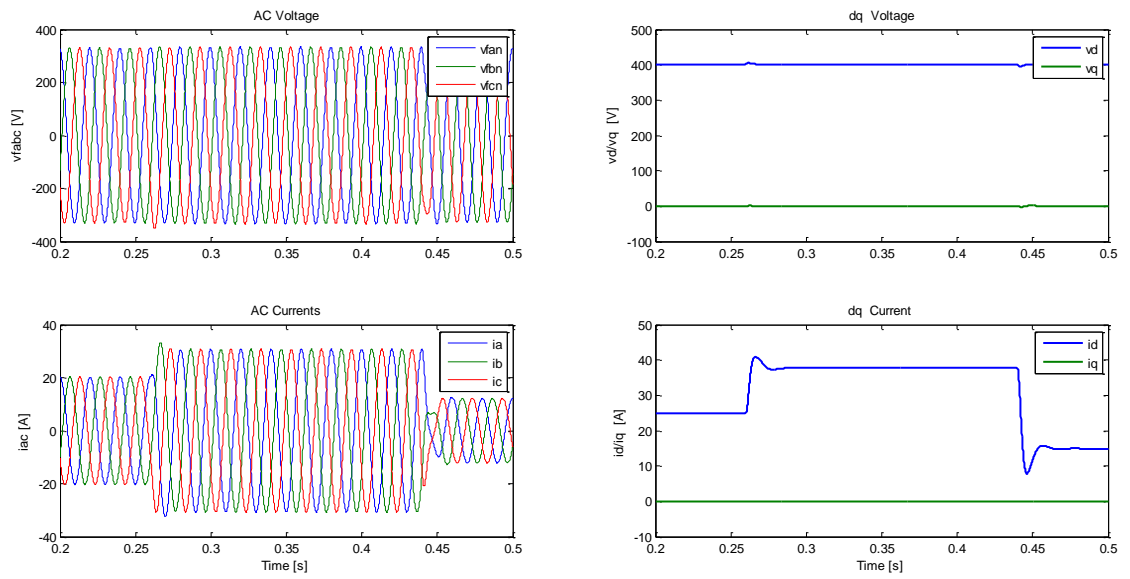


Figure 3-4 AC Currents and Voltages

To see how the system responds to the changes in grid characteristics, the system is simulated and the results are summarized in the following sections.

3.2.4 Response to Changes in Grid Voltage Amplitude

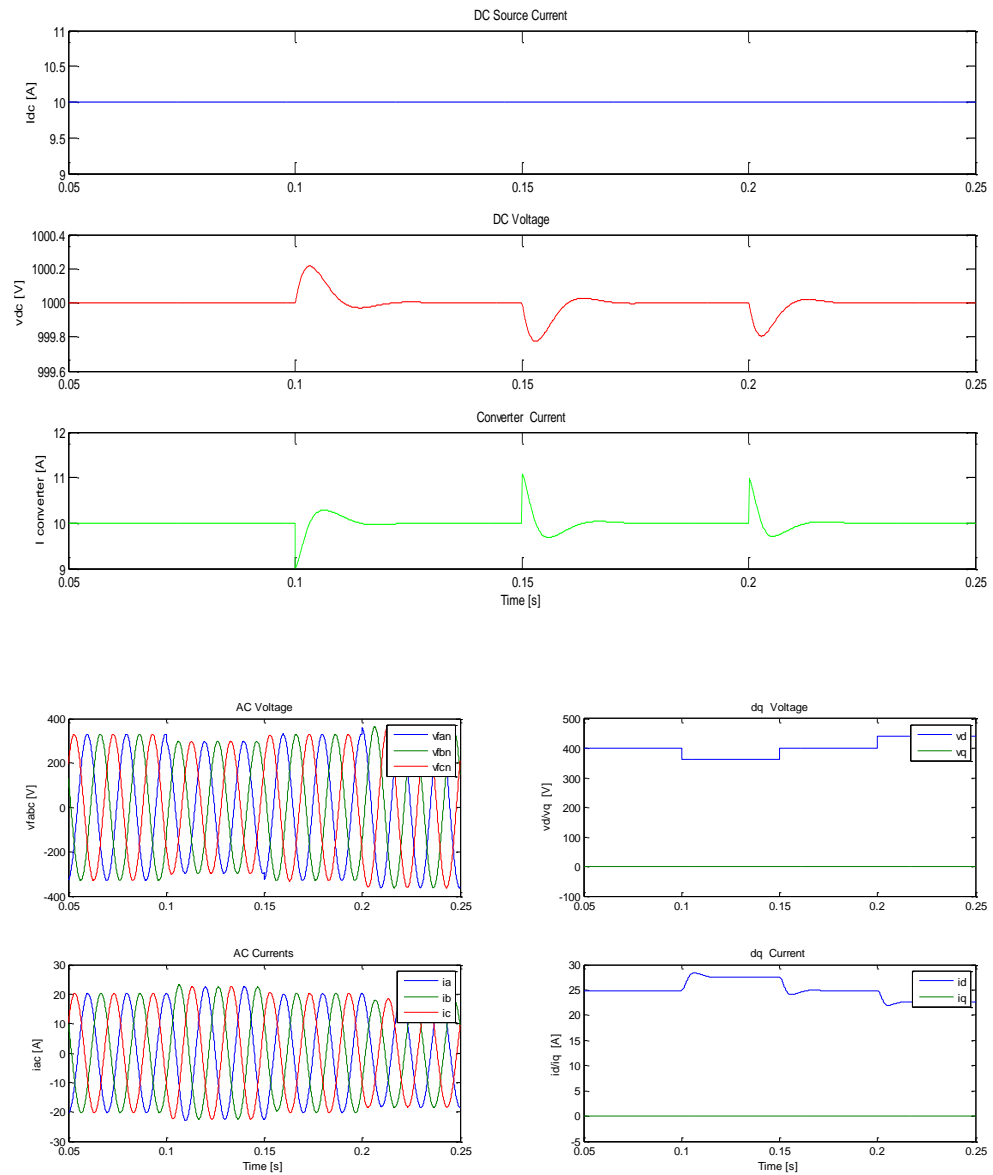


Figure 3-5 Response under Grid Voltage Changes ($\pm .1$ p.u.)

3.2.5 Response to Changes in Phase of Grid voltage

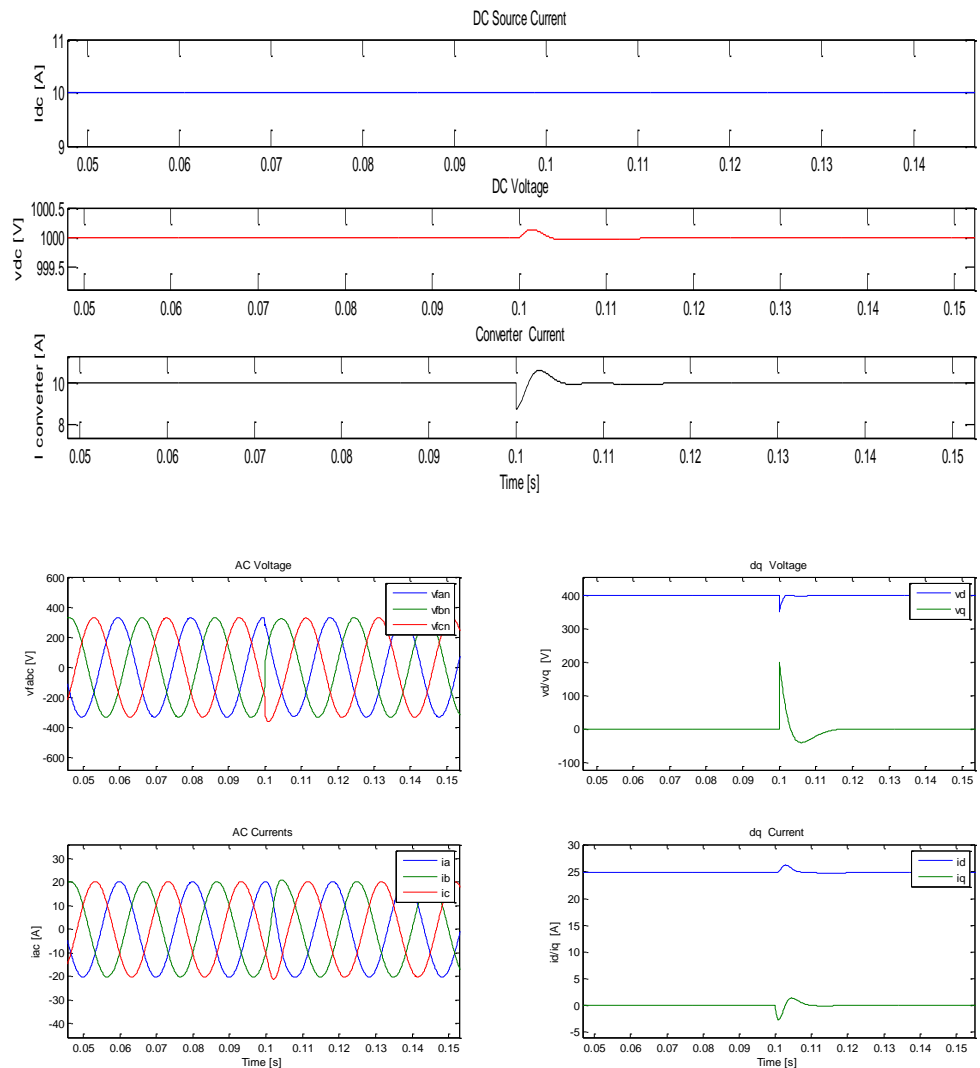


Figure 3-6 Response to Changes in Grid Voltage Phase

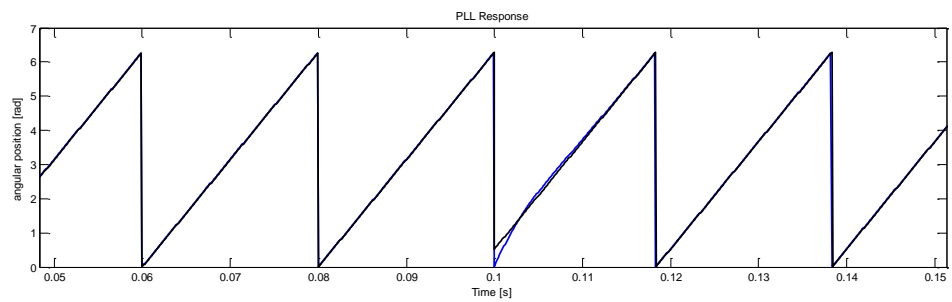


Figure 3-7 PLL Response

3.2.6 Response to Unsymmetrical Sags

When an unsymmetrical fault of type E (Two phase to ground) is applied at the grid, the AC currents are unsymmetrical and there is also a ripple in the power (P/Q) and dc voltage.

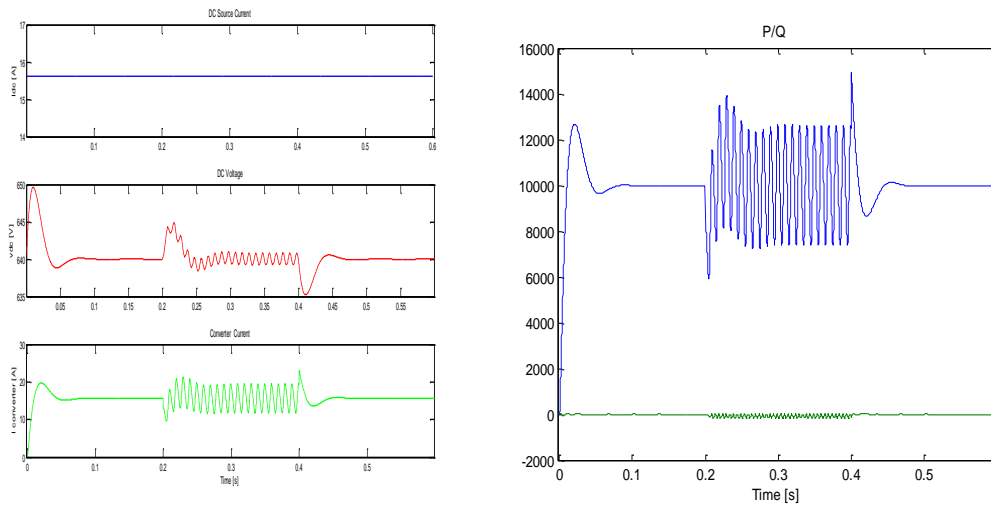


Figure 3-8 DC Voltage, P and Q Under Unsymmetrical Sags

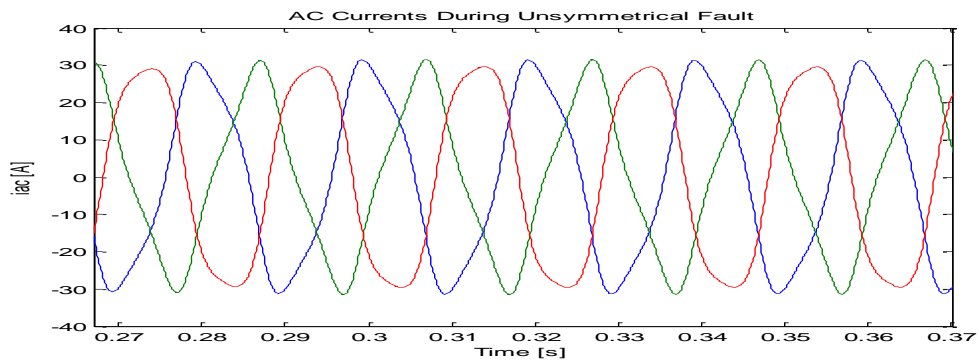


Figure 3-9 AC Currents Under Unsymmetrical Conditions

All above simulations are for a grid, with a grid inductance $1/10^{\text{th}}$ of the filter inductance.

Conclusions

The system works quiet adequately during all the scenarios that we have simulated. It rides properly through symmetrical faults in voltage amplitude and phase. During the

unsymmetrical faults, the system response is not quite good, as the AC currents are now not symmetric. As now the negative sequence components are not zero, the positive sequence components have oscillations at twice the fundamental frequency. For unsymmetrical faults, the scheme is to be modified.

4. Unsymmetrical Conditions

4.1 Introduction

As we concluded in chapter 3, the control scheme discussed above works well in case of normal operation and symmetrical voltage sags. In case of unsymmetrical voltage sags, we have unsymmetrical currents if we use the above scheme.

The most important thing to note here is the presence of negative sequence components in case of an unbalanced system. So, first we have to understand the concept of symmetrical components so that the control scheme can be modified to take these components into account. In this chapter, first an overview of the symmetrical components is presented and then different possible modifications are discussed.

4.2 Symmetrical Components

Any three phase voltage vector can be written in terms of its positive, negative and zero sequence components as, [6]

$$\mathbf{v}_{abc} = \begin{bmatrix} v_a \\ v_b \\ v_c \end{bmatrix} = \sum_{n=1}^{\infty} (\mathbf{v}_{abc}^{+n} + \mathbf{v}_{abc}^{-n} + \mathbf{v}_{abc}^{0n})$$

Where $+n, -n$ and $0n$ respectively represent the positive, negative and zero sequence components of the n th harmonic of the voltage vector \mathbf{v} .

At the fundamental frequency $n=1$, using phasors, the voltage components V^+, V^-, V^0 can be calculated using the Fortescue transformation.

$$[\mathbf{F}] = \frac{1}{3} \begin{bmatrix} 1 & 1 & 1 \\ 1 & a & a^2 \\ 1 & a^2 & a \end{bmatrix} ; \quad a = e^{j\frac{2\pi}{3}}$$

$$[\mathbf{F}]^{-1} = 3[\mathbf{F}]^* = \begin{bmatrix} 1 & 1 & 1 \\ 1 & a^2 & a \\ 1 & a & a^2 \end{bmatrix}$$

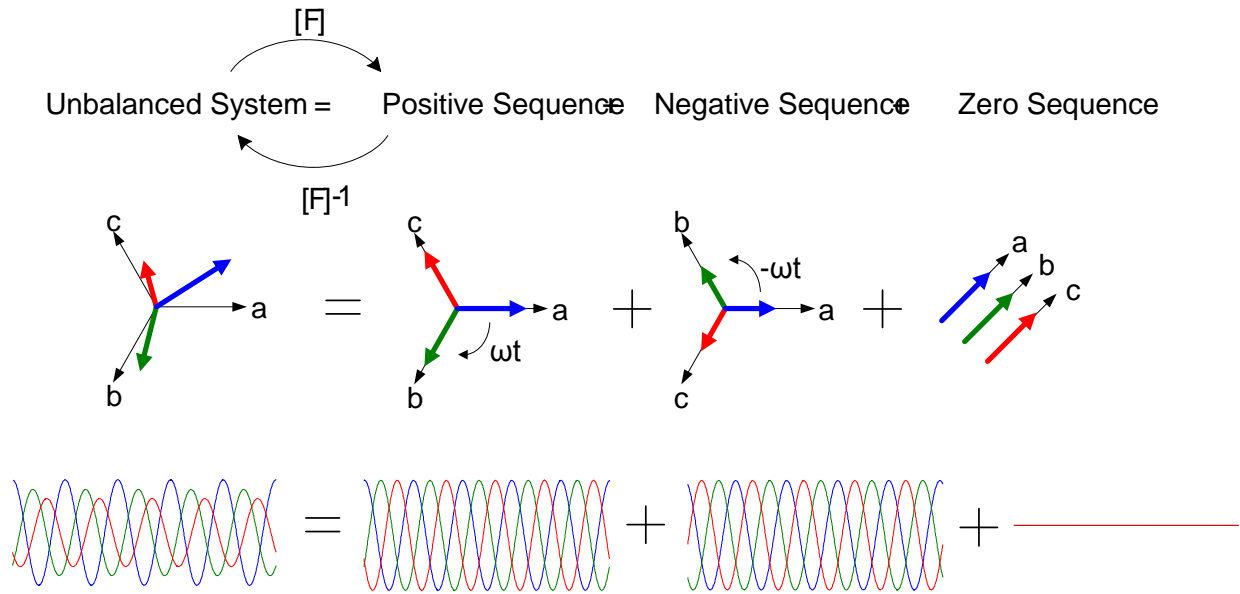


Figure 4-1 Symmetrical Components of Three Phase Voltage

Distributed systems are usually linked to the three-phase networks by using a three-wire system and hence they do not inject zero sequence current into the grid.

The advantage of symmetrical components is that this process converts the three phase unbalanced system to the sum of three balanced systems. For facilitation in the design of a control scheme, the components are converted using park transformation to DC quantities, as discussed in chapter 2.

4.2.1 Transformation of Symmetrical Components into dq Reference Frame

As we have seen in the previous section, the positive sequence components rotate with a frequency ωt and the negative sequence components rotate with $-\omega t$.

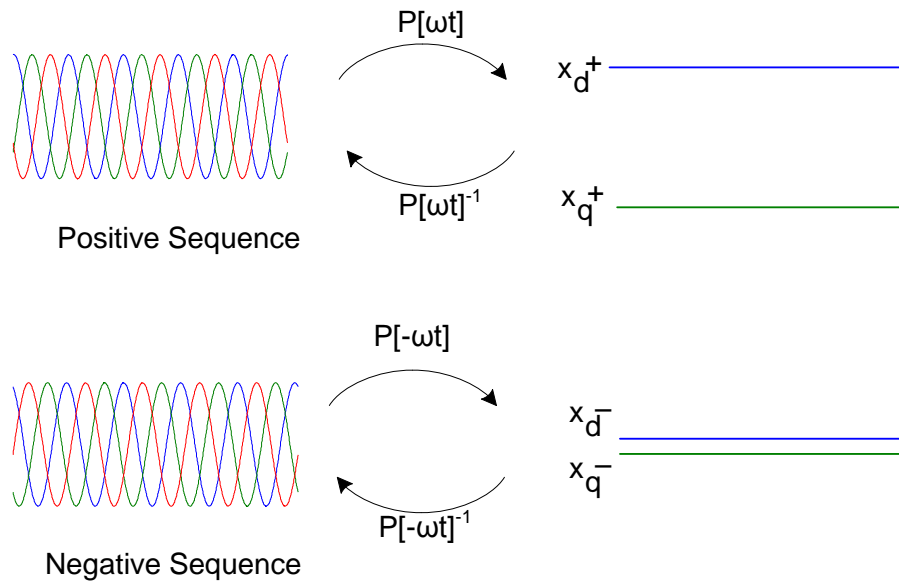


Figure 4-2 dq Transformation of Positive and Negative Sequence

4.3 Control Strategies

In this section first the current control and then DC bus voltage control strategies will be discussed.

4.3.1 Current Control

For a system containing both positive and negative sequence components, the most intuitive way to control a current vector is by using a controller based on the two synchronous reference frames, rotating with the fundamental grid frequency (ωt) in positive and negative directions respectively. A system based on the double synchronous reference frame DSRF [6].

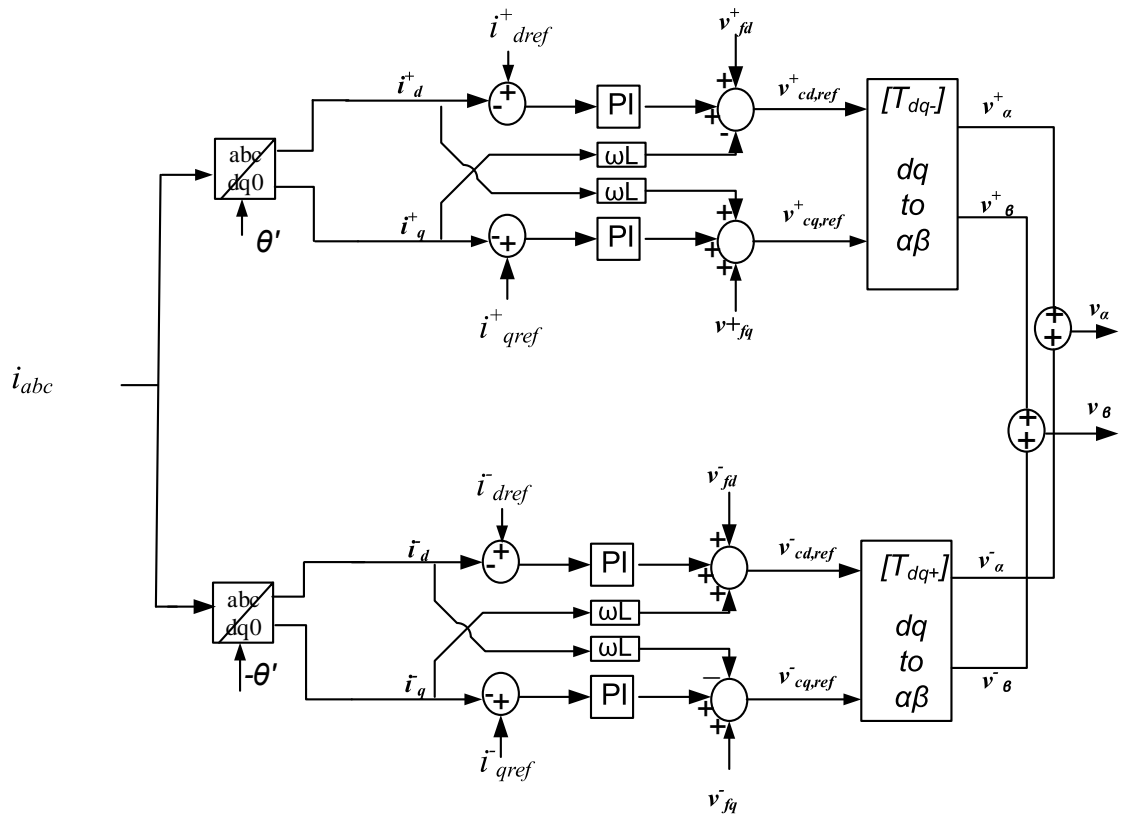


Figure 4-3 Double SRF Current Control

Where θ' is the phase angle detected by the PLL. We can see that the control scheme used is the same as the one use in case of the balanced case. The only difference is that the cross coupling terms now have opposite signs for the negative sequence due to the opposite rotation of the negative sequence.

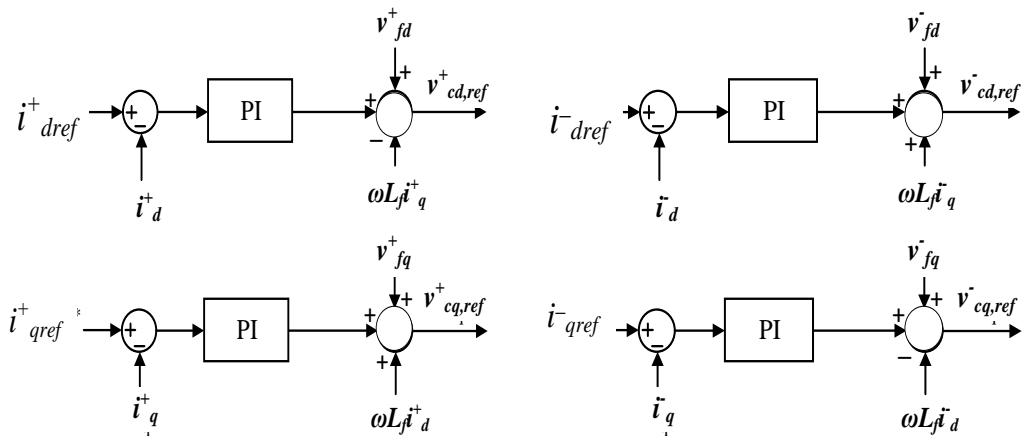


Figure 4-4 Positive and Negative Sequence Controllers

4.3.2 Cross Coupling and Introduction of Notch Filters

Consider a current vector composed of positive and negative sequence components as given below

$$\mathbf{i} = I^+ \begin{bmatrix} \sin(\omega t + \delta^+) \\ \sin(\omega t + \delta^+ - \frac{2\pi}{3}) \\ \sin(\omega t + \delta^+ + \frac{2\pi}{3}) \end{bmatrix} + I^- \begin{bmatrix} \sin(\omega t + \delta^-) \\ \sin(\omega t + \delta^- + \frac{2\pi}{3}) \\ \sin(\omega t + \delta^- - \frac{2\pi}{3}) \end{bmatrix}$$

The positive and negative synchronous reference frame projections can be written as [6]

$$\begin{aligned} \mathbf{i}_{dq}^+ &= \begin{bmatrix} i_d^+ \\ i_q^+ \end{bmatrix} = \begin{bmatrix} \bar{i}_d^+ \\ \bar{i}_q^+ \end{bmatrix} + \begin{bmatrix} \tilde{i}_d^+ \\ \tilde{i}_q^+ \end{bmatrix} = I^+ \begin{bmatrix} \cos(\delta^+) \\ \sin(\delta^+) \end{bmatrix} \\ &+ I^- \cos(\delta^-) \begin{bmatrix} \cos(2\omega t) \\ -\sin(2\omega t) \end{bmatrix} + I^- \sin(\delta^-) \begin{bmatrix} \sin(2\omega t) \\ \cos(2\omega t) \end{bmatrix} \end{aligned}$$

$$\begin{aligned} \mathbf{i}_{dq}^- &= \begin{bmatrix} i_d^- \\ i_q^- \end{bmatrix} = \begin{bmatrix} \bar{i}_d^- \\ \bar{i}_q^- \end{bmatrix} + \begin{bmatrix} \tilde{i}_d^- \\ \tilde{i}_q^- \end{bmatrix} = I^- \begin{bmatrix} \cos(\delta^-) \\ \sin(\delta^-) \end{bmatrix} \\ &+ I^+ \cos(\delta^+) \begin{bmatrix} \cos(2\omega t) \\ \sin(2\omega t) \end{bmatrix} + I^+ \sin(\delta^+) \begin{bmatrix} -\sin(2\omega t) \\ \cos(2\omega t) \end{bmatrix} \end{aligned}$$

The above equations show that there is a cross coupling present between the dq axis signals of both synchronous reference frames. This effect can be seen as a 2ω oscillation added to the DC signals on the dq axes.

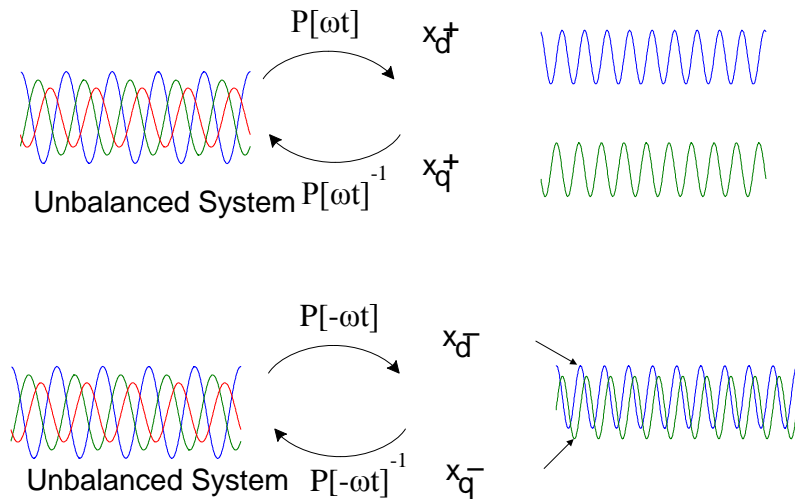


Figure 4-5 Oscillations in dq components of unbalanced quantities

Oscillations at 2ω in the measured signals can give rise to steady state errors when the PIs track the reference quantities. These oscillations have to be cancelled out so that the injected currents can be controlled fully under unbalanced conditions.

The most intuitive way is to use a notch filter tuned at 2ω to cancel out these oscillations.

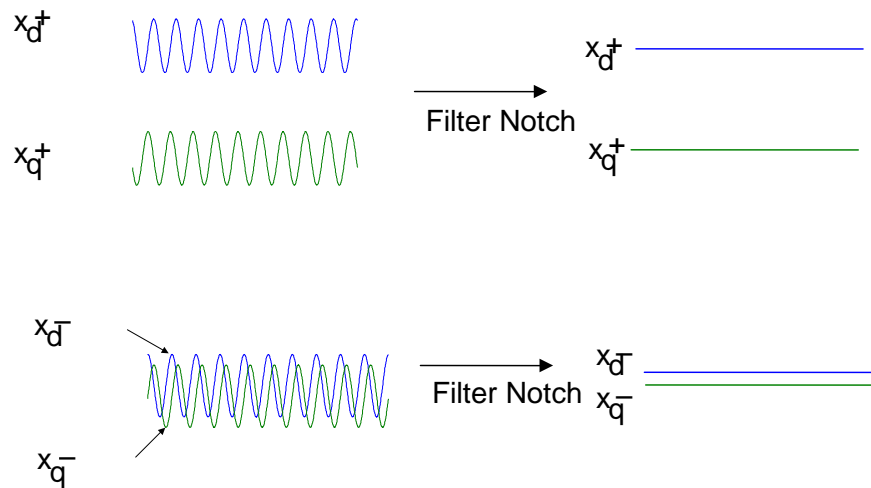


Figure 4-6 Removing the oscillations using notch filters

The notch filters are introduced for the dq quantities as shown in the figure below.

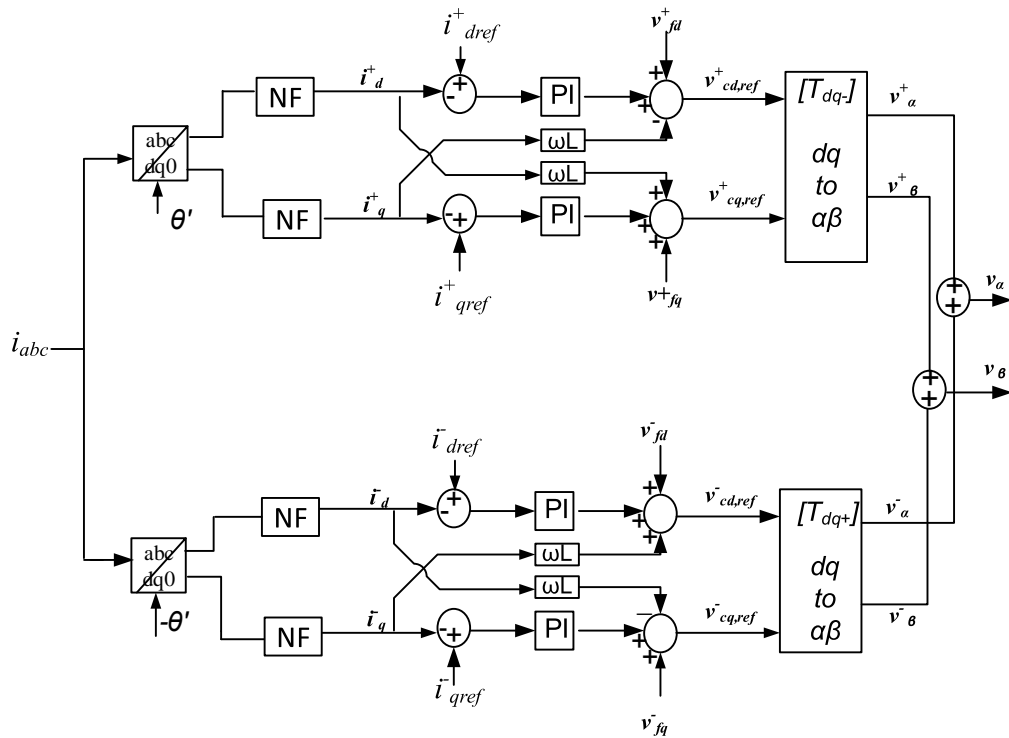


Figure 4-7 DSRF Current control with notch filters

4.3.3 Outer Loop Strategies for PQ Control

As we have seen in case of the balanced case, the output of the PI for the DC voltage control gives the current reference i_{dref} for the current controller set point. In case of unbalanced voltages, often there are different conditions that have to be met depending on the utility. For example, we may be needed to control active and reactive power, or we may be required to inject only symmetrical ac currents. For working in terms of power, another approach has to be used to calculate the reference currents. In literature there are many approaches for the outer loop. The main steps involved are calculating a reference power and then reference. Synchronous Frame VOC: PQ Open-Loop Control technique discussed in [6] is detailed in this section. Note that these techniques can also be used in the balanced voltages case as discussed earlier.

Synchronous Frame VOC: PQ Open-Loop Control

The DC voltage control modifies the active power reference. The d and q components of the reference current are calculated from these power signals, based on the type on control we want to achieve.

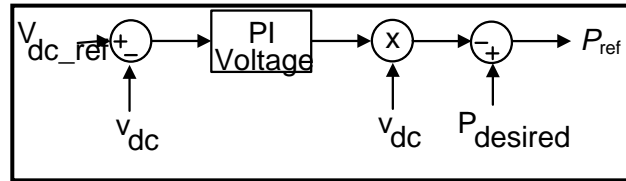


Figure 4-8 Reference power for the current reference calculation

In case of balance case, as discussed in section 2.8 the reference currents are calculated using the following matrix:

$$\begin{bmatrix} i_{d_ref} \\ i_{q_ref} \end{bmatrix} = \frac{1}{v_{fd}^2 + v_{fq}^2} \begin{bmatrix} v_{fd} & -v_{fq} \\ v_{fq} & v_{fd} \end{bmatrix} \begin{bmatrix} P_{ref} \\ Q_{ref} \end{bmatrix}$$

Where v_f is the measured grid voltage at the PCC. If Q_{ref} is taken as 0 and v_{fq} is taken as zero (voltage is aligned with the d axis), the reference $i_{d_ref} = \frac{P_{ref}}{v_{fd}}$ and $i_{q_ref} = 0$. In case of unbalanced voltages, i.e. presence of negative sequence components, the translation from the reference powers to currents depends on the type of control we want to achieve. This will be explained in the next sections.

4.3.4 Control Scheme Block Diagram

The block diagram of the complete control scheme is given below.

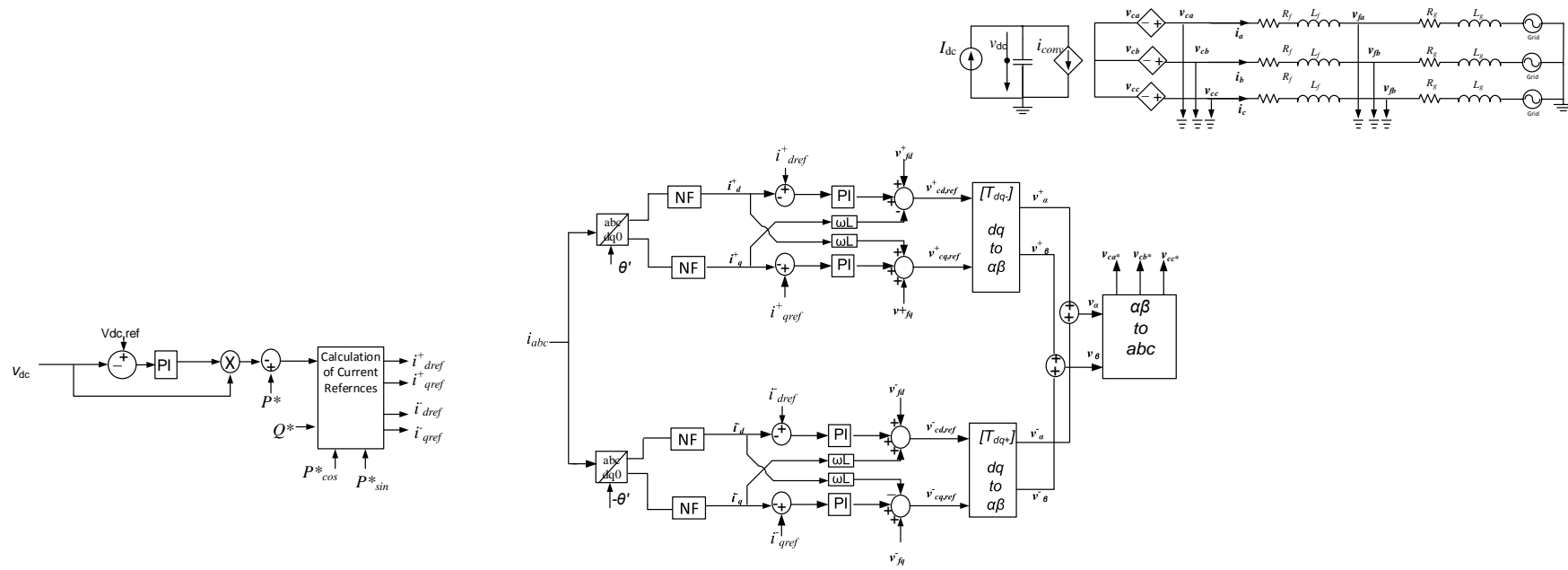


Figure 4-9 Control Scheme For PQ control in Double Synchronous Reference Frame

4.4 Current Reference Calculation

As we have seen earlier, power oscillating terms appear in case of unbalanced conditions due to the interaction between voltages and currents with different sequences. This gives rise to the requirement of the design of specific strategies for calculation of the injected currents by the power converter into the grid for the control of instantaneous active and reactive power. In this section, some of the techniques mentioned in [6] are briefly discussed.

4.4.1 Instantaneous Power Expressions

The apparent power is given by

$$\underline{s} = \underline{v} \underline{i}^*$$

Where

$$\underline{v} = v_d + jv_q \quad ; \quad \underline{i} = i_d + ji_q$$

During unbalance conditions, the voltage and current in the synchronous reference frame ($\Psi = \omega t + \theta_0$) are expressed as:

$$\underline{v} = e^{j(\omega t + \theta_0)} (v_d^+ + jv_q^+) + e^{-j(\omega t + \theta_0)} (v_d^- + jv_q^-)$$

$$\underline{i} = e^{j(\omega t + \theta_0)} (i_d^+ + ji_q^+) + e^{-j(\omega t + \theta_0)} (i_d^- + ji_q^-)$$

From the above equations, apparent power can be given as:

$$\begin{aligned} \underline{s} = & v_d^+ i_d^+ + v_q^+ i_q^+ + v_d^- i_d^- + v_q^- i_q^- + e^{j(2\omega t + 2\theta_0)} (v_d^+ i_d^- + v_q^+ i_q^-) + e^{-j(2\omega t + 2\theta_0)} (v_d^- i_d^+ + v_q^- i_q^+) \\ & + j \left[-v_d^+ i_q^+ + v_q^+ i_d^+ - v_d^- i_q^- + v_q^- i_d^- + e^{j(2\omega t + 2\theta_0)} (-v_d^+ i_q^- + v_q^+ i_d^-) + e^{-j(2\omega t + 2\theta_0)} (-v_d^- i_q^+ + v_q^- i_d^+) \right] \end{aligned}$$

Applying Euler's identity:

$$e^{\pm j\alpha} = \cos(\alpha) \pm j\sin(\alpha)$$

We get the apparent power in terms of its active and reactive components as:

$$\underline{s} = p + jq$$

$$= \begin{bmatrix} v_d^+ i_d^+ + v_q^+ i_q^+ + v_d^- i_d^- + v_q^- i_q^- \\ + \cos(2\omega t + 2\theta_0)(v_d^+ i_d^- + v_q^+ i_q^- + v_d^- i_d^+ + v_q^- i_q^+) \\ + \sin(2\omega t + 2\theta_0)(v_d^+ i_q^- - v_q^+ i_d^- - v_d^- i_q^+ + v_q^- i_d^+) \end{bmatrix} + j \begin{bmatrix} -v_d^+ i_q^+ + v_q^+ i_d^+ - v_d^- i_q^- + v_q^- i_d^- \\ + \cos(2\omega t + 2\theta_0)(-v_d^+ i_q^- + v_q^+ i_d^- - v_d^- i_q^+ + v_q^- i_d^+) \\ + \sin(2\omega t + 2\theta_0)(v_d^+ i_d^- + v_q^+ i_q^- - v_d^- i_d^+ - v_q^- i_q^+) \end{bmatrix}$$

Where:

$$p = P + P_{\cos} \cos(2\omega t + 2\theta_0) + P_{\sin} \sin(2\omega t + 2\theta_0)$$

$$q = Q + Q_{\cos} \cos(2\omega t + 2\theta_0) + Q_{\sin} \sin(2\omega t + 2\theta_0)$$

And the expressions for P , P_{\cos} , P_{\sin} , Q , Q_{\cos} , Q_{\sin} can be written in matrix form as:

$$\begin{bmatrix} P \\ P_{\cos} \\ P_{\sin} \\ Q \\ Q_{\cos} \\ Q_{\sin} \end{bmatrix} = \begin{bmatrix} v_d^+ & v_q^+ & v_d^- & v_q^- \\ v_d^- & v_q^- & v_d^+ & v_q^+ \\ v_q^- & -v_d^- & -v_q^+ & v_d^+ \\ v_q^+ & -v_d^+ & v_q^- & -v_d^- \\ v_q^- & -v_d^- & v_q^+ & -v_d^+ \\ -v_d^- & -v_q^- & v_d^+ & v_q^+ \end{bmatrix} \begin{bmatrix} i_d^+ \\ i_q^+ \\ i_d^- \\ i_q^- \end{bmatrix}$$

One of the main objectives in control of active rectifiers is to provide a constant DC output voltage. For any given grid voltage conditions, $[v_d^+, v_q^+, v_d^-, v_q^-]$, only four of the six power magnitudes can be controlled, as there are four degrees of freedom in calculation of the injected currents $[i_d^+, i_q^+, i_d^-, i_q^-]$. Many of the studies have collected the powers that have a direct influence on the DC bus voltage to be P , P_{\cos} , P_{\sin} . From the above matrix, the equations for the reference currents can be calculated by inverting the 4x4 matrix obtained after removing Q_{\cos} , and Q_{\sin} :

$$\begin{bmatrix} i_d^{+*} \\ i_q^{+*} \\ i_d^{-*} \\ i_q^{-*} \end{bmatrix} = \begin{bmatrix} v_d^+ & v_q^+ & v_d^- & v_q^- \\ v_d^- & v_q^- & v_d^+ & v_q^+ \\ v_q^- & -v_d^- & -v_q^+ & v_d^+ \\ v_q^+ & -v_d^+ & v_q^- & -v_d^- \end{bmatrix}^{-1} \begin{bmatrix} P^* \\ P_{\cos}^* \\ P_{\sin}^* \\ Q^* \end{bmatrix}$$

From the above matrix, the reference values for the currents can be calculated based on the type of results we want to achieve.

4.5 PLL Modifications

The synchronous reference frame PLL (SRF-PLL) has satisfactory performance during balanced conditions. However, in case of unbalanced conditions, its performance is influenced by the distortions. This is depicted in the figure below:

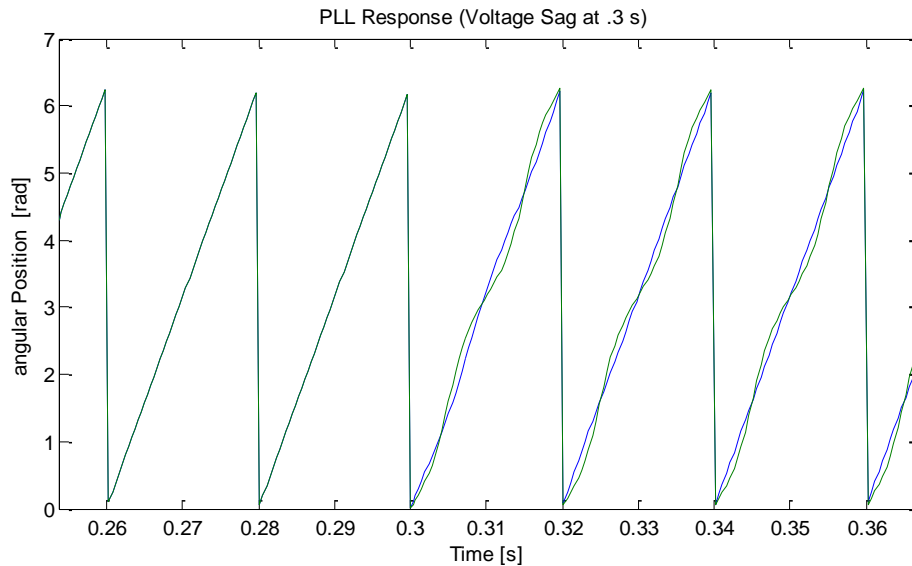


Figure 4-10 PLL behavior before and during sag

Some of the improvements for this PLL to tackle unbalanced conditions are presented in [9]. One of the techniques uses the Second Order Generalized Integrator (SOGI) to generate signals in quadrature. Two SOGI quadrature signal generators generate the two signals for the α and β components of the input voltage vector [6]. From the four signals thus generated, i.e. $v'_\alpha, qv'_\alpha, v'_\beta, qv'_\beta$, a positive and negative sequence calculation block computes the sequence components.

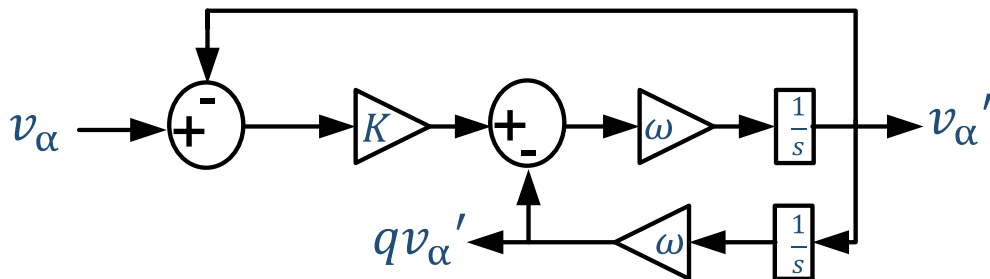


Figure 4-11 SOGI Quadrature Signals Generator

An SRF-PLL is then used to translate the positive sequence voltage to dq synchronous reference and estimate the angle.

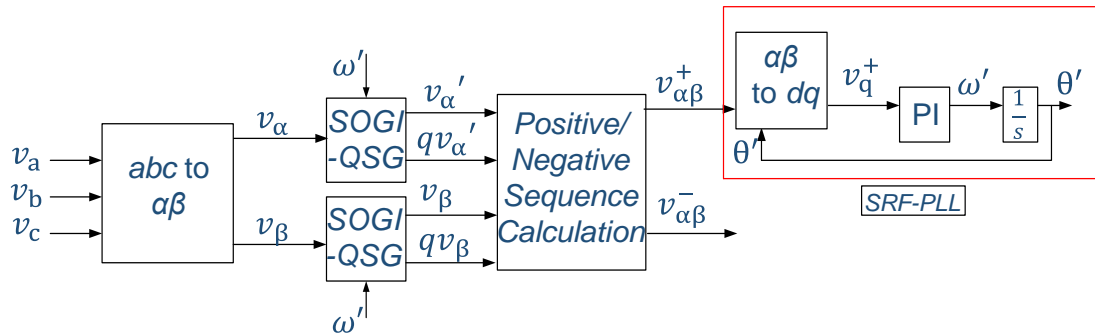


Figure 4-12 DSOGI PLL Block Diagram

4.6 Simulation Results

For the simulation purposes, a voltage sag of type E and type B are modeled at the grid. The negative current components are forced to zero, so is the q component of positive sequence current. The idea is to force a three phase symmetric current on the AC bus.

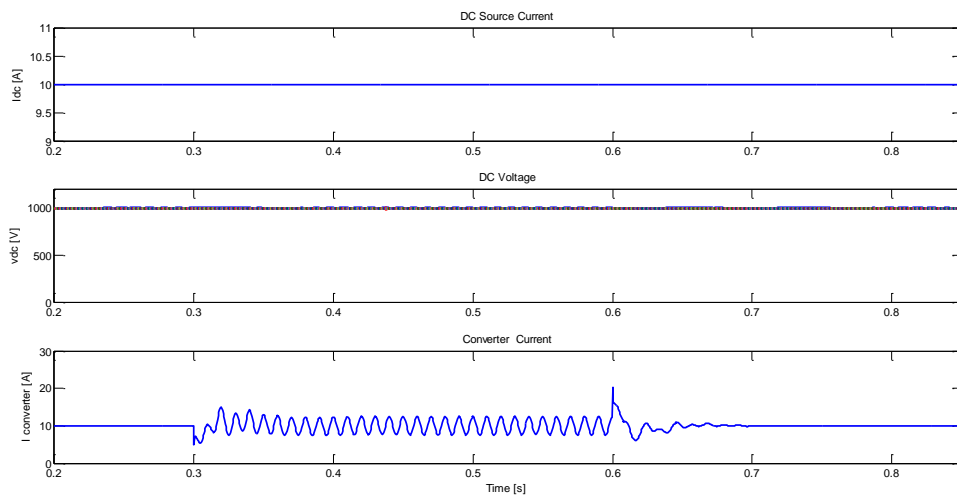


Figure 4-13 System behavior during type E Voltage Sags (DC Voltage and Current)

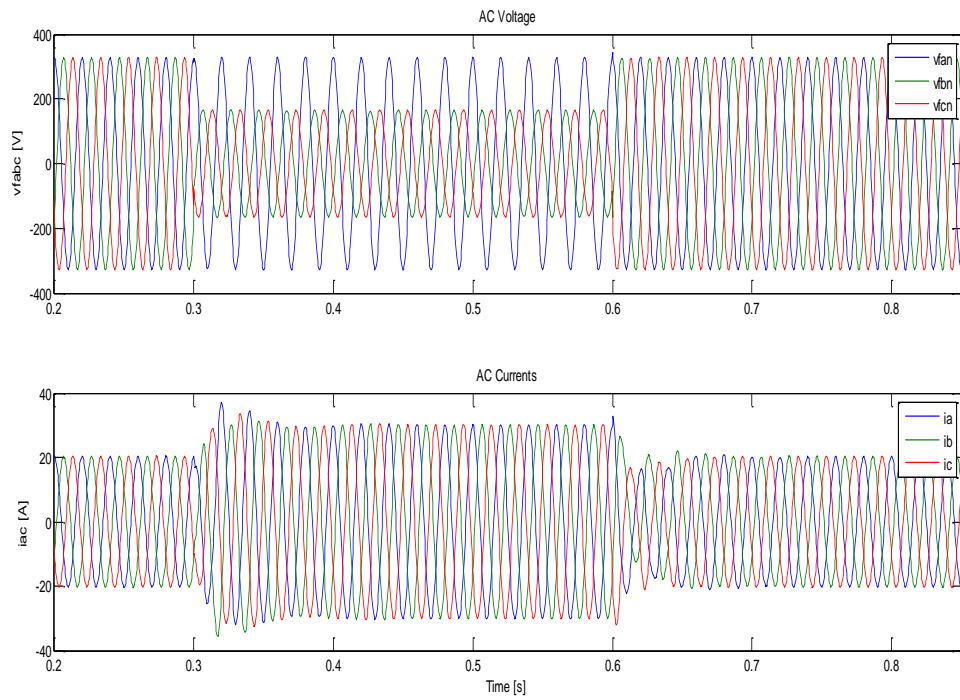


Figure 4-14 System behavior during type E Voltage Sags (AC Voltage and Current)

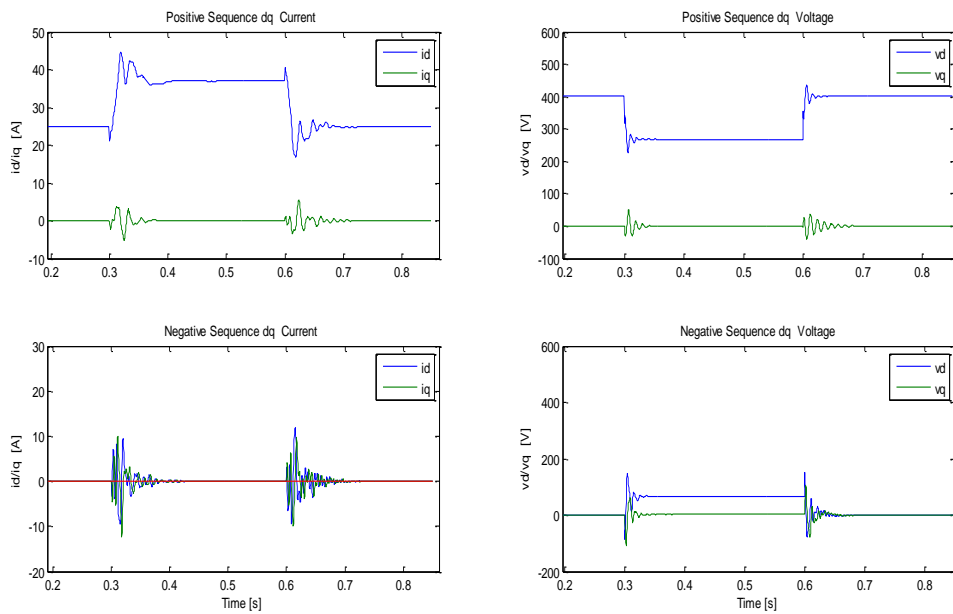


Figure 4-15 System behavior during type E Voltage Sags (dq components)

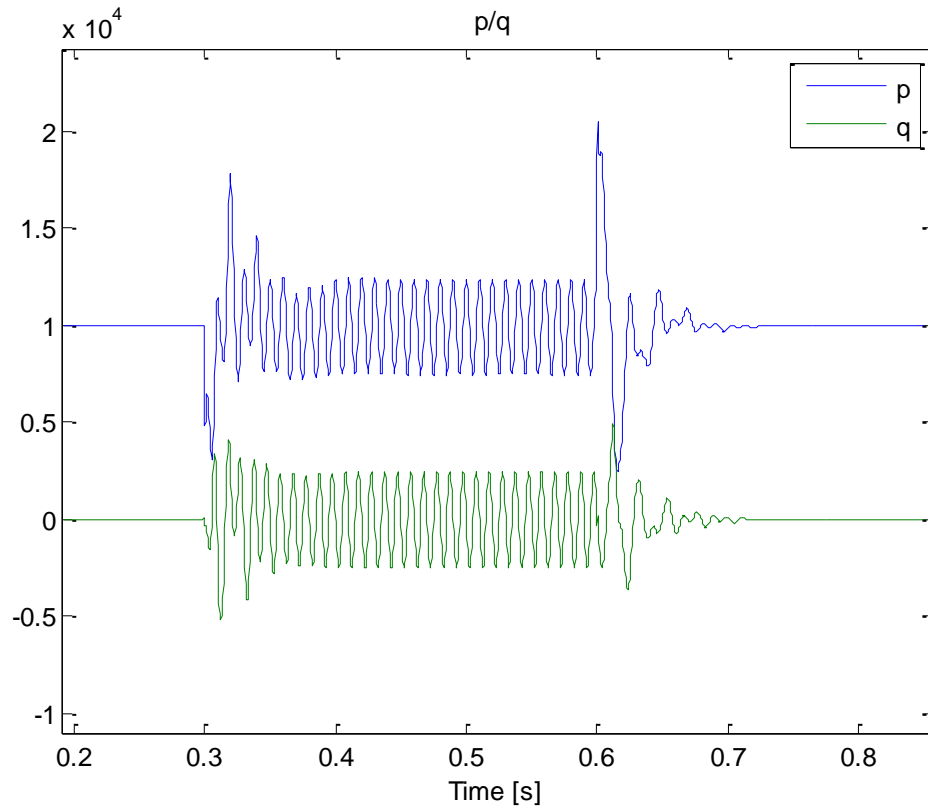


Figure 4-16 System behavior during type E Voltage Sags (P and Q)

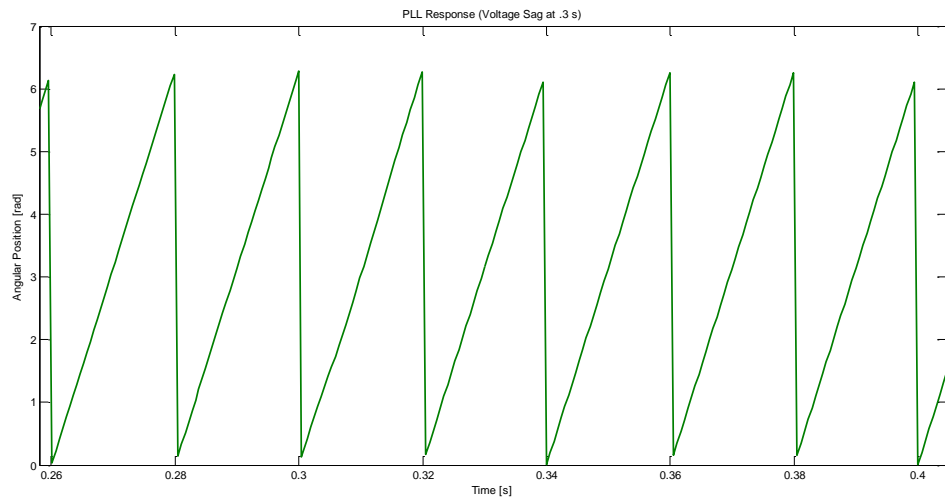


Figure 4-17 PLL Response

Type B: Single Phase to Ground Faults

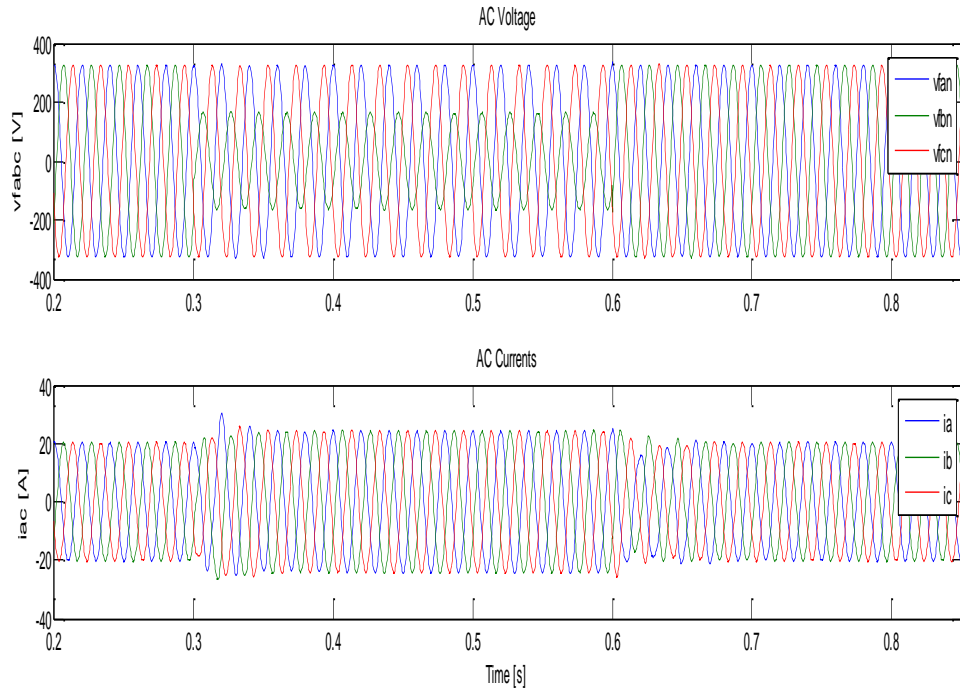


Figure 4-18 System behavior during type B Voltage Sags (AC voltages and currents)

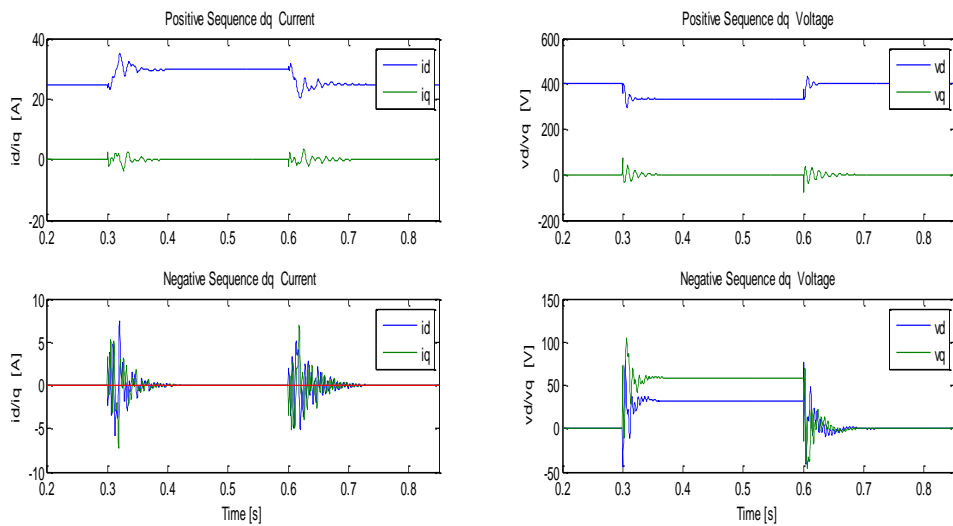


Figure 4-19 System behavior during type B Voltage Sags (qd Components)

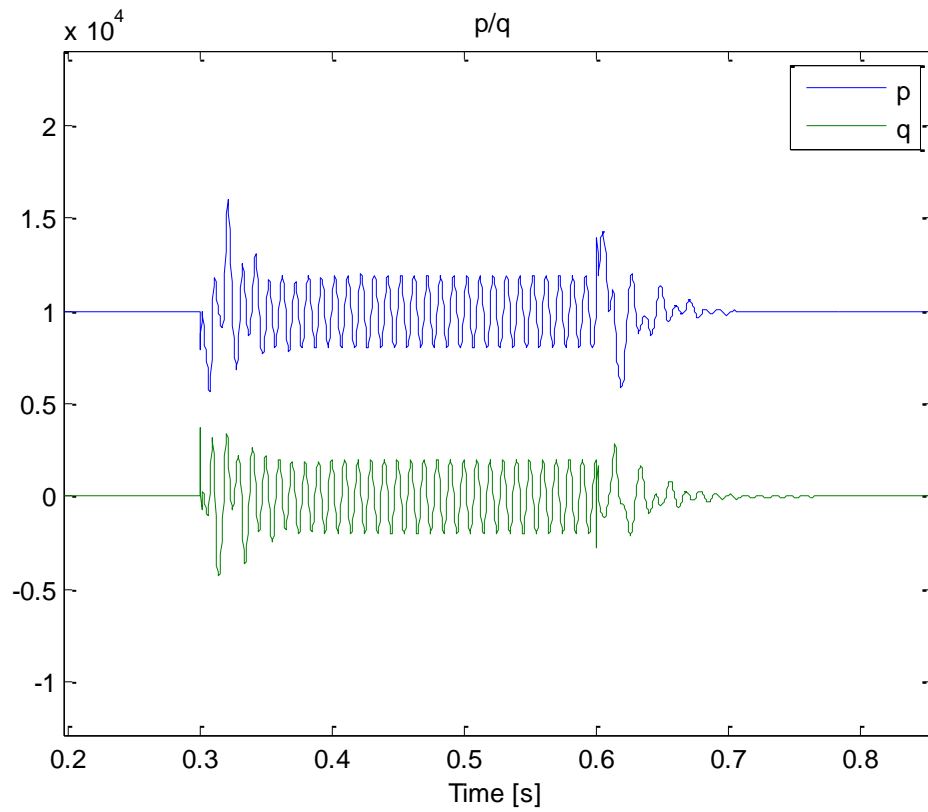


Figure 4-20 System behavior during type B Voltage Sags (P and Q)

Type A: Three Phase to Ground Fault

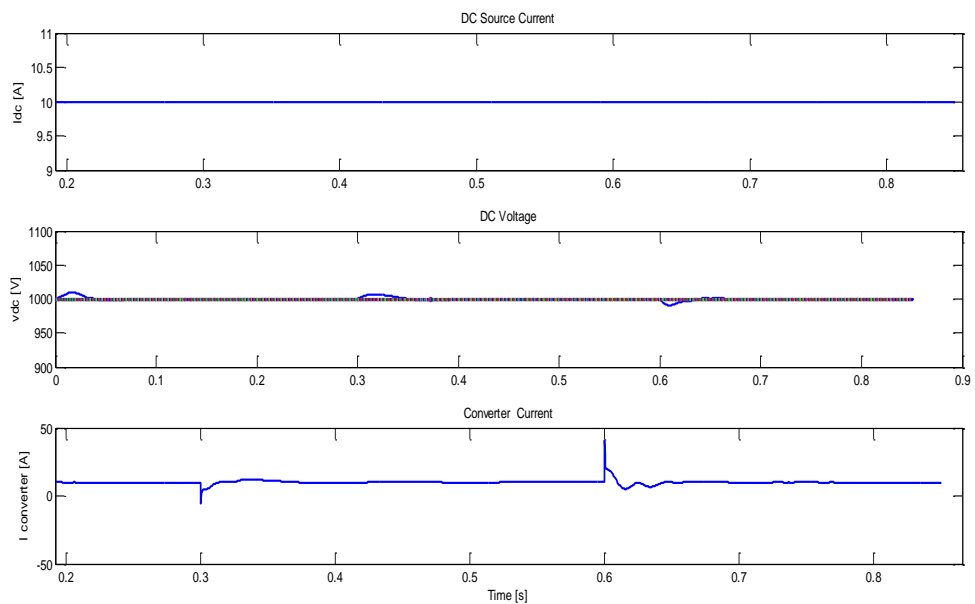


Figure 4-21 System behavior during type A Voltage Sags (DC Side Voltage and Currents)

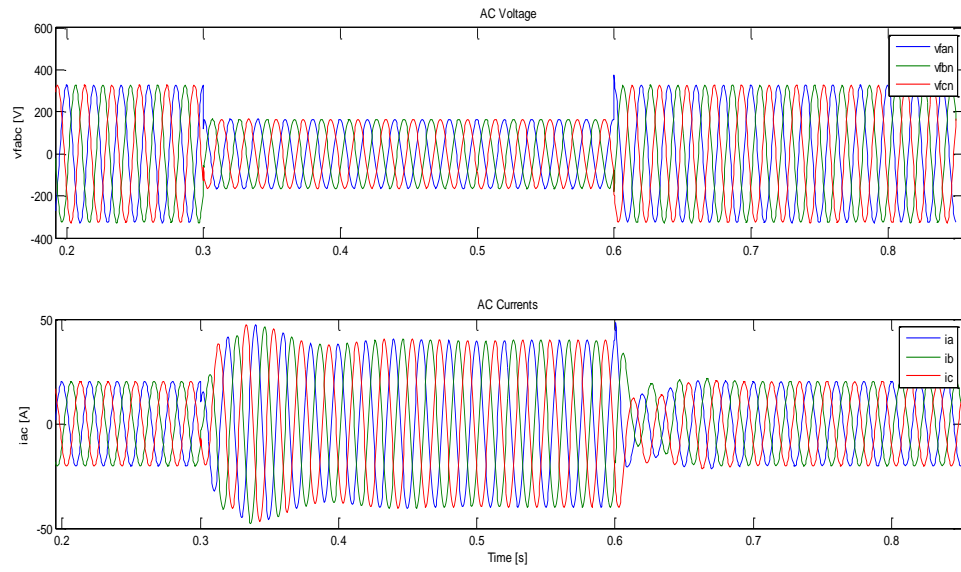


Figure 4-22 System behavior during type A Voltage Sags (AC voltages and Currents)

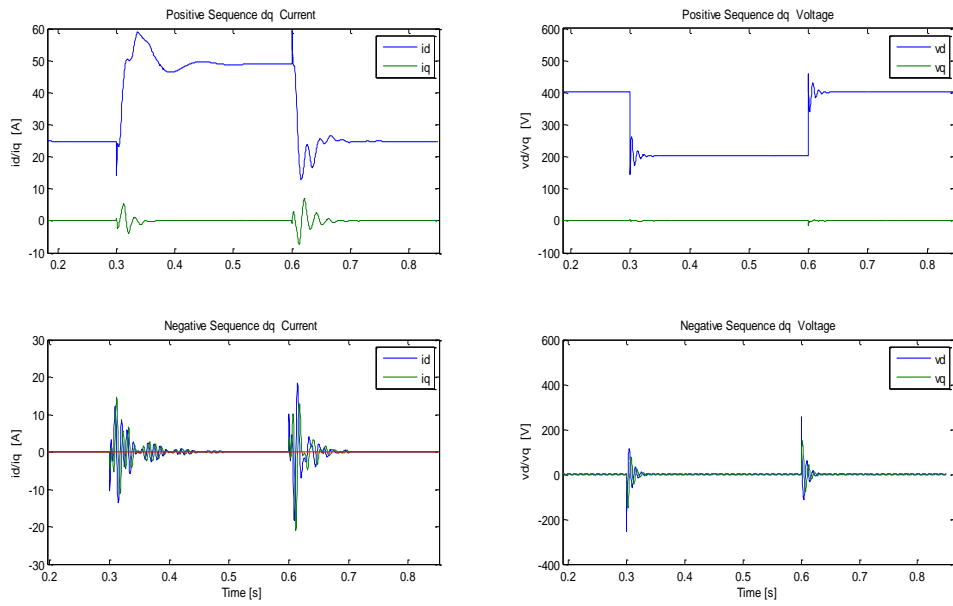


Figure 4-23 System behavior during type A Voltage Sags (qd components)

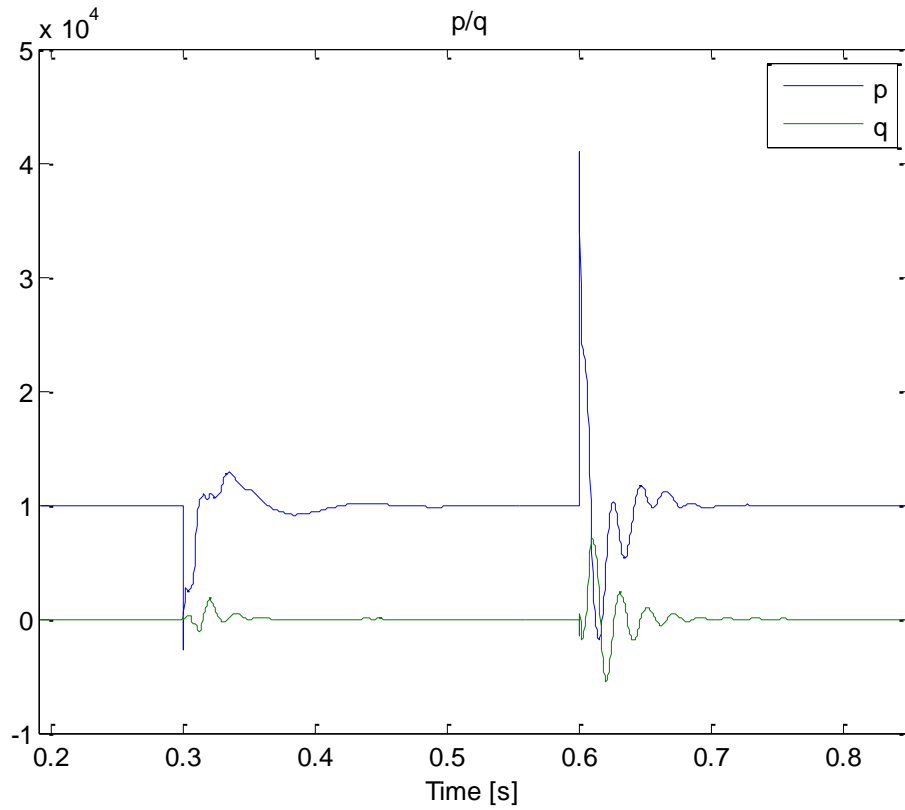


Figure 4-24 System behavior during type A Voltage Sags (P and Q)

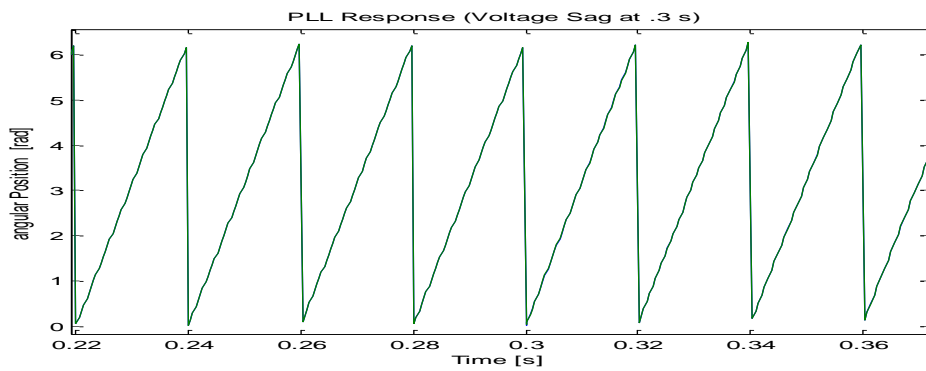


Figure 4-25 PLL behavior during symmetrical sag (type A)

Conclusions

The modifications in the control scheme for the unbalanced grid voltage conditions mainly depend on the type of the desired control we want to achieve. We have simulated the results for the case where we want to inject symmetrical AC currents during the voltage sag.

There are many possible improvements in the control scheme. For example a better synchronization system (PLL) can be adopted for the determination of the synchronous reference components to facilitate the control scheme [6].

5. Discrete Inverter Influence

5.1 Introduction

After testing the control system with the continuous model, the average model of the VSC is replaced with an inverter. To implement this, the voltages now have to be generated by the inverter, and pulses have to be provided by modulating the reference voltages using a modulation technique. In this thesis, Space Vector Pulse Width Modulation (SVPWM) is used due to its advantages over the carrier based PWM that will be explained in the following sections.

In this chapter, first the modulation scheme used i.e. SVPWM, is discussed. After that the simulation results using this technique and Inverter are presented. The different issues faced during the conversion from continuous to discrete model are discussed along the way.

5.2 Space Vector PWM

The space vector pulse width modulation (SVPWM) is known for its effectiveness, simplicity for implementation, harmonics reduction.

The study of space vector modulation technique reveals that space vector modulation technique utilizes DC bus voltage more efficiently and generates less harmonic distortion when compared with Sinusoidal PWM (SPWM) technique.

The space vector concept is based on the rotating field of the induction motor. When a three phase voltage is applied to the AC machine, there is a rotating flux in the air gap of the machine, which can be represented by a single rotating voltage vector. The magnitude and angle of the rotating vector can be found by converting the voltages into $\alpha\beta$ reference frame using the following transformation.

$$\begin{bmatrix} V_\alpha \\ V_\beta \\ V_\gamma \end{bmatrix} = \frac{2}{3} \begin{bmatrix} 1 & \frac{-1}{2} & \frac{-1}{2} \\ 0 & \frac{\sqrt{3}}{2} & \frac{-\sqrt{3}}{2} \\ \frac{1}{2} & \frac{1}{2} & \frac{1}{2} \end{bmatrix} \begin{bmatrix} V_{an} \\ V_{bn} \\ V_{cn} \end{bmatrix}$$

In an inverter, there are eight possible combinations for the on/off patterns of the three upper switches (a b c). The lower switches have on/off states that are opposite to the corresponding upper switches. Consider a switching variable vector $[a \ b \ c]^t$. The relationship between this vector and the phase voltage vector $[V_{an} \ V_{bn} \ V_{cn}]^t$ is

$$\begin{bmatrix} V_{an} \\ V_{bn} \\ V_{cn} \end{bmatrix} = \frac{V_{dc}}{3} \begin{bmatrix} 2 & -1 & -1 \\ -1 & 2 & -1 \\ -1 & -1 & 2 \end{bmatrix} \begin{bmatrix} a \\ b \\ c \end{bmatrix}$$

When the phase voltages corresponding to the eight states are transformed into the $\alpha\beta$ frame, we get 2 zero voltages and 6 non-zero voltages. As an example, consider the transformation corresponding to the state [1 0 0]

$$\begin{bmatrix} V_{an} \\ V_{bn} \\ V_{cn} \end{bmatrix} = \frac{V_{dc}}{3} \begin{bmatrix} 2 & -1 & -1 \\ -1 & 2 & -1 \\ -1 & -1 & 2 \end{bmatrix} \begin{bmatrix} 1 \\ 0 \\ 0 \end{bmatrix} = \frac{V_{dc}}{3} \begin{bmatrix} 2 \\ -1 \\ -1 \end{bmatrix}$$

and

$$\begin{bmatrix} V_{\alpha} \\ V_{\beta} \\ V_{\gamma} \end{bmatrix} = \frac{2}{3} \begin{bmatrix} 1 & \frac{-1}{2} & \frac{-1}{2} \\ 0 & \frac{\sqrt{3}}{2} & \frac{-\sqrt{3}}{2} \\ \frac{1}{2} & \frac{1}{2} & \frac{1}{2} \end{bmatrix} \begin{bmatrix} V_{an} \\ V_{bn} \\ V_{cn} \end{bmatrix} = \begin{bmatrix} \frac{2}{3} \\ 0 \\ 0 \end{bmatrix}$$

The reference voltage v_{abc} is converted to a rotating voltage V_{ref} with a magnitude and an angle which can be found from the $\alpha\beta$ components as:

$$|\bar{V}_{ref}| = \sqrt{V_{\alpha}^2 + V_{\beta}^2}$$

$$\alpha = \tan^{-1}\left(\frac{V_{\beta}}{V_{\alpha}}\right)$$

The possible voltages in abc and $\alpha\beta$ can be summarized as shown in the following table

Voltage Vectors	Switching vectors			Phase Voltages (abc frame)			$\alpha\beta$ frame	
	a	b	c	V_{an}	V_{bn}	V_{cn}	V_{α}	V_{β}
V_0	0	0	0	0	0	0	0	0
V_1	1	0	0	2/3	-1/3	-1/3	2/3	0
V_2	1	1	0	1/3	1/3	-2/3	1/3	$1/\sqrt{3}$
V_3	0	1	0	-1/3	2/3	-1/3	-1/3	$1/\sqrt{3}$
V_4	0	1	1	-2/3	1/3	1/3	-2/3	0
V_5	0	0	1	-1/3	-1/3	2/3	-1/3	$-1/\sqrt{3}$
V_6	1	0	1	1/3	-2/3	1/3	1/3	$-1/\sqrt{3}$
V_7	1	1	1	0	0	0	0	0

Table 5-1 Switching Vectors and Corresponding voltages in abc and alpha-beta frames

All voltages to be multiplied by V_{dc}

The six non-zero vectors form the axis of a hexagon, with the angle between two adjacent axes being 60 degrees while the two zero vectors are at the origin and apply zero voltage to the load. The desired reference voltage vector is approximated using the eight switching patterns.

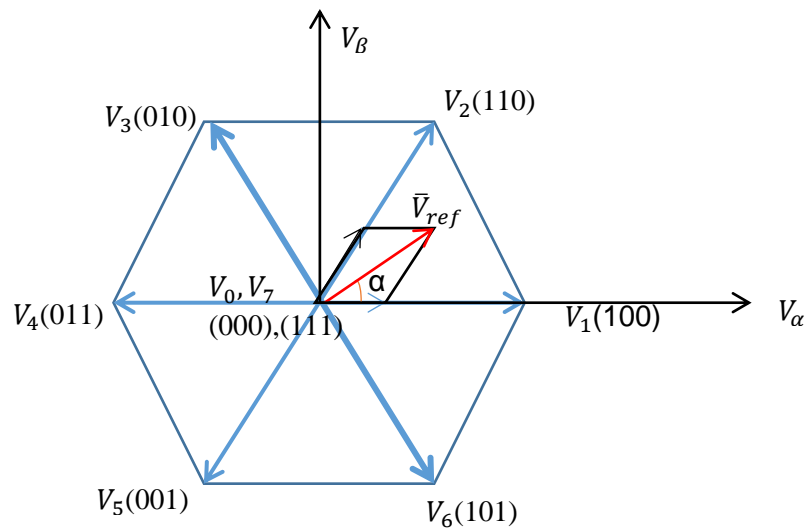


Figure 5-1 The eight Space Vectors forming a hexagon

The Voltage V_{ref} is given by [8]

$$\bar{V}_{ref} = \frac{1}{T_{PWM}} (T_0V_0 + T_1V_1 + T_2V_2 + \dots + T_7V_7)$$

Practically, only the two adjacent states (V_x and V_{x+60}) of the reference voltage phasor and the zero states should be used [9] as demonstrated by the example in figure. The reference voltage \bar{V}_{ref} can be approximated by having the inverter in switching states V_x and V_{x+60} for T_1 and T_2 duration of time respectively.

$$\bar{V}_{ref} = \frac{1}{T_{PWM}} (T_1V_x + T_2V_{x+60})$$

As is evident from the above equation, the voltages V_x and V_{x+60} should be known, so that they are applied for the corresponding times. These voltages depend on the sector of the reference voltage. Thus determination of the sector is an important step in the SVPWM.

The sum of the times T_1 and T_2 should be less than or equal to T_{PWM} . If the sum is less than T_{PWM} , one or both the zero vector voltages are applied for the remainder of the time, that is:

$$T_0 = T_{PWM} - T_1 - T_2$$

Thus the time T_0 is filled by one or both of the zero vectors, as shown in the figure below:

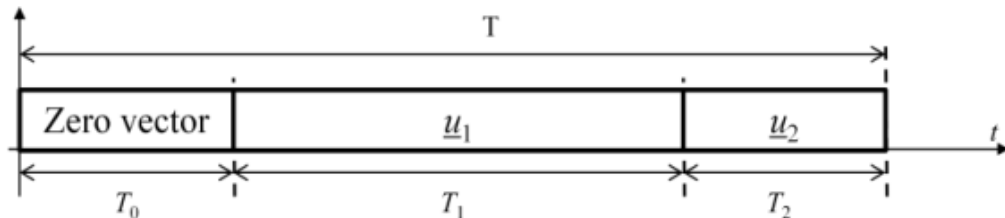


Figure 5-2 Application of Zero and Non-Zero Vectors

The calculation of the times, depending on each sector, can be done according to the following table [8]

Sector I ($0 \leq \omega t \leq \frac{\pi}{3}$)	Sector II ($\frac{\pi}{3} \leq \omega t \leq \frac{2\pi}{3}$)	Sector III ($\frac{2\pi}{3} \leq \omega t \leq \pi$)
$T_1 = \frac{\sqrt{3}}{2}mT_s \cos(\omega t + \frac{\pi}{6})$	$T_2 = \frac{\sqrt{3}}{2}mT_s \cos(\omega t + \frac{11\pi}{6})$	$T_3 = \frac{\sqrt{3}}{2}mT_s \cos(\omega t + \frac{3\pi}{2})$
$T_2 = \frac{\sqrt{3}}{2}mT_s \cos(\omega t + \frac{3\pi}{2})$	$T_3 = \frac{\sqrt{3}}{2}mT_s \cos(\omega t + \frac{7\pi}{6})$	$T_4 = \frac{\sqrt{3}}{2}mT_s \cos(\omega t + \frac{5\pi}{6})$
$T_0 + T_7 = T_s - T_1 - T_2$	$T_0 + T_7 = T_s - T_2 - T_3$	$T_0 + T_7 = T_s - T_3 - T_4$
Sector IV ($\pi \leq \omega t \leq \frac{4\pi}{3}$)	Sector V ($\frac{4\pi}{3} \leq \omega t \leq \frac{5\pi}{3}$)	Sector VI ($\frac{5\pi}{3} \leq \omega t \leq 2\pi$)
$T_4 = \frac{\sqrt{3}}{2}mT_s \cos(\omega t + \frac{7\pi}{6})$	$T_5 = \frac{\sqrt{3}}{2}mT_s \cos(\omega t + \frac{5\pi}{6})$	$T_6 = \frac{\sqrt{3}}{2}mT_s \cos(\omega t + \frac{\pi}{2})$
$T_5 = \frac{\sqrt{3}}{2}mT_s \cos(\omega t + \frac{\pi}{2})$	$T_6 = \frac{\sqrt{3}}{2}mT_s \cos(\omega t + \frac{\pi}{6})$	$T_1 = \frac{\sqrt{3}}{2}mT_s \cos(\omega t + \frac{11\pi}{6})$
$T_0 + T_7 = T_s - T_4 - T_5$	$T_0 + T_7 = T_s - T_5 - T_6$	$T_0 + T_7 = T_s - T_1 - T_6$

Table 5-2 Calculation of Times in Different Sectors [8]

A more detailed study of the selection of the sector algorithm and the equations for the determination of the turn on times is given in [9]

From the times and voltages to be applied determined based on the reference voltage and the sectors the switching times for the individual switches need to be calculated. The times determined above only indicate which vectors should be applied for how much time, not the switching times. The switching times depend on the adjacent voltage vectors that we have to apply.

For example, consider the voltage vectors to be applied are \underline{V}_{100} and \underline{V}_{110} , respectively. the possibilities of the switching sequence are shown in the figures below.

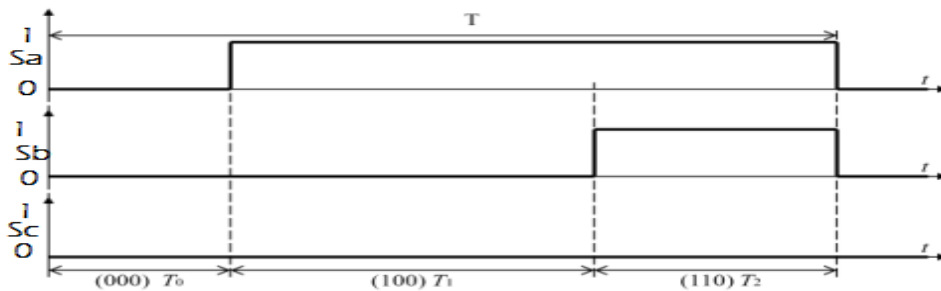


Figure 5-3 Switching Pattern with asymmetric pulsation

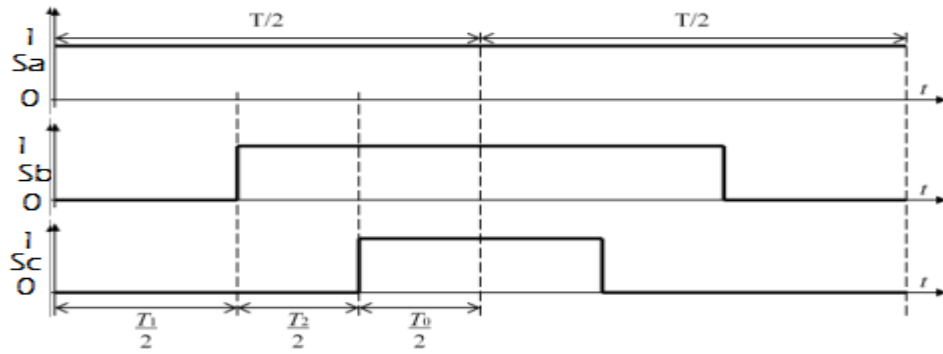


Figure 5-4 Symmetric pulsation using $\underline{V}_r(111)$ as zero vector

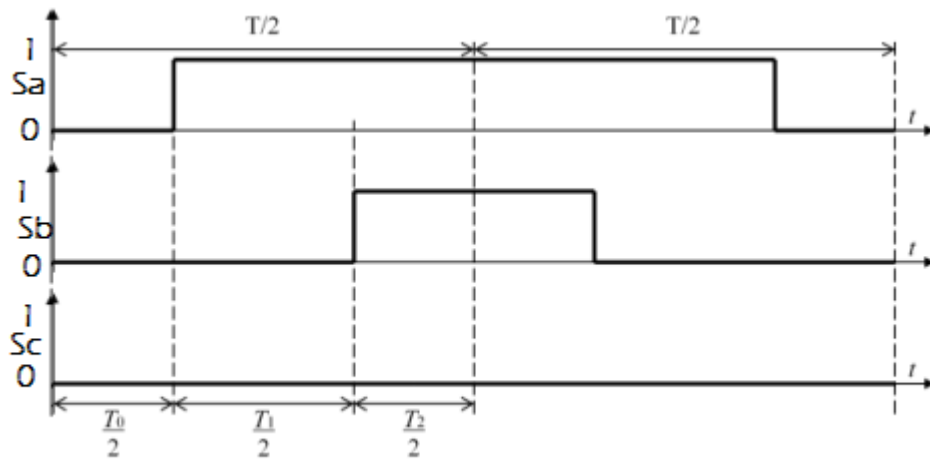


Figure 5-5 Symmetric pulsation using $\underline{V}_o(000)$ as zero vector

In the first figure, two switches are switched at certain time, would generate more harmonics, so it is not normally used. In the other schemes, only one switch is switched at any time. In all above cases, only one zero voltage vector is applied during one period. Another option is to use both the zero vectors, which is shown below:

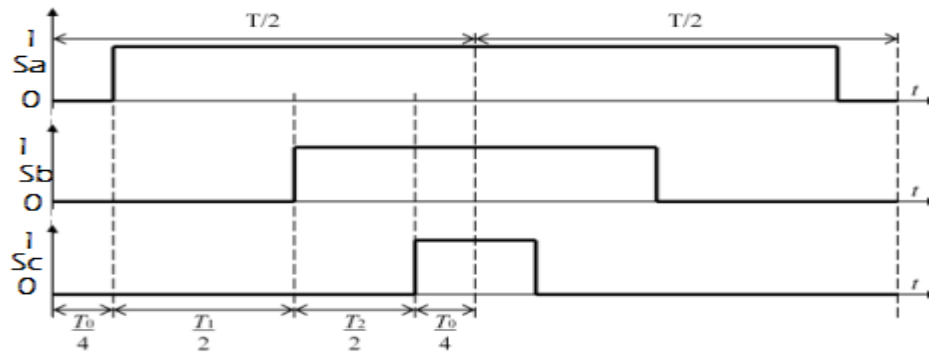


Figure 5-6 Symmetric pulsation using $\underline{V}_7(111)$ and $\underline{V}_0(000)$ as zero vector

The total harmonic distortion is minimum when the last pattern with both zero vectors is used [9].

The control signals for the three upper switches are obtained by comparing the time intervals with a repeating sequence during each SVPWM period.

The maximum line to line and phase output voltages without going into over modulation are

$$V_{line,max(rms)} = \sqrt{\frac{3}{2}} V_{phase,max(peak)} = \sqrt{\frac{3}{2}} * \frac{2}{3} V_{dc} \cos(30^\circ) = \frac{V_{dc}}{\sqrt{2}}$$

Which is higher than the value in sinusoidal PWM ($\frac{V_{dc}}{2}$).

5.3 Simulations

After getting an idea about the type of modulation we are going to use, the next step is to test the control scheme with the selected modulation scheme (SVPWM) and an inverter.

5.3.1 Results

The most intuitive step is to replace the continuous model with an inverter and SVPWM without making any other changes. The SVPWM block generates pulses according to the voltage references given by the control. The Block diagram is given below

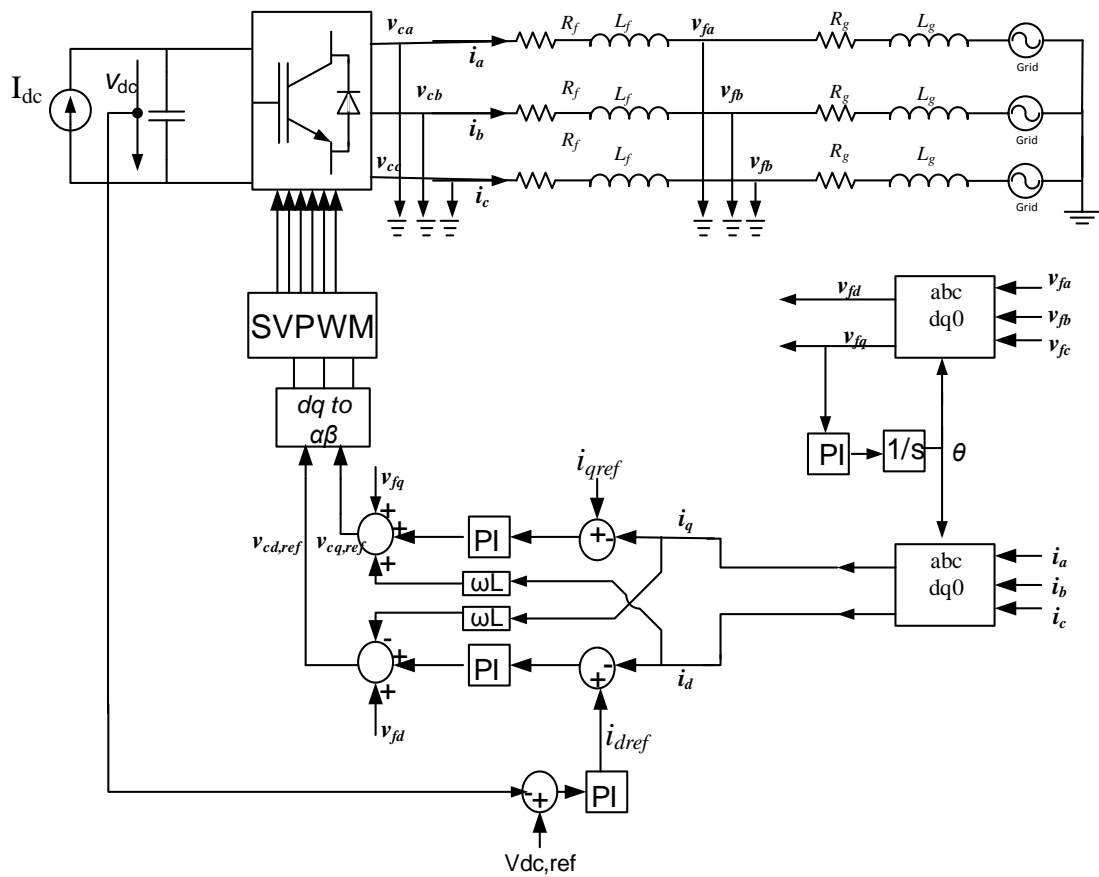


Figure 5-7 Control Scheme with Inverter and SVPWM

The behavior of the system is given in the figures below:

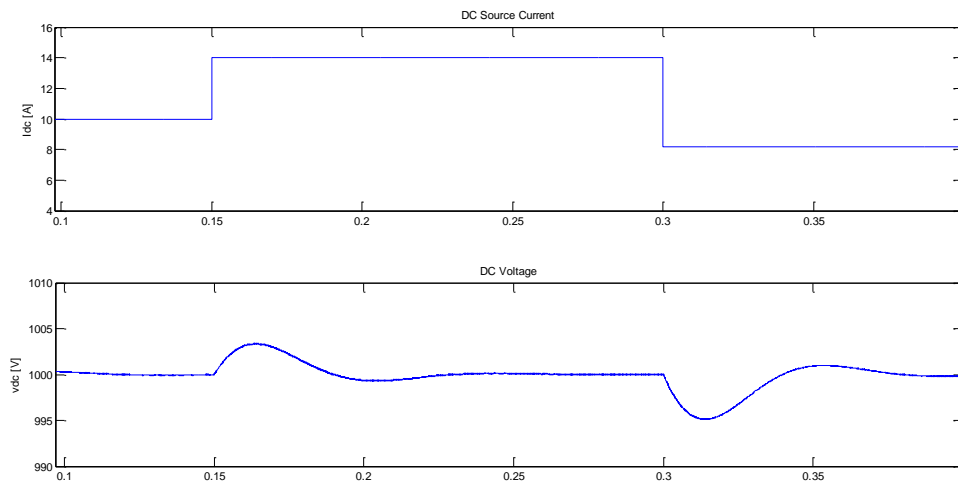


Figure 5-8 DC Voltage when DC Current Reference is Changed

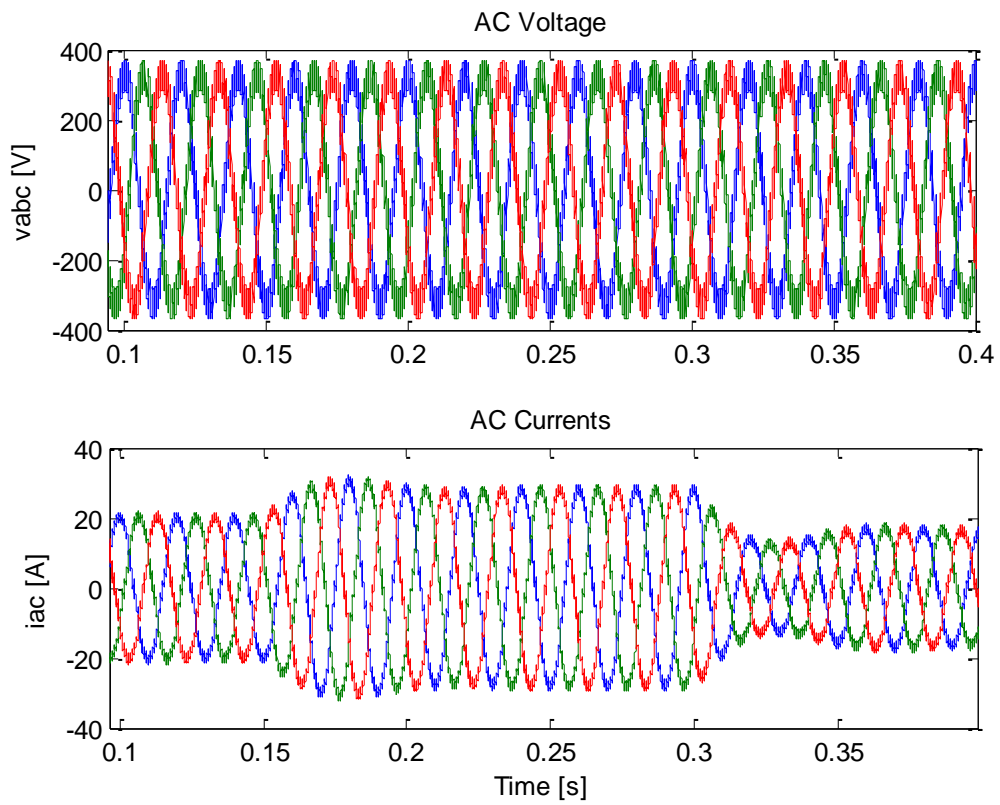


Figure 5-9 AC Voltages and Currents

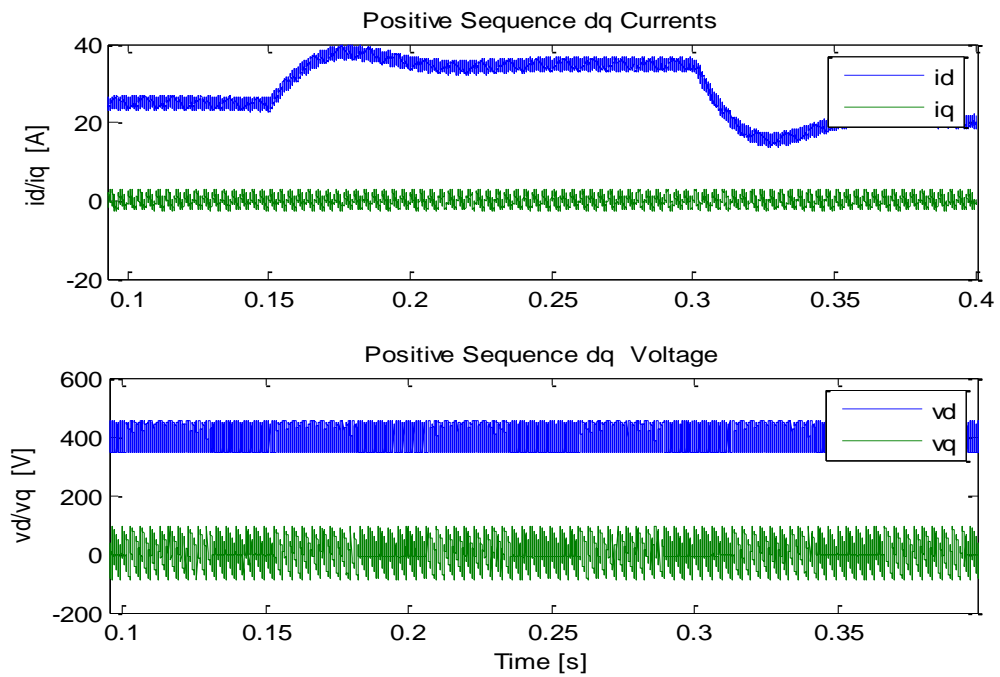


Figure 5-10 dq Currents and Voltages

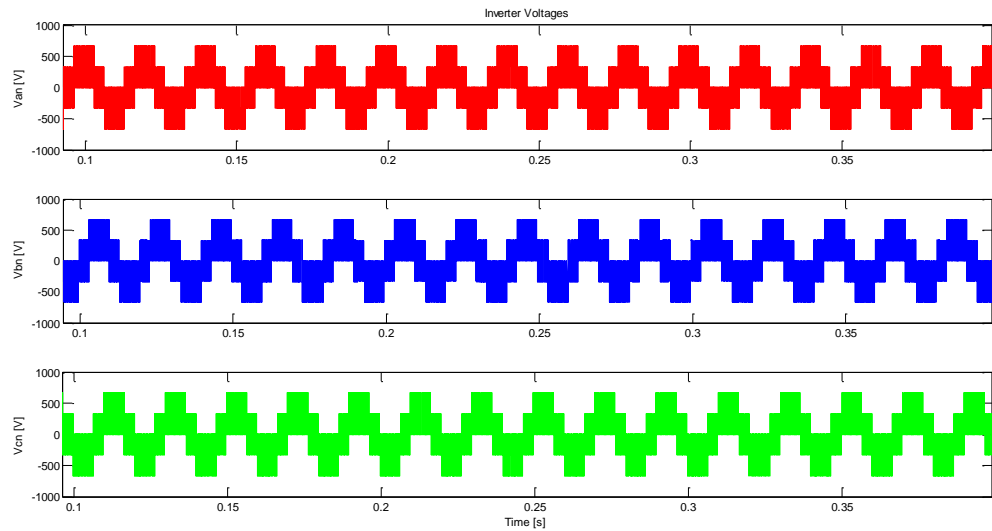


Figure 5-11 Inverter Voltages

As we can see from the simulation results that the voltage and currents are not of very good quality and have a lot of noise due to switching. The switching frequency used in the simulations is 5 kHz. Increasing the frequency decreases the switching noise. Some of the basic techniques to tackle this problem involve the introduction of low pass filters. Increasing the switching frequency decreases the switching noise.

As we can see from the results, the input currents to the control have a lot of noise due to switching. Below are some techniques to remove this noise.

5.3.2 Introduction of Low-Pass Filters

One option is to introduce low pass filters after converting the abc quantities into the dq quantities. Another option is to pre-filter the quantities after measuring them at the PCC and then do the conversion to the dq reference frame.

In this thesis the second approach is used.

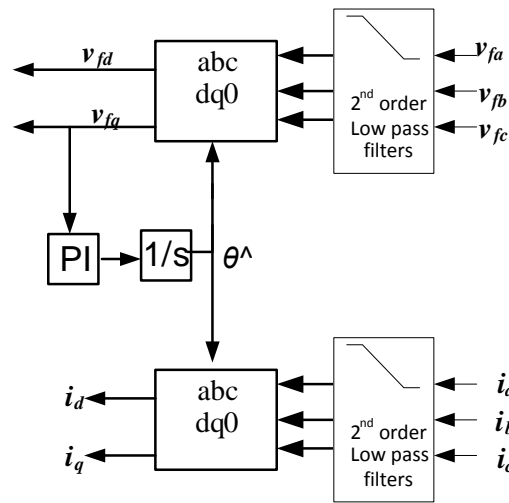


Figure 5-12 Introduction of Filters

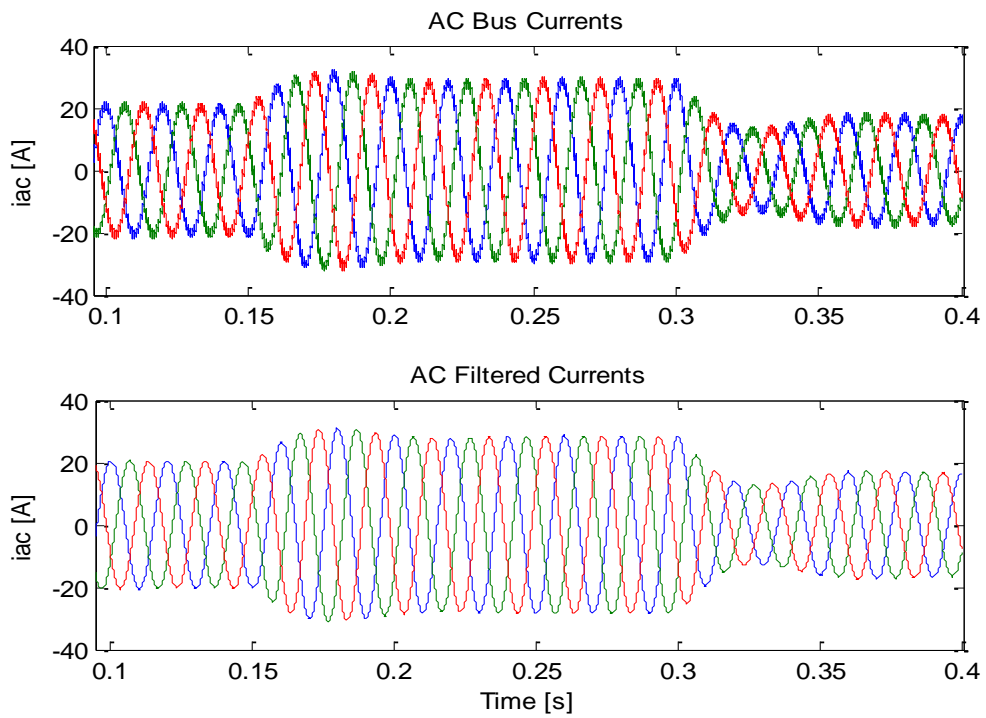


Figure 5-13 AC Voltages before and after the Filters

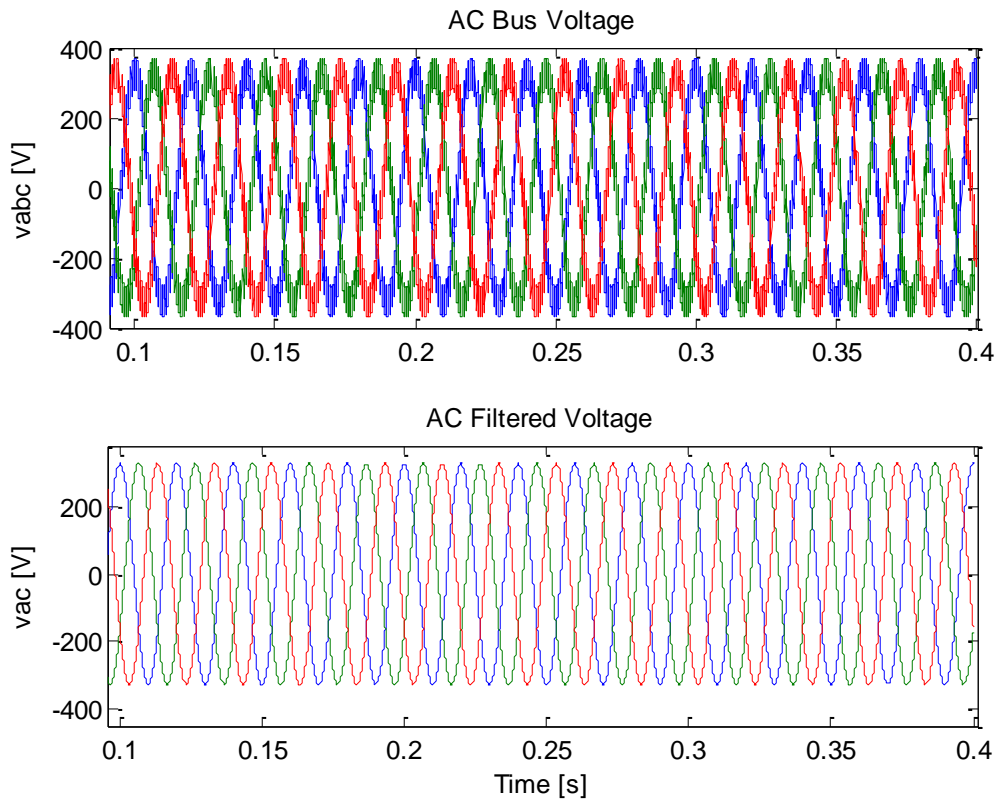


Figure 5-14 AC Currents before and after the Filters

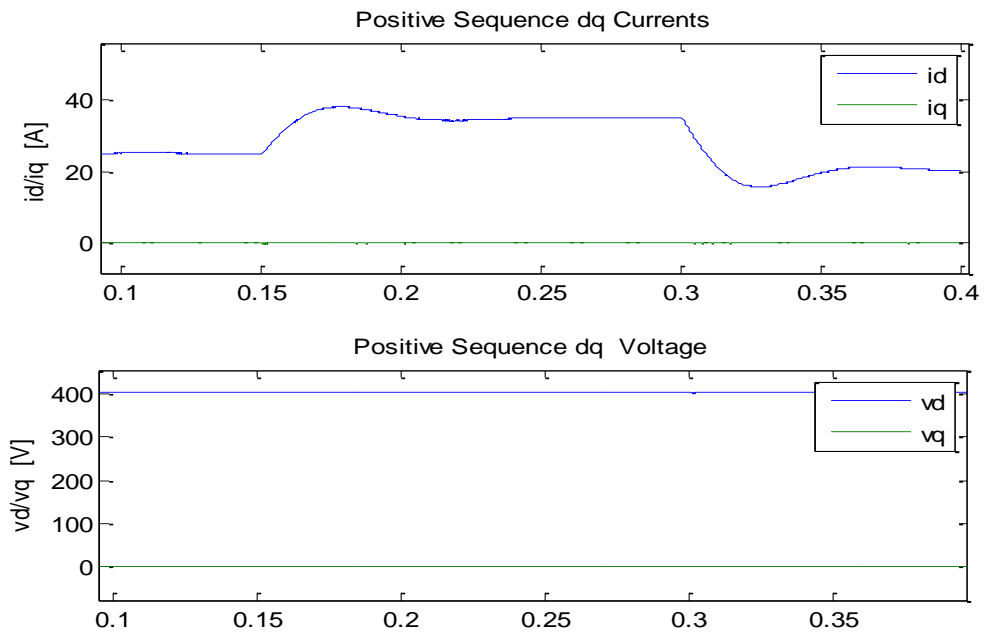


Figure 5-15 dq Components of the filtered quantities

The pre-filtering removes the noise from the qd components before they are fed to the control. This may help improve the performance of the control. The reference voltages that have to be imposed by the inverter are now perfectly sinusoidal.

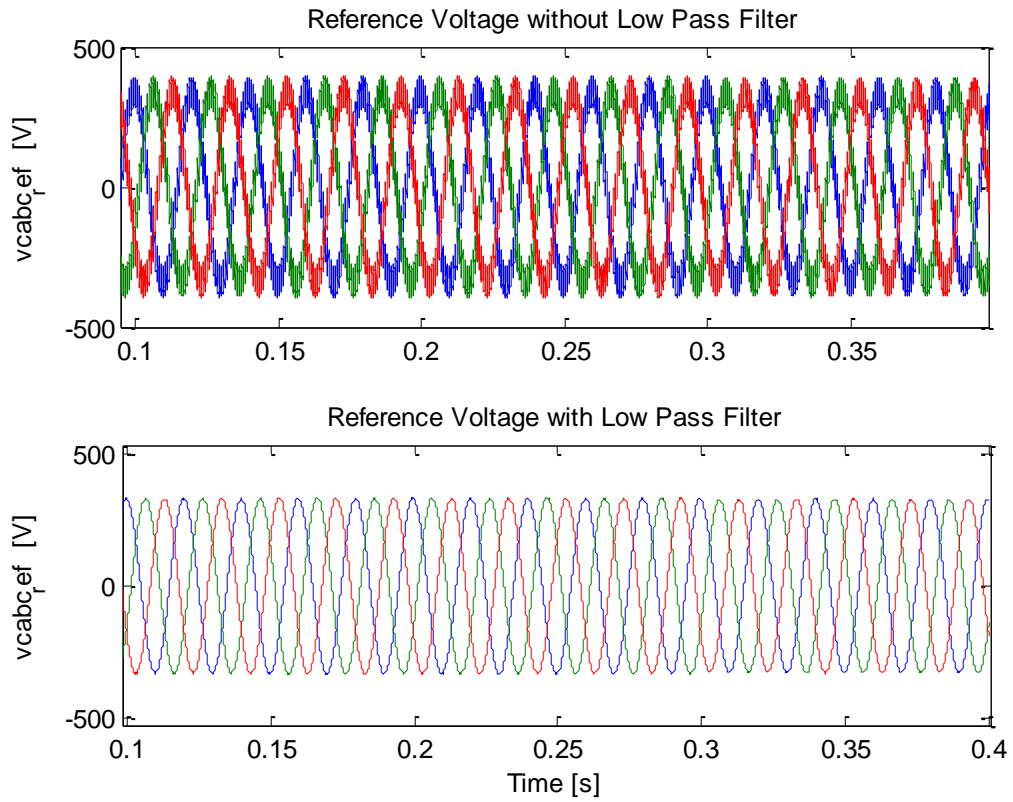


Figure 5-16 Reference voltages without and with the use of filters

5.4 Unsymmetrical Conditions

The response of the system under unsymmetrical conditions, for example in case of a Type E fault is shown in the figures below:

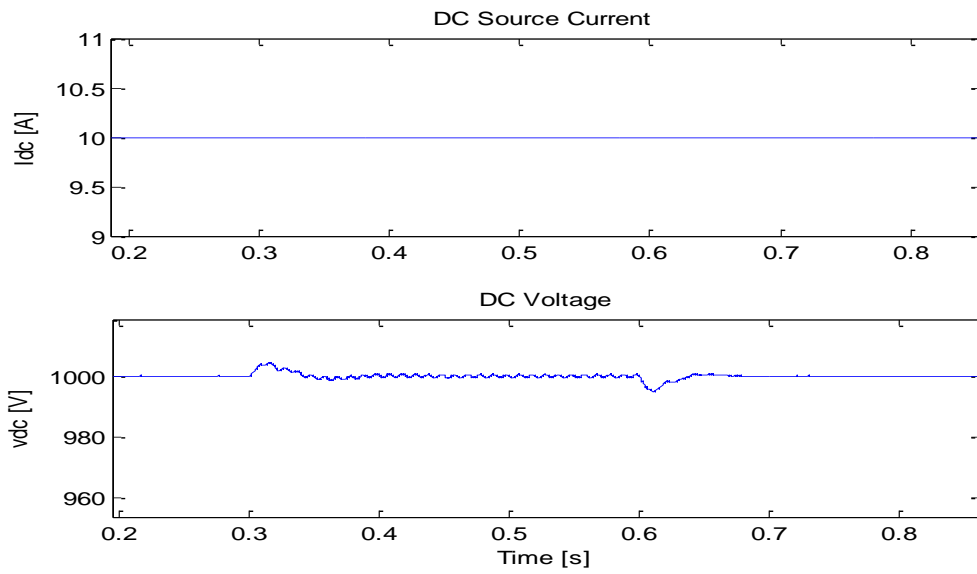


Figure 5-17 System behavior during type E Voltage Sags (DC Voltage and Current)

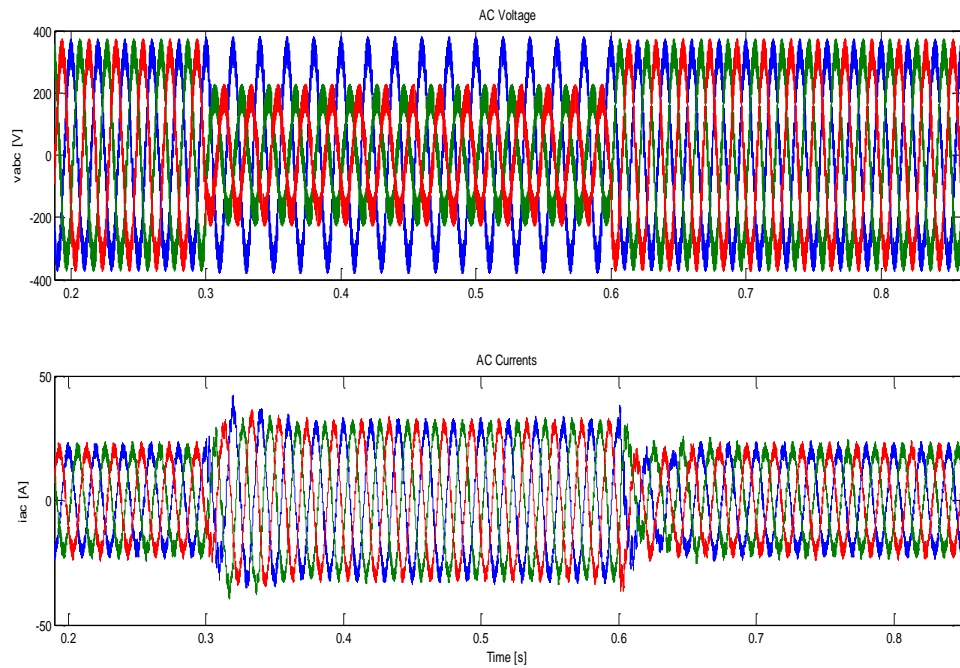


Figure 5-18 System behavior during type E Voltage Sags (AC Voltage and Current)

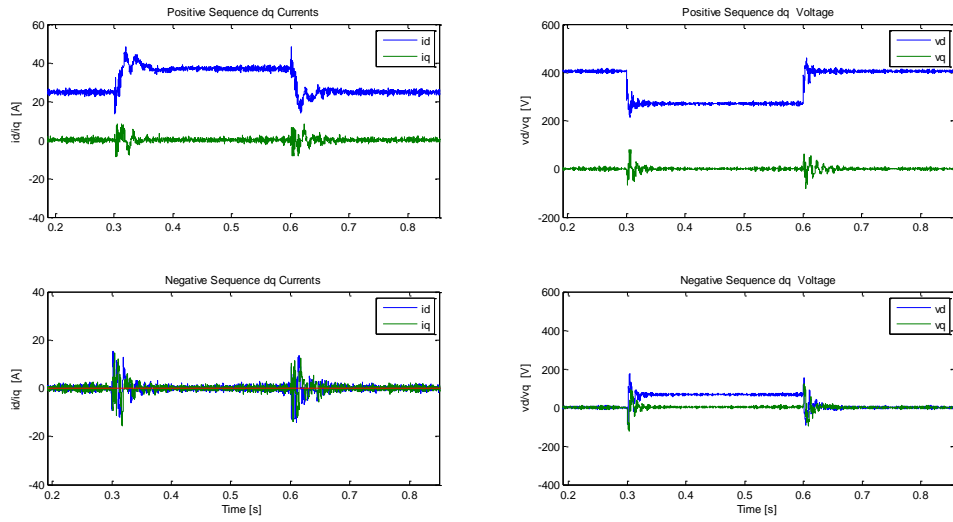


Figure 5-19 System behavior during type E Voltage Sags (dq Voltage and Current)

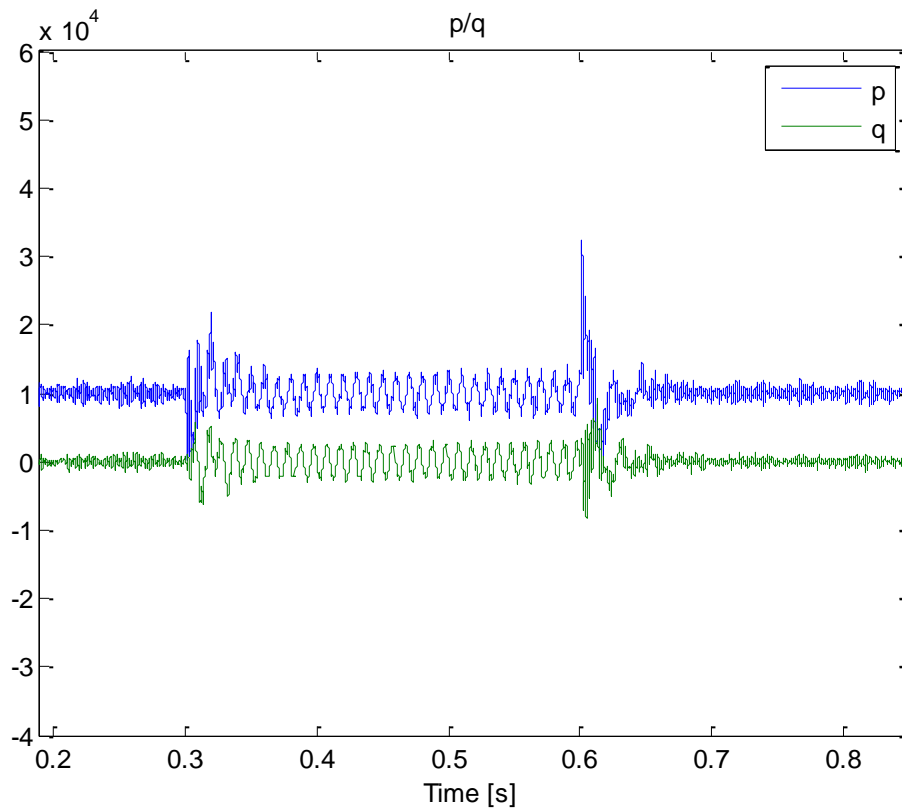


Figure 5-20 System behavior during type E Voltage Sags (p and q)

Conclusions

As we have seen during the course of this chapter, using the SVPWM and inverter, the control scheme is able to track any changes in the current input of the DC source (thus the power input, as DC voltage is constant), maintaining a constant DC side voltage and ensuring the power balance between the AC and DC side.

6. Implementation

6.1 Introduction

After the simulations of the control scheme in Simulink, the next step is to implement the model using dSPACE (1104) which allows the interfacing of Matlab/Simulink with input and output signals. In this chapter the setup for these tests is introduced and the results of the tests in the laboratory are discussed.

6.2 Block Diagram

The setup that is used in the laboratory for the tests can be represented by the following block diagram:

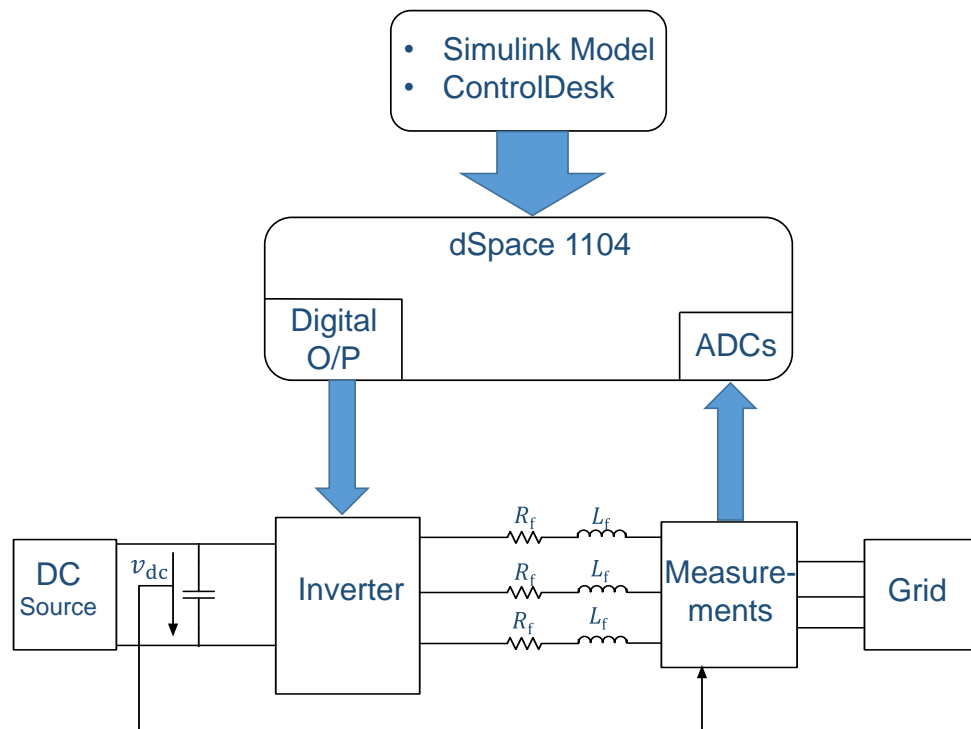


Figure 6-1 dSpace Setup

6.3 The Hardware

An overview of the main hardware used in the experiments is given below.

6.3.1 dSPACE 1104

With Real-Time Interface (RTI), function models can be easily implemented on the DS1104 R&D Controller Board. The RTI I/O blocks can be inserted into a Simulink block diagram to connect the function model with the I/O interfaces and to configure all I/O

graphically. After the configuration, the real-time model code can be generated, compiled and downloaded to the DS1104 automatically [10]

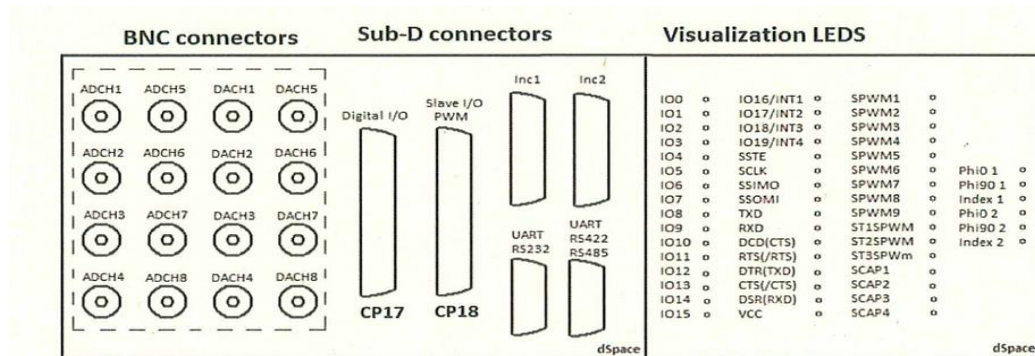


Figure 6-2 dSpace pin-out and display

6.3.2 The Inverter

The DC bus from a 30 V power supply will be connected to the corresponding polarity \pm VDC DC BUS power input. Six IGBT power transistors (Q0 to Q5) will be connected to the three inductors of the filter. Each of the six transistors is switched on/off by means of the corresponding pin that can be found on the inverter box (e.g. transistor Q1 is controlled by a digital signal in PIN 9). The digital signals to control the transistors will come from the dSPACE system.

A C code is generated by Matlab for the Simulink Model which we make, which is sent to the dSPACE connected to the computer. Any real time control actions can be performed in the Control Desk Software, by building a suitable interface containing all the control variable as required.

Some information about the inverter components is given in the table below:

V_{ac}	400Vrms
I_{ac}	15Arms
$V_{dc,max}$	800V
$f_{sw,max}$	20kHz
Rated Power	10kVA
IGBTs	SKiiP 23NAB12T4V1
Capacitor Bank	6x680 μ F (Equivalent Capacitance 1020 μ F)

Table 6-1 Inverter Information

6.4 Control Desk

When the model is built in Simulink,(incremental build), an .sdf file is generated which can be loaded into the Control desk software. Various block outputs and variable values can be seen in the software, and its can also be used to modify these values to get the desired control functions (like Start/Stop etc). A layout needs to be built for the experiment according to the needs.

6.5 The Simulink Model

The Simulink model is now modified, as the inverter, grid and DC source all are now to be replaced with actual components instead of Simulink models. Some control functionalities can also be added to the Simulink model, for example, Enabling/Disabling the Control system, starting the IGBTs etc. One key point to note here is that if these functionalities are added to the system, a reset should be added to the Integrators so that their value is reset when the control system is enabled, otherwise, their value will keep on increasing when the system is not working.

The ADC of dSpace is used to read the AC voltage, AC currents and the DC voltage to be used in the control scheme. The maximum input at the ADC can be between +10V and -10V. The ADC then divides the input by a factor of ten. Thus to read a voltage in the order of 20-30 V, it has to be divided by a factor of 10 so that the limit of the ADC is not violated. In the Simulink model, the value read by the ADC has to be multiplied by a factor of 100 (10 for the probe attenuation factor and 10 for the ADC attenuation).

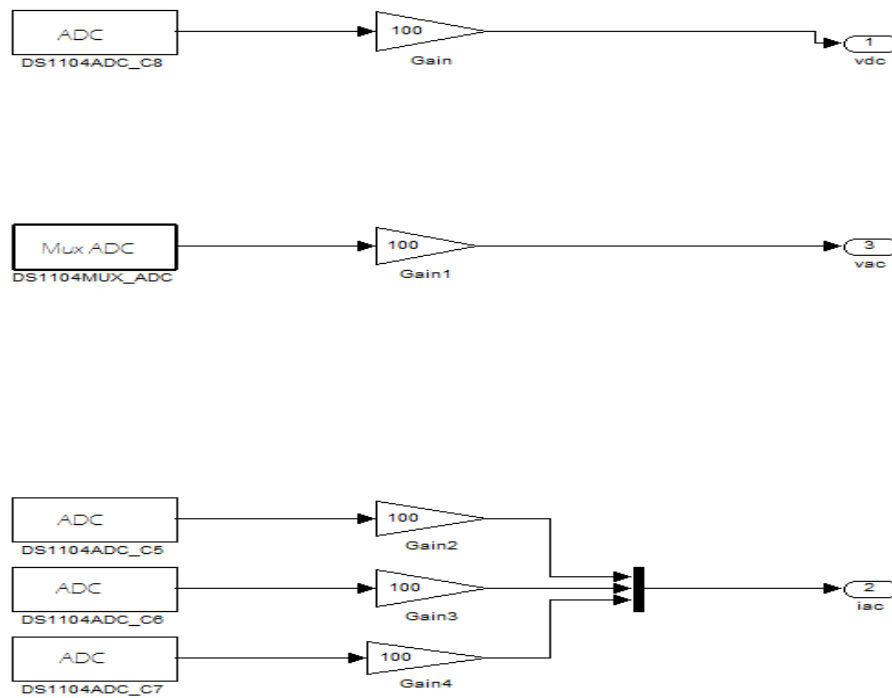


Figure 6-3 Simulink model to read and scale inputs

A start button is incorporated into the system for safety, so that when the button is off, all the IGBTs are disabled. The DC side is connected to the AC side only when the IGBTs are enabled through this button. ControlDesk can be used to change the value in real time. The Simulink model for this functionality is given in the appendix C.

As mentioned earlier the resetting of the integrator in the PI should be kept in notice. As when the IGBTs are disabled, the integrator will try to set the error to zero, which can not be done because all the IGBTs are off. Thus the integrator value will keep on increasing. One way to do this is to reset the integrator when the IGBTs are enabled. Another way is to make the K_i value zero when the switches are disabled.

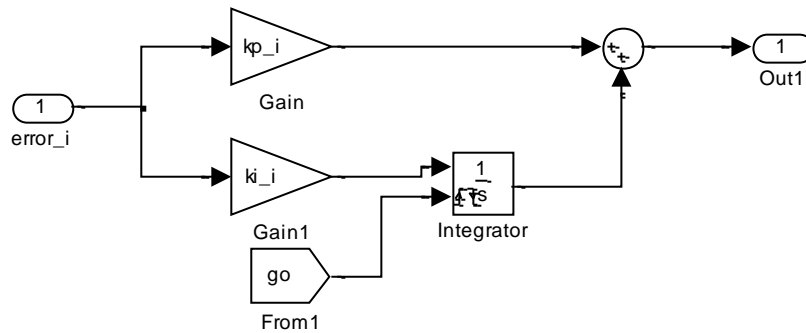


Figure 6-4 Mechanism to reset the integrator

6.6 Tests and Results

In the first step, tests were performed at a very low voltage, 28V DC and 12 V V_{rms} . The only current source available provided 3A maximum current. The tests were performed by changing the dc current set point and analyzing the behavior of the system.

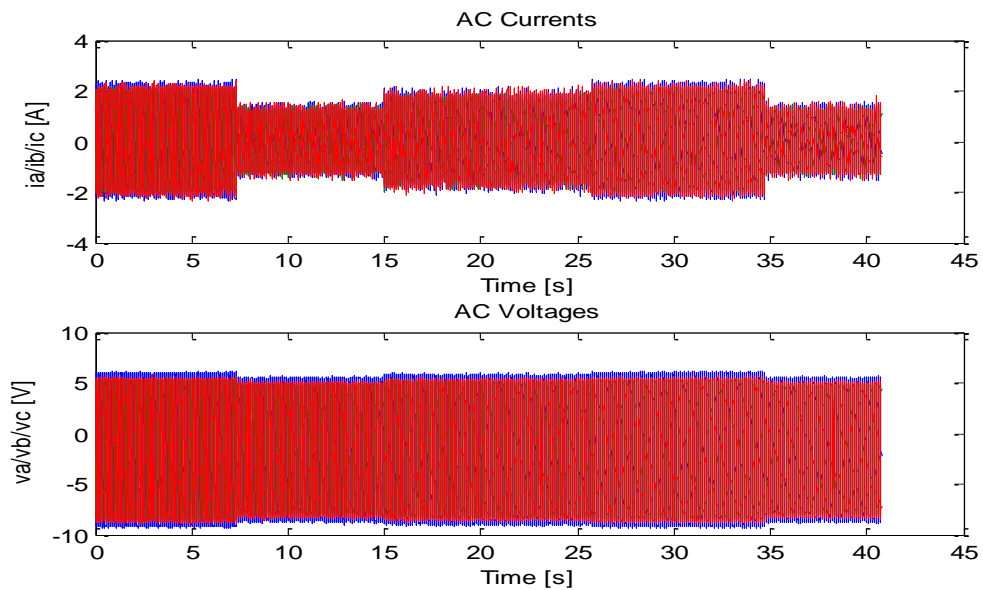


Figure 6-5 AC Currents and Voltages

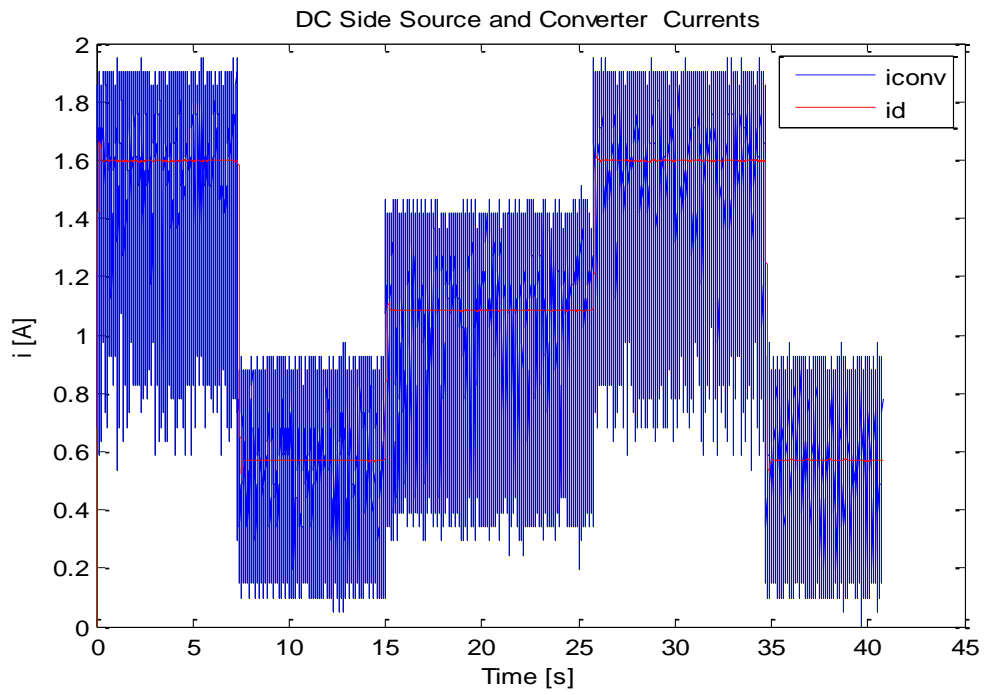


Figure 6-6 DC Current Changes

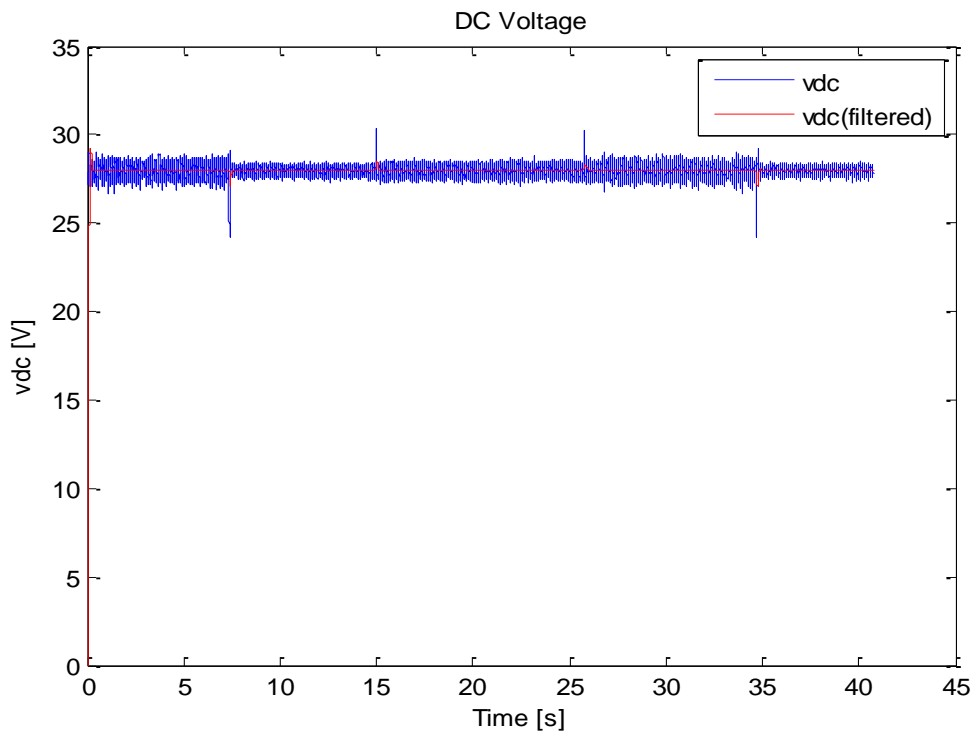


Figure 6-7 DC Voltage

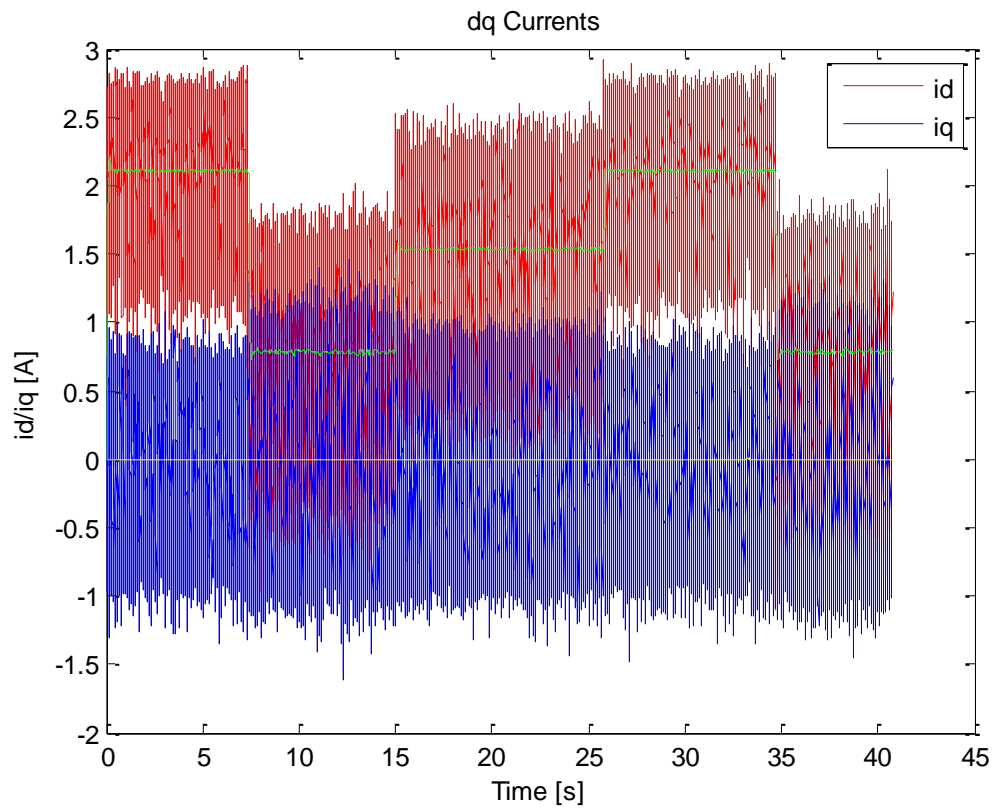


Figure 6-8 dq Currents

Further experiments were performed for testing the AC current control at higher voltages. The parameters used in the experiment are tabled below:

Parameter	Value
V_{dc}	208 V
V_{rms} (line to line)	87V
L_f	9 mH

Table 6-2 Parameters used in dSpace tests

The tests are performed by changing the dc current set point and analyzing the behavior of the system.

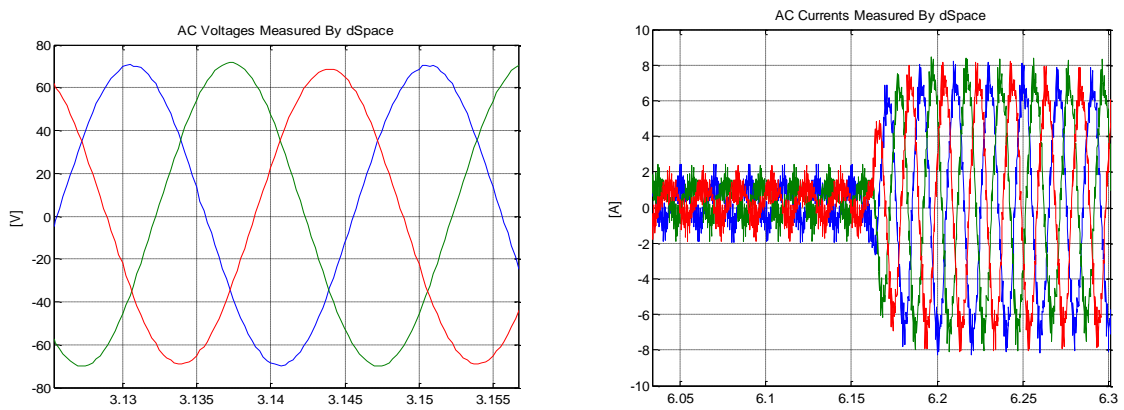


Figure 6-9 AC Currents and Voltages

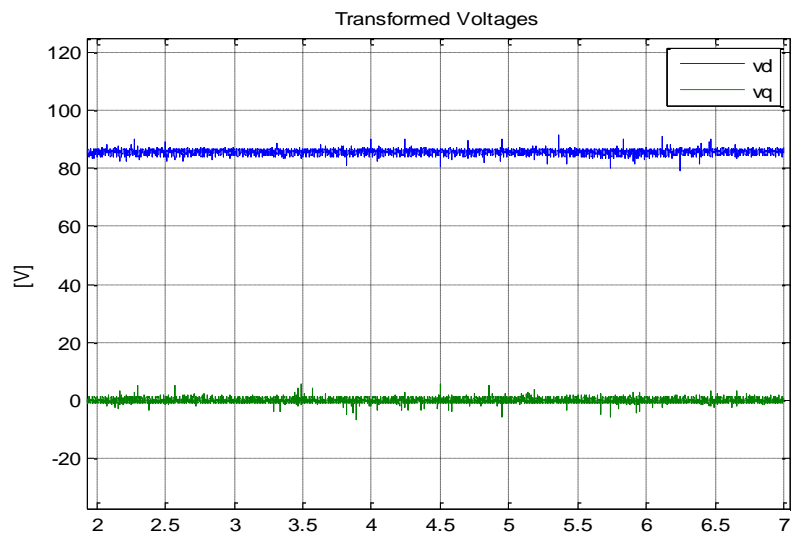


Figure 6-10 Transformed Voltages in dq frame

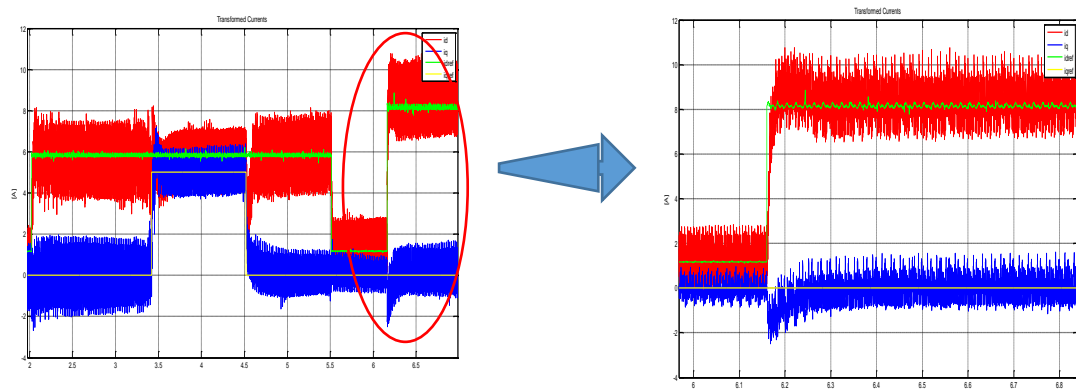


Figure 6-11 Transformed Currents in dq frame

Conclusions

As we can see from the results, the DC voltage is kept at around 28V set point by the control. AC side current changes accordingly with the changes in DC side current (changes in injected power). The low voltages used in the experiment make it difficult to view the quantities properly because of the switching noise present. Also there are no filters applied, which would have facilitated the control system.

7. Conclusions and Recommendations

A control system for the interconnection between a DC source and an AC grid was studied and simulated during this thesis. The control system keeps the DC bus voltage at a constant level under different changes in the system.

The implementation of the system is done at low voltage levels which provide difficulties in monitoring the system behavior under different circumstances. Also due to the limitations of the laboratory equipment, for example unavailability of the desired filter inductance and resistance pose problems in realizing the system properly. Further experiments using the proper elements are necessary for proper conclusions to be drawn for the control. Nevertheless, the simulations provided the necessary results.

The control can also be modified further to control different quantities depending on different current reference calculation strategies, for example, IARC, PNSC, AARC, BPS.

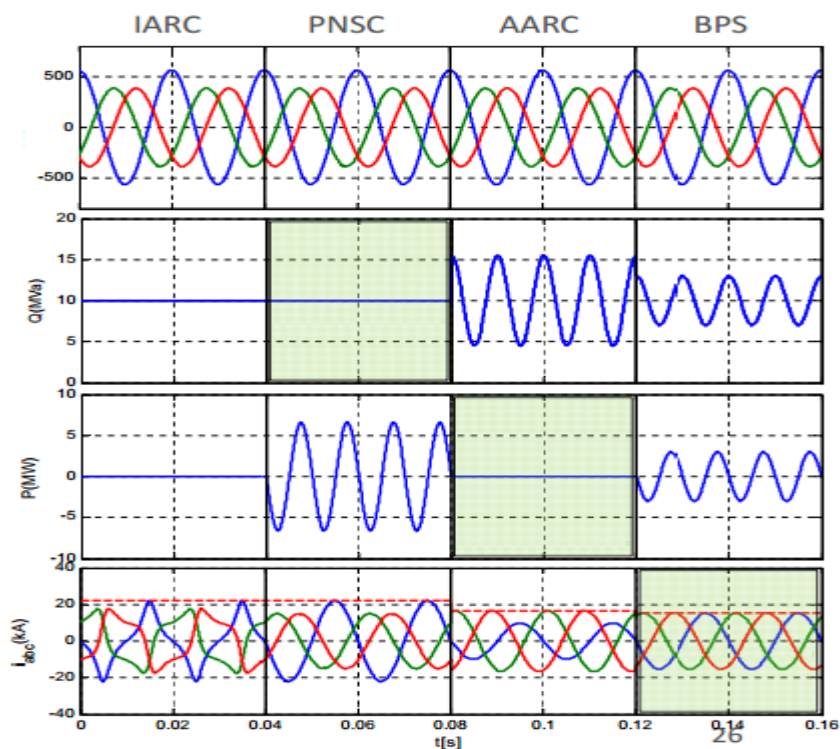


Figure 7-1 Performance of IARC, PNSC, AARC and BPS [6]

References

- [1] Renewable Energy Policy Network for the 21st Century, "Renewables 2015 Global Status Report," [Online]. Available: <http://www.ren21.net/status-of-renewables/global-status-report/>.
- [2] F. Blaabjerg, R. Teodorescu and M. Liserre, "Overview of Control and Grid Synchronization for Distributed Power Generation Systems," *IEEE TRANSACTIONS ON INDUSTRIAL ELECTRONICS*, vol. 53, no. 5, October 2006.
- [3] A. Egea-Alvarez, *Multiterminal HVDC transmission systems for offshore wind*, Barcelona, 2014.
- [4] K. Ogata, *Ingeniería de Control Moderna*, 4ª Edición, Madrid: Prentice-Hall, 2007.
- [5] L. Harnefors and . H.-P. Nee, "Model-based current control of AC machines using the internal model control method," *IEEE TRANSACTIONS ON INDUSTRY APPLICATIONS*, vol. 34, no. 01, JANUARY/FEBRUARY 1998.
- [6] R. Teodorescu, M. Liserre and P. Rodriguez, *Grid Converters for Photovoltaic and Wind Power Systems*, John Wiley and Sons, 2011.
- [7] R. Pena, J. Clare and G. Asher, "Doubly fed induction generator using back-to-back PWM converters and its application to variable-speed wind-energy generation," *Electric Power Applications, IEE Proceedings*, vol. 143, no. 3, May 1996.
- [8] S.-K. Chung, "A Phase Tracking System for Three Phase Utility Interface Inverters," *IEEE TRANSACTIONS ON POWER ELECTRONICS*, vol. 15, no. 3, May 2000.
- [9] H. A. Pereira, A. F. Cupertino and . S. R. Silva, "Influence of PLL in Wind Parks Harmonic Emissions," *IEEE PES Conference On Innovative Smart Grid Technologies Latin America (ISGT LA)*, 15-17 April 2013.
- [10] K. Zhou and D. Wang, "Relationship Between Space-Vector Modulation and Three-Phase Carrier-Based PWM:A Comprehensive Analysis," *IEEE TRANSACTIONS ON INDUSTRIAL ELECTRONICS*, vol. 49, no. 1, February 2002.
- [11] E. Hendawi, F. Khater and A. Shaltout, "Analysis, Simulation and Implementation of Space Vector Pulse Width," *AEE'10 Proceedings of the 9th WSEAS international conference on Applications of electrical engineering*, 2010.
- [12] [Online]. Available: <https://www.dspace.com/en/pub/home/products/hw/singbord/conledpanels.cfm>.

Appendices

A. Continuous Model Simulink Blocks

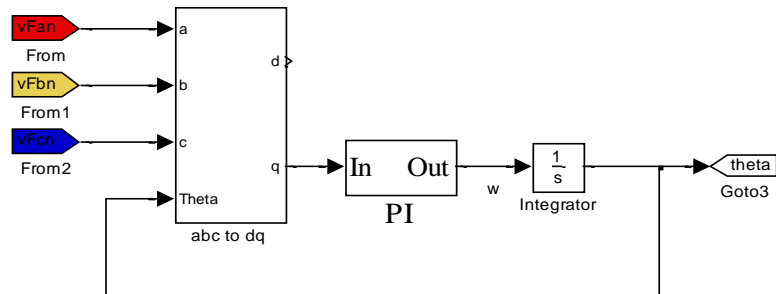


Figure A 1 PLL Simulink Block

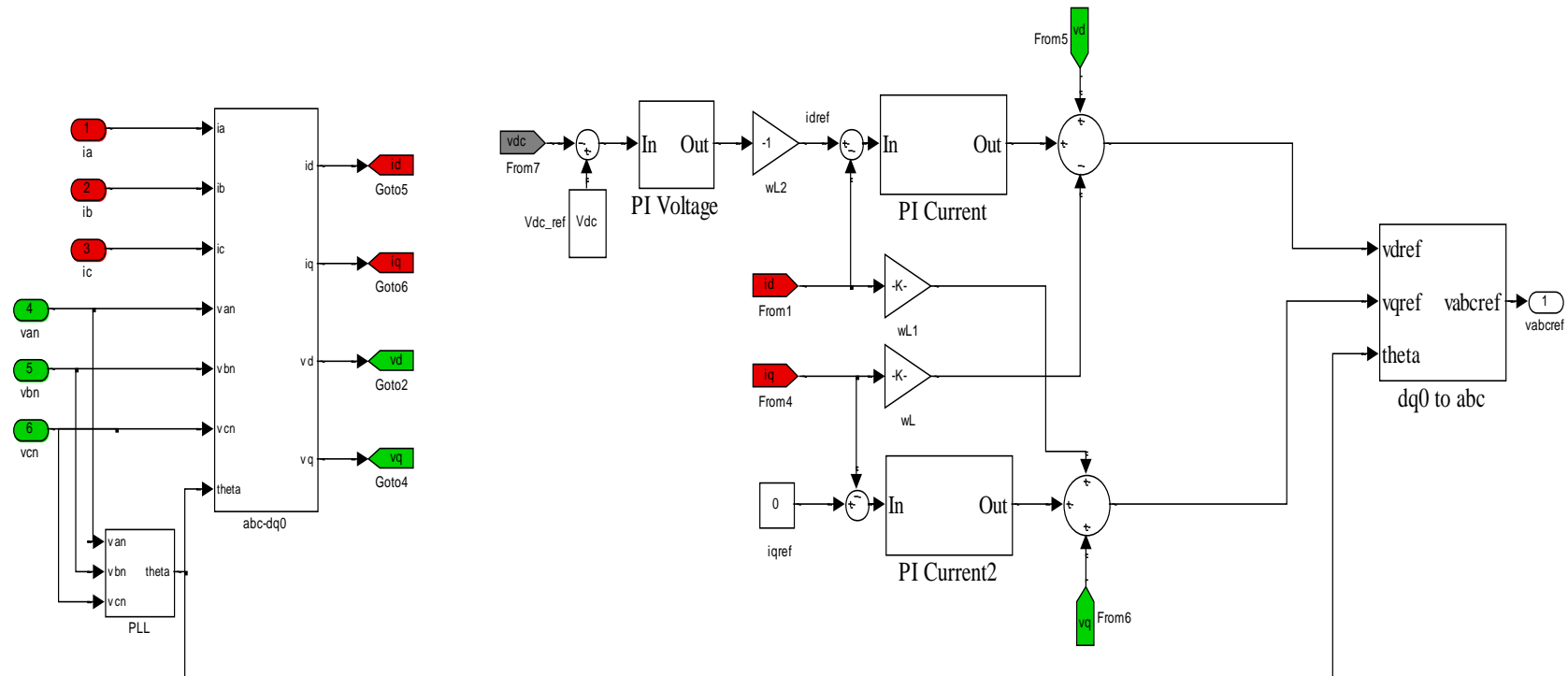


Figure A 3 Control Block in Simulink

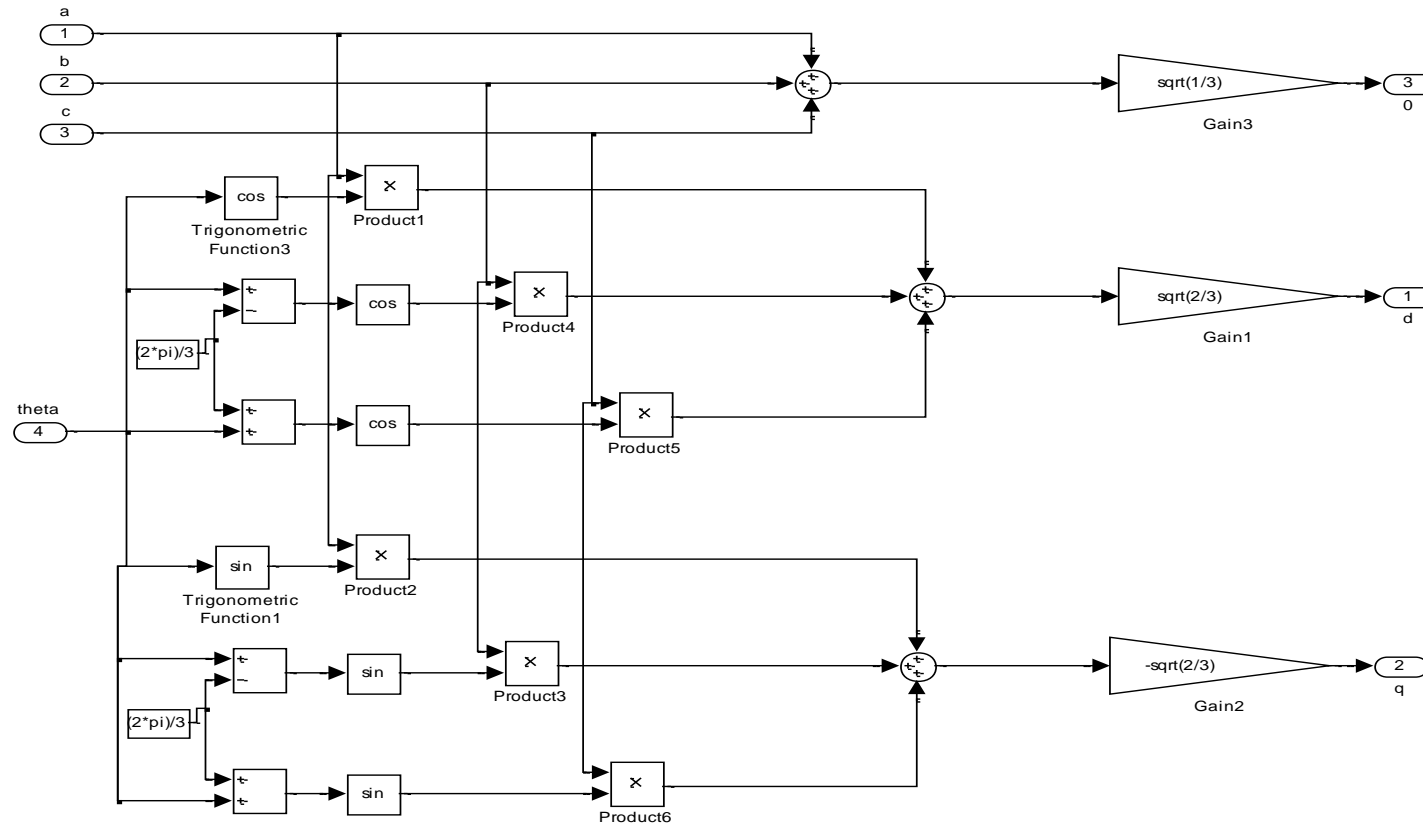


Figure A 4 abc to dq transformation block

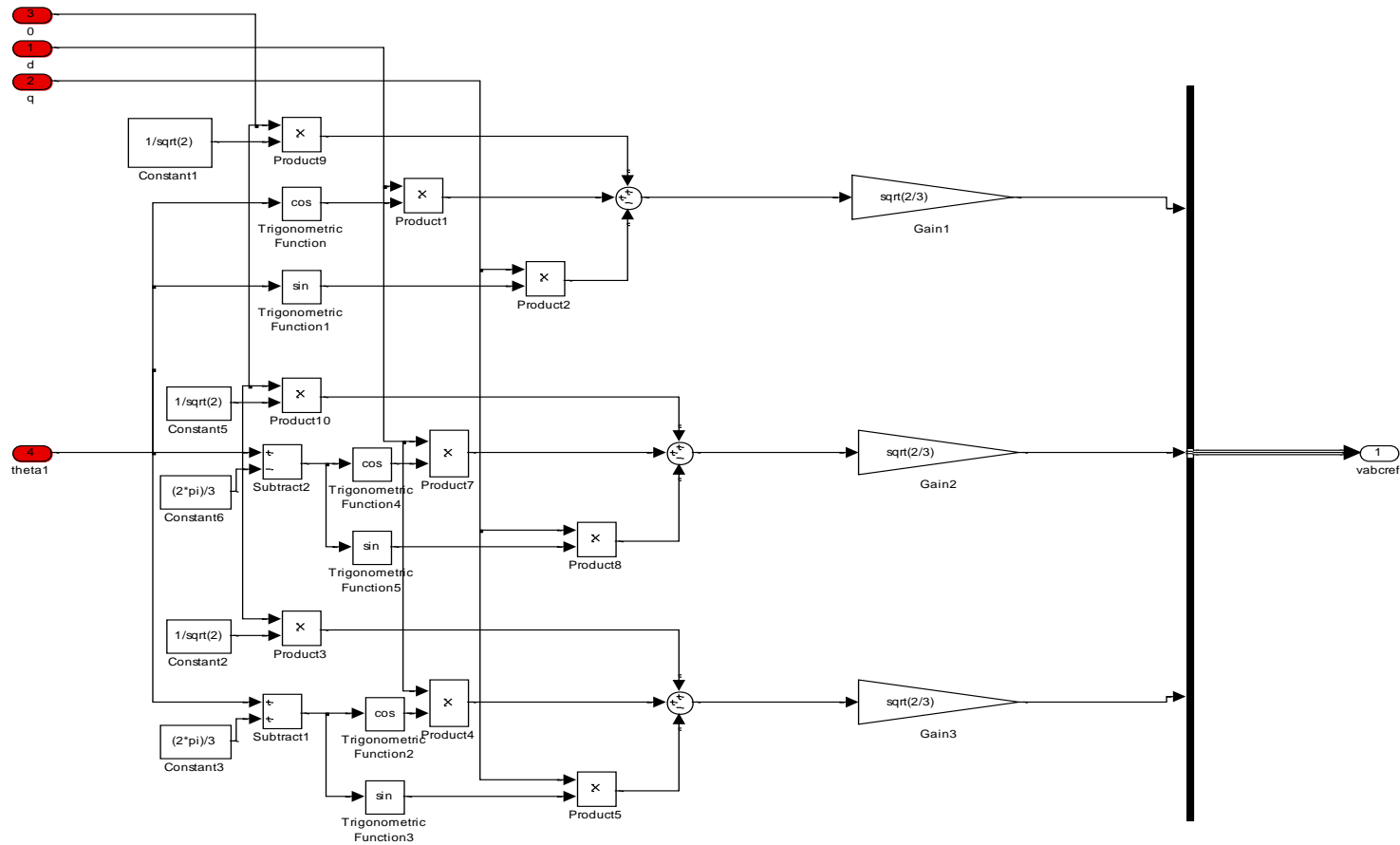


Figure A 5 dq0 to abc transformation block

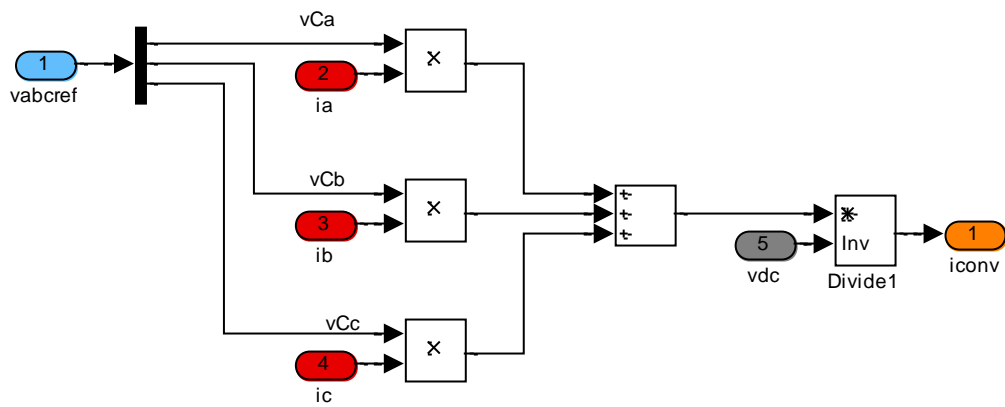


Figure A 6 Converter DC side Current Calculation

B. Discrete Models in Simulink

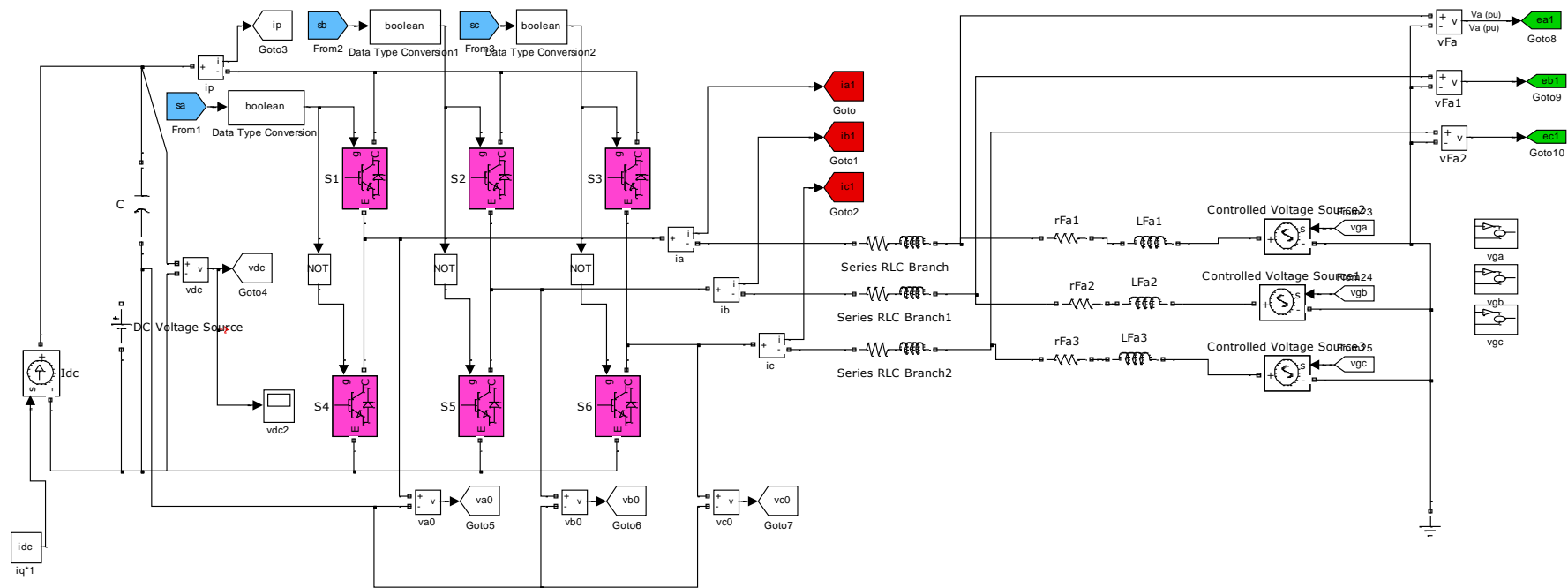


Figure B 1 Main System Model in Simulink

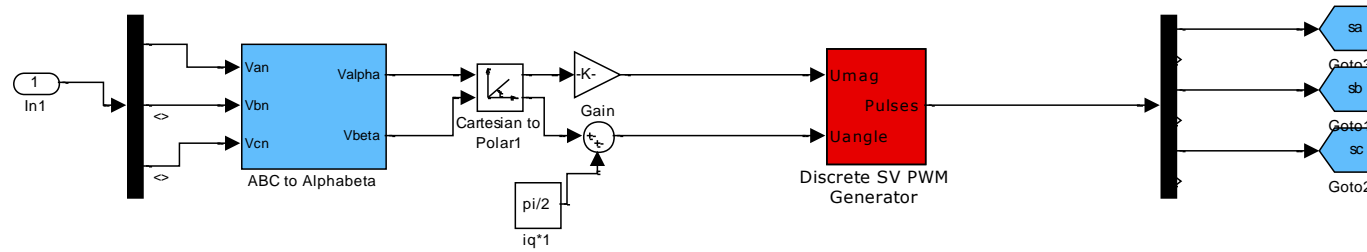


Figure B 2 SVPWM Generation Block

C. Simulink Models for Real Time Implementation on dSpace

RTI Data...

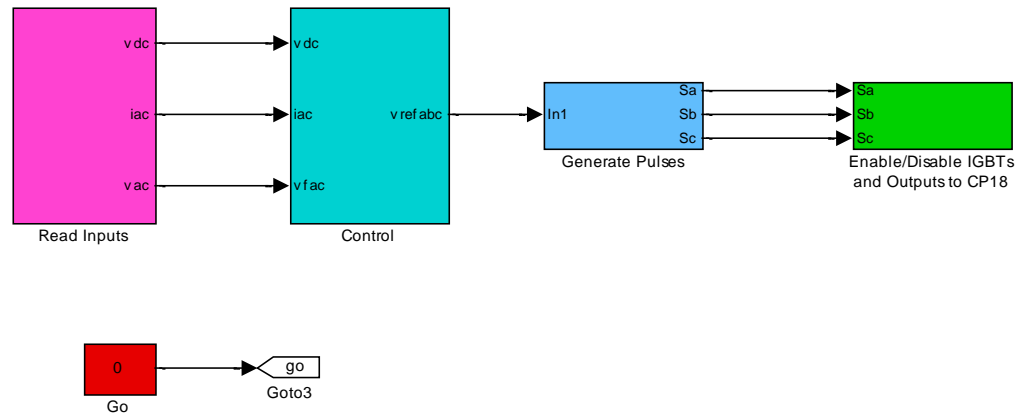


Figure C 1 Simulink top level model for real time implementation

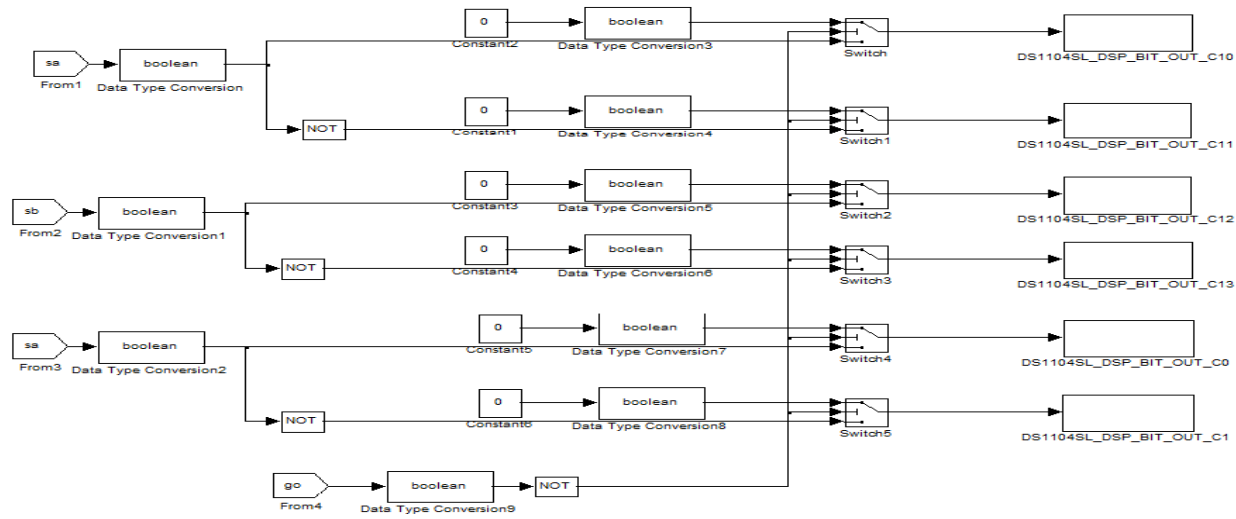


Figure C 2 Simulink block for enabling/disabling the IGBTs